

03

STIF

ERTS III

"Made available under NASA sponsorship
in the interest of early and wide dis-
semination of Earth Resources Survey
Program information and without liability
for any use made thereof."

E7.6-10331

CR-147212

RECEIVED
NASA STI FACILITY
ACQ. BR

MAY 18 1976

DCAF#

10028745

1 2 3 4 5

(E76-10331) REGIONAL TECTONIC EVALUATION OF
THE TUSCAN APENINE, VOLCANISM, THERMAL
ANOMALIES AND THE RELATION TO STRUCTURAL
UNITS Final Report, Oct. 1972 - May 1975
(Zentralstelle fuer Geo-Photogrammetrie)

N76-24656

Hc \$6.00

Unclas

G3/43

00331

Original photography may be purchased from:
EROS Data Center
10th and Dakota Avenue
Sioux Falls, SD 57198

ORIGINAL CONTAINS
COLOR ILLUSTRATIONS

1332A

ZGF

- ZENTRALSTELLE FÜR GEO-PHOTOGRAMMETRIE UND FERNERKUNDUNG (DFG)

am Institut für allgemeine und angewandte Geologie der Universität, Luisenstr. 37, D-8 München 2

RECEIVED

MAR 22 1976

SIS/902.6

1. SR No. 332	2. Type of Report III	3. Recipient's Catalog No.
4. Title: Regional tectonic evaluation of the Tuscan Apenine, Vulcanism, thermal Anomalies and the relation to structural units		5. Report Data May 1975
		6. Period Covered Oct. 72 - May 75
7. Principal investigator Prof. Dr. J. Bodechtel <i>etc.</i>		8. Number of Pages 133
9. Name and Address of Principal Investigators Organization Zentralstelle für Geo-Photogrammetrie und Fernerkundung		10. Principal Investigator Rept. No.
		11. GSFC Technical Monitor James Broderick
12. Sponsoring Agency and Address Deutsche Forschungsgemeinschaft BONN-Bad Godesberg Kennedyallee 40		13. Key Words (Selected by PI) Geology, Land use, data processing
<p>Supplementary notes</p> <p>This report consists of the results of research work carried out at the Zentralstelle für Geo-Photogrammetrie und Fernerkundung der Deutschen Forschungsgemeinschaft (Central Laboratory of geophotogrammetry and remote sensing of the German Research Council)</p>		
<p>Summary:</p> <p>Based on LANDSAT-1 data (photographic products and CCTs) methodological and application oriented investigations were carried out. The geological interpretation on data exhibiting the Italian peninsula (lineament evaluation) led to the recognition of tectonic features which are explained by a clockwise rotation of various blocks along left-handed transform faults. These faults can be interpreted as resulting from shear due to main stress directed north-eastwards.</p> <p>A landuse map of the mountainous regions of Italy was produced on a scale of 1:250.000. Several levels, I, II and III categories could be mapped.</p> <p>For the digital treatment of MSS-CCTs an image processing software was written in FORTRAN IV. The software package includes descriptive statistics and also classification algorithms. Statistical investigations on redundancy and user-oriented application of LANDSAT-data led to investigations concerning data reduction and to analogue-digital data processing techniques. At least laser-optical processing techniques (Fourier analysis) applied on LANDSAT-data were considered.</p>		

The following Report was prepared
by the Staff of the Zentralstelle:

Prof.Dr.J. Bodechtel
Dr.R. Haydn
Dr.J. Nithack
Dipl.Phys. R. Dittel
Cand. Geol. G. di Bernado
Dipl. Geol. K. Hiller
Dipl. Geol. F. Jaskolla
Cand. Geol. H. Leisen
Cand. Geol. U. Münzer
Dipl. Geol. A. Smolka
Dr. R.P. Gupta ⁺)

⁺) Guest scientist from the Department of Geology
and Geophysics, University of Roorkee, India

CONTENTS

PART I:

Scientific and application-oriented investigations
(Geology, Tectonics, Landuse-mapping)

A) Geologic evaluation of Central Italy.....	3
1. Methodological aspects of space-imagery interpretation	4
1.1. Multitime image interpretation	4
1.2. Detection of tectonic movements from morphological features	7
2. Lineament patterns of the North and Central Apennines	10
2.1. Regional lineaments evaluated from LANDSAT-data	11
2.2. Lineament tectonic evaluation of the Tuscan-Umbrian Apennines	12
3. General tectonic model for the Northern and Central Apennines	14
3.1. Tuscan-Umbrian Apennines	14
3.2. Central Apennines	16
3.3. Northern Apennines	16
4. Relationship between Northern Apennines, Po-Valley and the Southern Alps	18
5. Comparison of lineament pattern with tectonic ground truth measurement	22
5.1. Geology at the test site	25
5.2. Evaluation of a LANDSAT-1 image of the Tuscany, with special regard to the ground- truth area	28
5.3. Relation between field work and phototectonic interpretation of aerial photographs	30
5.4. Some methodological aspects on the evaluation of meso-tectonical measurements	34
5.5. Tectonic systems derived from pole-diagrams	37
B) Geo-tectonic studies in Eastern Alps	40
C) Application of LANDSAT data for land-use mapping by conventional interpretation techniques	57

1. Data source	58
2. Evaluation techniques	58
2.1. Background information	58
2.2. Interpretation key	59
2.2.1. LANDSAT-1 multispectral scanner data	59
2.2.2. SKYLAB data	62
2.3. Gray tone and colour tone	62
2.3.1. The impact of natural parameters on the photographic density	63
2.3.2. Impact of technical factors on the photo- graphic density	63
3. Possibilities and limitations of the conventional classification	66
4. Discussion of the results	72
4.1. Mapping of land-use categories	72
4.2. Cartographic accuracy	76
4.3. Comparison with other methods of mapping	76
4.4. Comparison with automatic digital classification	76

PART II

Methodological investigations

(Digital analog investigations)

A) Digital image data processing	80
1. Image data processing package -IMAGIN-.....	81
1.1. Preparation of data for digital evaluation	81
1.2. Check of data quality	83
1.3. Descriptions of IMAGIN routines	83
2. Selection of data material and test sites	86
3. Statistical evaluation	89
4. Data reduction	96
4.1. Data compression by principal components transformation	98
4.2. Application oriented data compression	99
5. Automatic classification	105
5.1. Supervised classification	105

5.2. Non supervised classification	108
5.3. The "Slope-Method"	109
B) Analog/digital treatment of multispectral data	112
1. Enhancement of class seperability	112
2. Color coding by operating in the three-dimen- sional color space	115
3. Analog electronic data evaluation	120
C) Fourier analytical evaluation of LANDSAT data by an optical computer	122
1. Image manipulation	122
2. Quantitative measurements	125

PART I

SCIENTIFIC AND APPLICATION-ORIENTED INVESTIGATIONS

(GEOLOGY, TECTONICS, LANDUSE-MAPPING)

INTRODUCTION

This final report on LANDSAT-1 investigations is the result of activities conducted during the years 1973 - 1975. With respect to our research activities in the LANDSAT program and in the field of remote sensing in general, this report must be considered an intermediate work statement of progress to date.

It is necessary to continue and to intensify future work on the following aspects: methodological investigations concerning the applicability of LANDSAT data for various earth scientific disciplines; development of data handling techniques, such as digital evaluation of LANDSAT data; and the analog electronic treatment of images. From a pure scientific point of view, LANDSAT data have delivered a great deal of new information.

With regard to LANDSAT-2, we are optimistic that further scientific results can be derived by evaluation data acquired over a longer period of time.

Pure scientific investigations lead automatically to practical applications and the practical use especially of LANDSAT data. In order to define and to identify potential applications of spaceborne remote sensing techniques, a first-order task is to bring to the attention of potential users the importance of such data.

The Zentralstelle für Geo-Photogrammetrie und Fernerkundung has been founded and is funded by the German Research Council in order to promote remote sensing activities in Germany and to help establish this new technology for various potential applications. The enclosed book on ERTS and partly on SKYLAB ("Die dritte Entdeckung der Erde") must be considered as a step toward achieving this goal. The distribution of this

REPRODUCIBILITY OF THE
ORIGINAL PAGE IS POOR

book has already resulted in increased interest by potential users, such as ministries and other agencies involved in environmental planning and surveillance.

The LANDSAT-1 data provides us, for the first time, with very high resolution sequential multispectral satellite data. Our first approach in the evaluation of this data has been carried out under earth scientific aspects using more or less conventional interpretation techniques. These activities consist of structure-tectonical investigations and also the evaluation of LANDSAT data for land-use planning purposes.

Investigations into the more methodological aspects concerning the digital treatment of LANDSAT data has been intensified after receiving the first tapes near the end of 1973

Within the scope of the above-mentioned investigations, the following activities were conducted: software development for the treatment of MSS-data, the application of analog digital and optical techniques.

According to our various activities, the following report is subdivided into two main parts entitled: Part I, scientific and application-oriented investigations and Part II, methodological investigations.

A) GEOLOGIC EVALUATION OF CENTRAL ITALY

The geological investigations described are based on conventional photo interpretation techniques applied to LANDSAT imagery. For some demonstration purposes also EREP data were applied.

The methods described were used to investigate the tectonic significance of identifiable linear features by utilising multistage imagery and the results of fieldwork (Fig. 1). The geological field investigations are restricted to some areas near Volterra and Siena in the Central Tuscany.

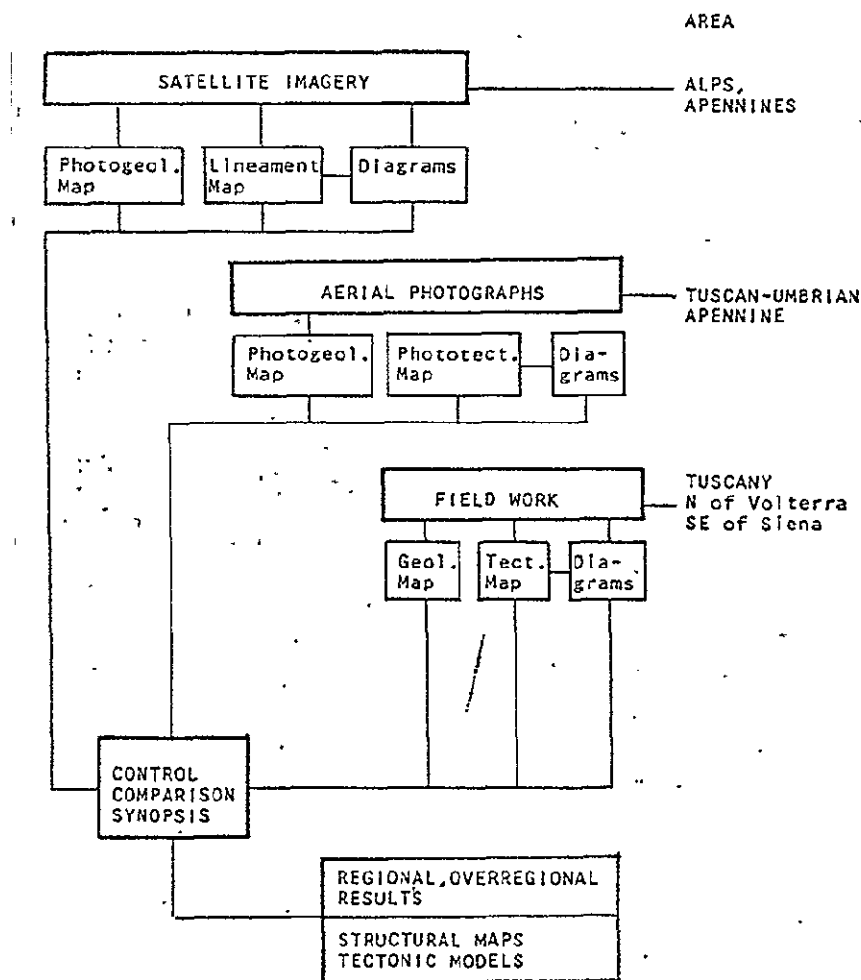


Fig. 1 Scheme for the geologic-tectonic research in the Apennines

1. Methodological Aspects of Space-Imagery Interpretation

1.1 Multitime Image Interpretation

The ability to recognise and interpret linear features within mountain regions strongly depends on shadow effects provided by the distinct relief. As shadow effects are also a function of Sun angle. ERTS images offer optimum possibilities for the statistical comparison of lineament maps with respect to seasonal illumination conditions.

Figure 2 shows a statistical representation of lineament directions derived from three sequential ERTS images of the Molise, northwest of the Gargano Peninsula, Italy (ERTS-1, 8.8.72, 27.8.72, 5.2.73). Comparison of the three histograms shows that all possible linear-feature directions are present in each ERTS frame. The distributions of the maxima, however, have shifted to a certain degree. Depending on the azimuth and elevation of the Sun, this effect has to be taken into consideration, especially when performing tectonic interpretations on the basis of statistical lineament distributions.

In order to minimise the above effects, it is necessary to superimpose the results of as many multitime lineament evaluations as possible as in the following table.

The significance of the distribution maxima obtained by combining sequential data is discussed in Chapter 4.

-10°	-20°	-30°	-40°	-50°	-60°	-70°	-80°	-90°	sector
3,9	14,6	9,5	15,5	14,2	23,4	12,5	2,7	2,2	relative value
-100°	-110°	-120°	-130°	-140°	-150°	-160°	-170°	-180°	sector
3,0	8,6	1,4	4,5	3,7	9,1	5,0	7,1	9,7	relative value

REPRODUCIBILITY OF THE
ORIGINAL PAGE IS POOR

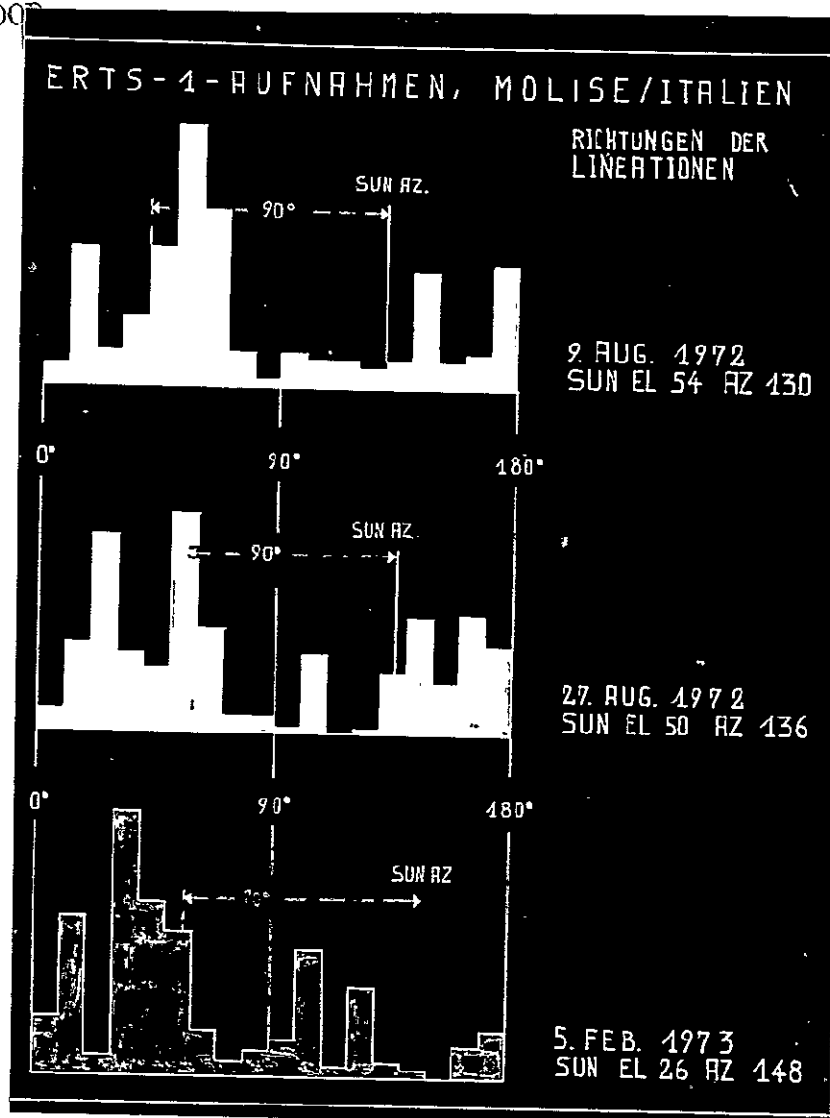


Fig. 2 Histograms of lineament distributions derived from sequential images

The need for multitime evaluations is also apparent from Figure 3. Many linear features could be identified and traced over large areas by using images from different seasons. The reason for this is that, in Central Europe at least the detection of lineaments depends on morphology and vegetation. When using multitime imagery, regional patterns become more obvious.

REPRODUCIBILITY OF THE
ORIGINAL PAGE IS POOR

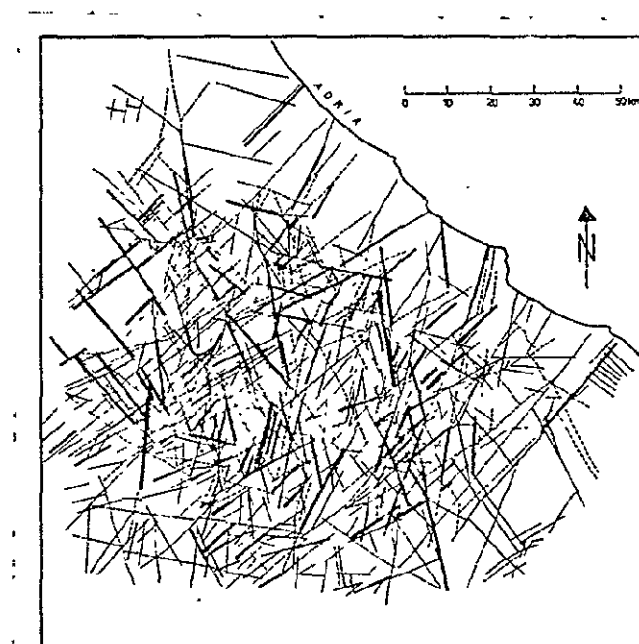


Fig.3 Composed lineament map of temporal imagery
LANDSAT-1 images
MOLISE/ITALY

Lineations (MSS 7)

— 9.Aug.1972

- - - 27.Aug.1972

..... 5.Feb.1973

— overlapping lineations

1.2 Detection of Tectonic Movements from Morphological Features

By using morphological features for the evaluation of synoptic satellite imagery, it is possible to obtain information on tectonic movements along fracture systems. Regions comparable in terms of petrography and tectonic stress fields are characterised by a similar morphological pattern if the same climatological conditions can be assumed. If a displacement of such comparative units is detectable along a linear feature in a first approach, it can be described as a fault. A more detailed description of the fault is only feasible if the dipping direction of the strata can be detected, because vertical displacement of tilted strata results in a pseudo-horizontal displacement at the surface. Vertical movements can be determined only for fold structures, basin or graben fringes. Sigmoidal oriented valleys and mountain ridges can mask younger horizontal movements. Furthermore, it can be observed that fold structures cut by faults often show displacements with respect to the movement of the fault.

Examples of the above phenomena are shown in Figure 4, which represents part of a Skylab image (S 190A, September 1973) showing the Umbrian Apennines between the Lago di Trasimeno and the Adriatic coast.

Figure 5 clearly shows the feasibility of thematic mapping of geologic tectonic phenomena. This map, which covers the the Latium volcanic region and the northeastern area between the Umbrian Apennines and the Abruzzi, shows the advantages that synoptic satellite imagery offers in this field. Besides different volcanic phenomena and the strike and dip of strata, regional relationships between distinct, identifiable linear features are also evident.

Two types of faults in particular can be differentiated: transform or shear faults and vertical fractures.

In this area, the shear faults form a narrow-angle system. The first, approximately north-south oriented, is represented by a zone which cuts the Apennines east of the well-

known Rieti line. Along this fault, horizontal movement can be detected, with a relative dislocation of the western part towards the south. Forming an angle of about 45° , this system is cut by southwest-northeast directed shear faults. For the north-west oriented fault system, clockwise rotation of the western and eastern blocks is assumed.



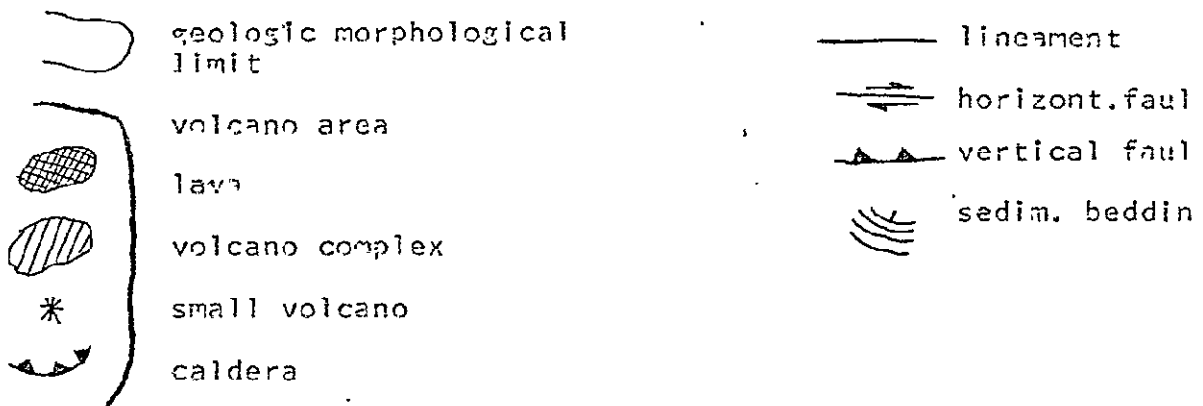
Fig. 4 Umbrian Arc, Skylab S 190 A; Examples for detecting faults by morphological features

REPRODUCIBILITY OF THE
ORIGINAL PAGE IS POOR

Further detectable northwest-southeast striking vertical fault systems are correlated with the chain of Tuscan-Latium volcanoes. These vertical faults, together with the above northeast-southwest oriented transform faults, form a system of bc and ac joints that were originated by a southwest-northeast directed stress field.

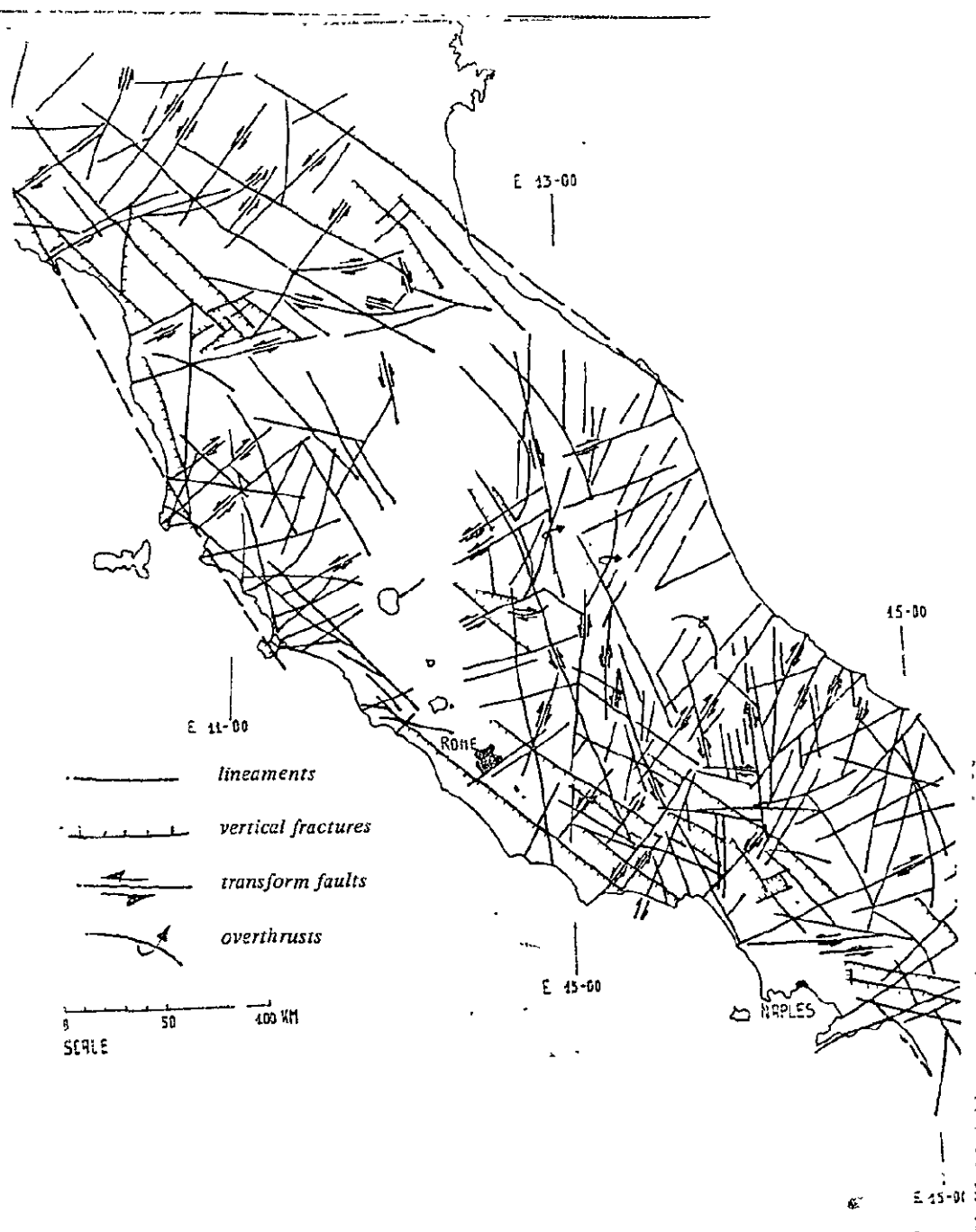


Fig. 5: Geologic tectonic map of LATIUM, ITALY
LANDSAT-1, 6.Feb.1973, MSS 7



2. Lineament Patterns of the North and Central Apennines

Owing to the synoptic nature of satellite data, the extensive major fault systems could be identified and explained in relation to stress directions and fold systems.



- Fig. 6 Main faults in Italy revealed by ERTS-1

Regional Lineaments Evaluated from LANDSAT-Data

Figure 6 shows a view of the main lineations in the northern and central Apennines. The arrows indicate the senses of the horizontal displacements (see Chapter 1). The statistical distribution of the transform and vertical faults corresponds with the results derived by aerial photo-interpretation and fieldwork (Fig. 7). Of importance for the further interpretation are the distribution peaks at 40° , 70° , 130° and 160° (see Chapter 4).

Intensive ground studies have proved that these directions can be correlated directly with an older tectonic system, with a-axis 70° and b-axis 160° , which was rotated clockwise from a primary system (b 140°), and with a younger system again in the primary stress with a = 40° and b = 140° .

The excellent correlations between the results derived from satellite images, aerial photographs and ground truth serve to demonstrate the feasibility of the evaluation methods applied.

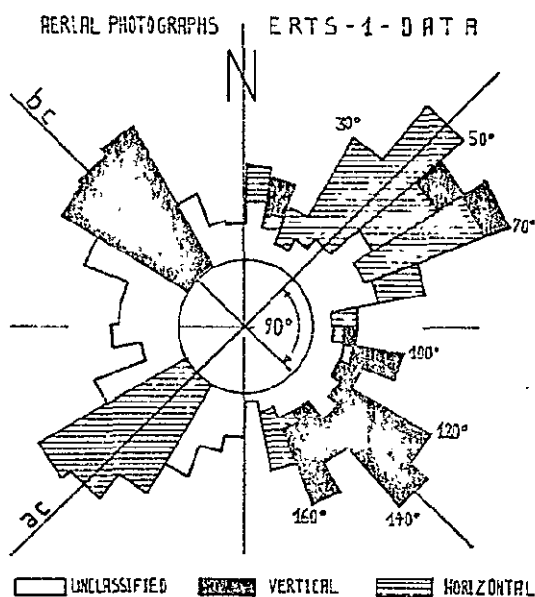


Fig. 7 Rose-diagram of fault directions revealed by aerial photographs and ERTS-1 data

2.2 Lineament Tectonic Evaluation of the Tuscan-Umbrian Apennines

The complex tectonics of the Umbrian arc are demonstrated by Fig. 9 which shows the main lineaments and accompanying minor lineations. Taking into account also the information derived from ERTS data (Fig. 7), the same tectonic systems as above ($a_1 = 70^\circ$, $b_1 = 160^\circ$; $a_2 = 40^\circ$, $b_2 = 140^\circ$) could be derived. In addition to these main lineations, shear faults at 10° and 110° can be observed.

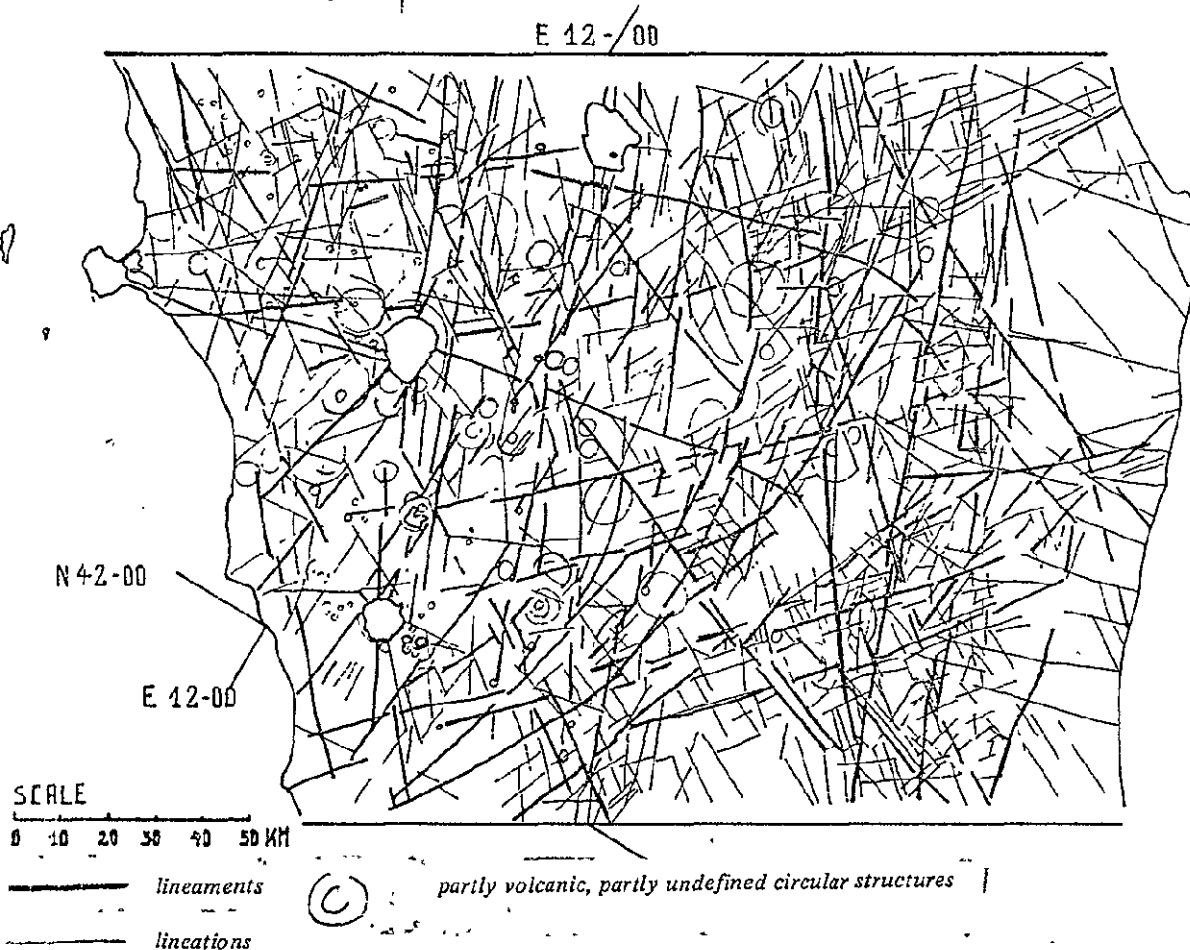


Fig. 8 Photo-tectonic interpretation, Tuscan-Umbrian Apennines

REPRODUCIBILITY OF THE
ORIGINAL PAGE IS POOR

Some information could also be derived concerning the age of the various systems. A sequential description could be drawn up for the latest movements. A model for a "tectonic schedule" is illustrated in Figure 10 and can be described as follows:

- 1) Beginning of the folding phase, which is characterised by northwest-southeast oriented fold axis and a perpendicular striking ac-system (primary 140° b and b_2).
- 2) With respect to the further compression, displacement of the various blocks occurs along the ac-system. This results in a relative displacement towards the northeast of the northwestern part.

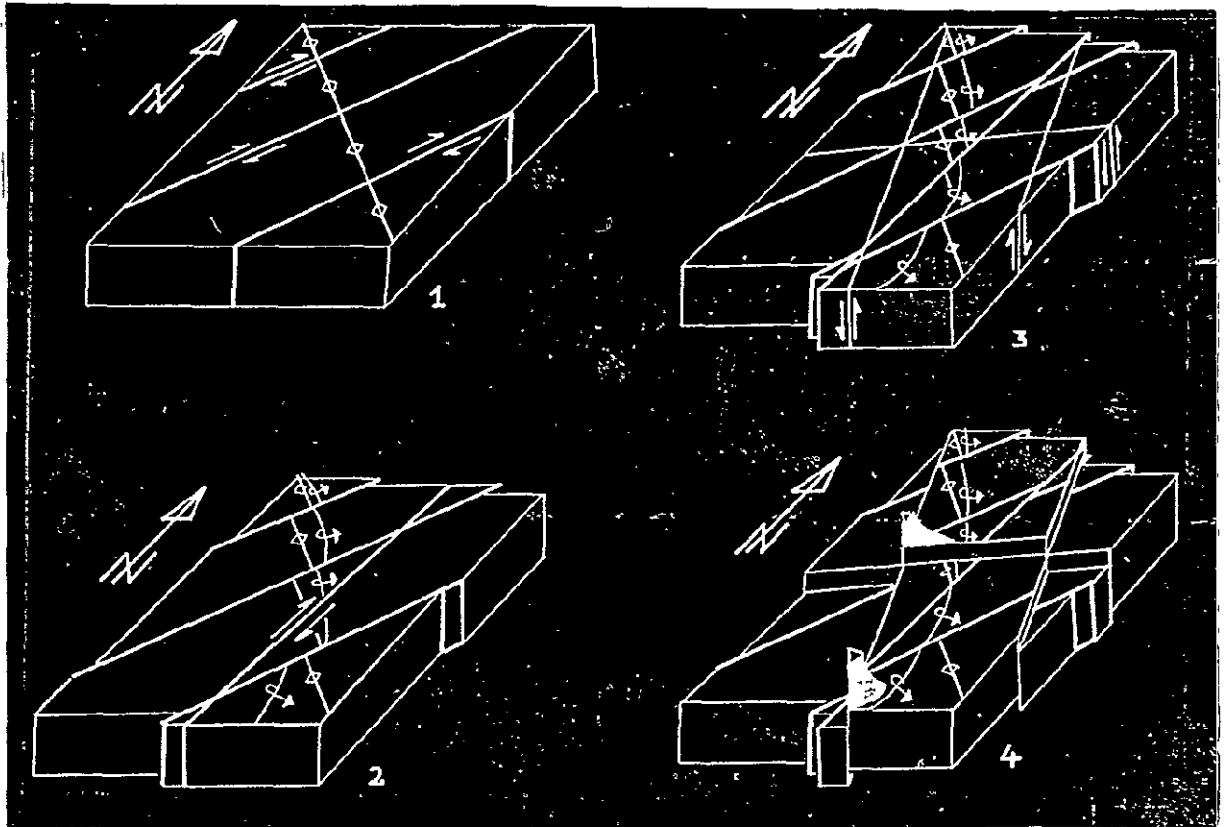


Fig. 9 Fracture development in the Tuscan Umbrian Apennine

3) Besides north-south oriented transform faults, a continuation of the shearing process causes a north east directed displacement of the southeastern part. The repeated displacements of the folds and overthrusts from the "Umbrian Arc".

4) In a last phase, vertical movements occur especially along 70° , 110° and 160° striking planes. Along these fractures, the region of the Latium and Tuscan volcanoes was depressed.

3. General Tectonic Model for the Northern and Central

3.1 Apennines

Tuscan-Umbrian Apennines

As is clearly shown in Figure 7, the directions of the main lineations of the region between the Arno River and the Abruzzi Mountains differ from those in the northern and southern areas. The tectonic unit of the Tuscan-Umbrian Apennines is bordered by the following fracture zones:

- In the north, a transform fault striking about 80° and following the Arno Valley. Along this fault, the Tuscan-Umbrian block was displaced to the east.
- In the east, a north-south striking transform fault, beginning east of the city of Latina and ending at the Adriatic coast northwest of Ancona. The relative movement of the Tuscan-Umbrian unit was directed to the south.

A clockwise rotation of the Tuscan-Umbrian Apennines results from the combination of movements described. Diagrams* obtained from fieldwork show two rectangular joint systems: and older ($b_1 = 160^{\circ}$) and a younger ($b_2 = 140^{\circ}$) system. In his theory of the orogenesis of the Apennines, Wunderlich (1966) postulates an anti-clockwise rotation of the main stress from west to southwest. Such a rotation could have caused the difference between the older and younger b-axes. As regards

* see next chapter

tectonic movements revealed by satellite data, it must, however, be pointed out that such studies mainly highlight features of relative movements.

Assuming the Tuscan-Umbrian region to be a static block, the forming stress would have shifted from west to southwest. However, taking the direction of stress as a stable element, the Tuscan-Umbrian block must be rotated clockwise (Fig. 11). This second possibility is confirmed by:

- the movements along the bordering main transform faults,
- the internal fault pattern of the block,
- the overthrusts in the Abruzzi Mountains,
- the reduction in overthrusting intensity from north to south along the border between the Umbrian Apennines and the Abruzzi.

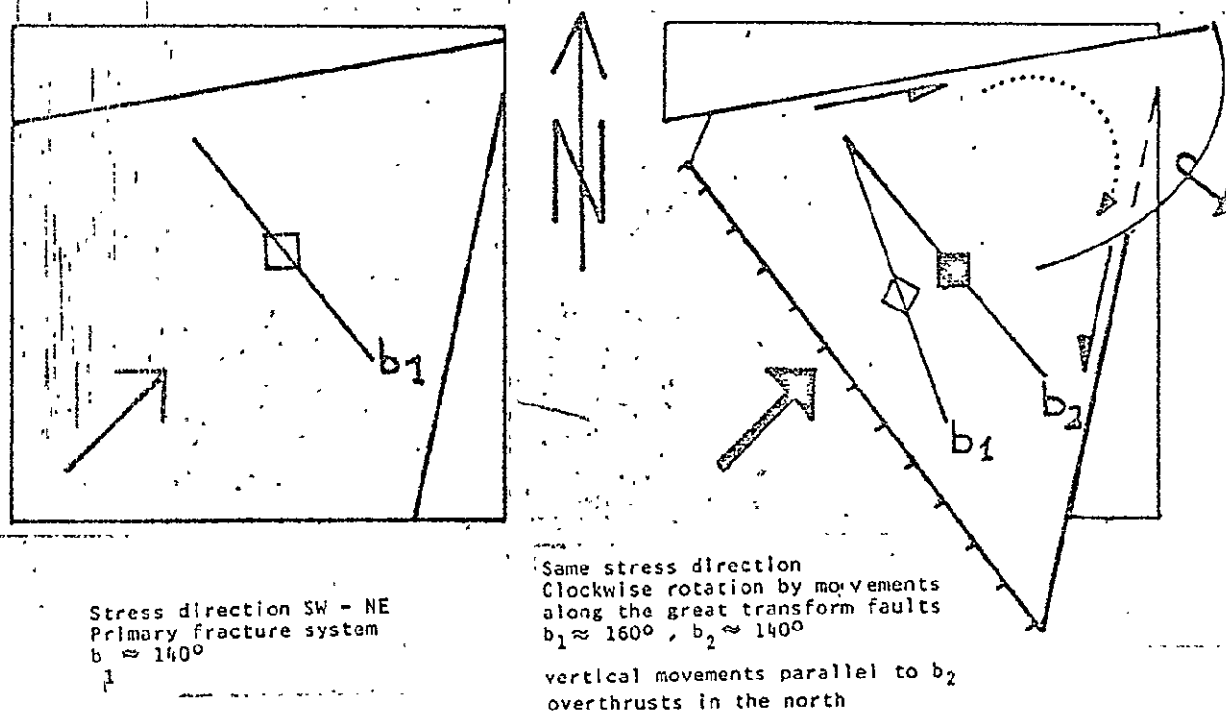


Fig. 10 Tectonic model of the Tuscan - Umbrian Apennines

3.2 Central Apennines (Abruzzi Mountains)

The tectonic concept, described for the Tuscan-Umbrian Apennines based on the relative movement observable in ERTS and Skylab data has to be seen in connection with the neighbouring areas north and south.

Based on the tectonic map (Fig. 7), a movement of the Central Apennines, the Abruzzi Mountains, similar to that of the Tuscan-Umbrian block can easily be derived. But the Abruzzi are further southwest than the Tuscan-Umbrian Apennines. This could be caused by a combination of clockwise rotation and northeastward drift tendency of the Tuscan-Umbrian Apennines, whereas the Abruzzi block was a relatively stable element.

3.3 Northern Apennines

In the west, the Northern Apennines are cut off by a NNE striking transform fault beginning in the Gulf of Genoa and forming the eastern border of the Monferrato. The southern limit is the Arno Valley fault, which borders the Tuscan-Umbrian Apennines.

According to the relative movements along the two bordering transform faults, the Northern Apennines must also have been rotated clockwise. In this case too, the rotation could be combined with drift in a northeastern direction.

These movements may explain the triangular shape of the Po Valley, the northwestern part of the Northern Apennines being moved further northeast than their southwestern part.

A sketch of above tectonic model, evaluated from ERTS and Skylab data, is shown in Figure 12. The "block-bordering" transform faults can be interpreted as a shearing system with a main stress lying SW-NE. This stress caused a general drifting of the Apennines to the northeast. The drift

intensity decreased from northwest to southeast and caused clockwise rotation of the three blocks of the Northern Apennines, the Tuscan-Umbrian Apennines, and the Abruzzi Mountains.

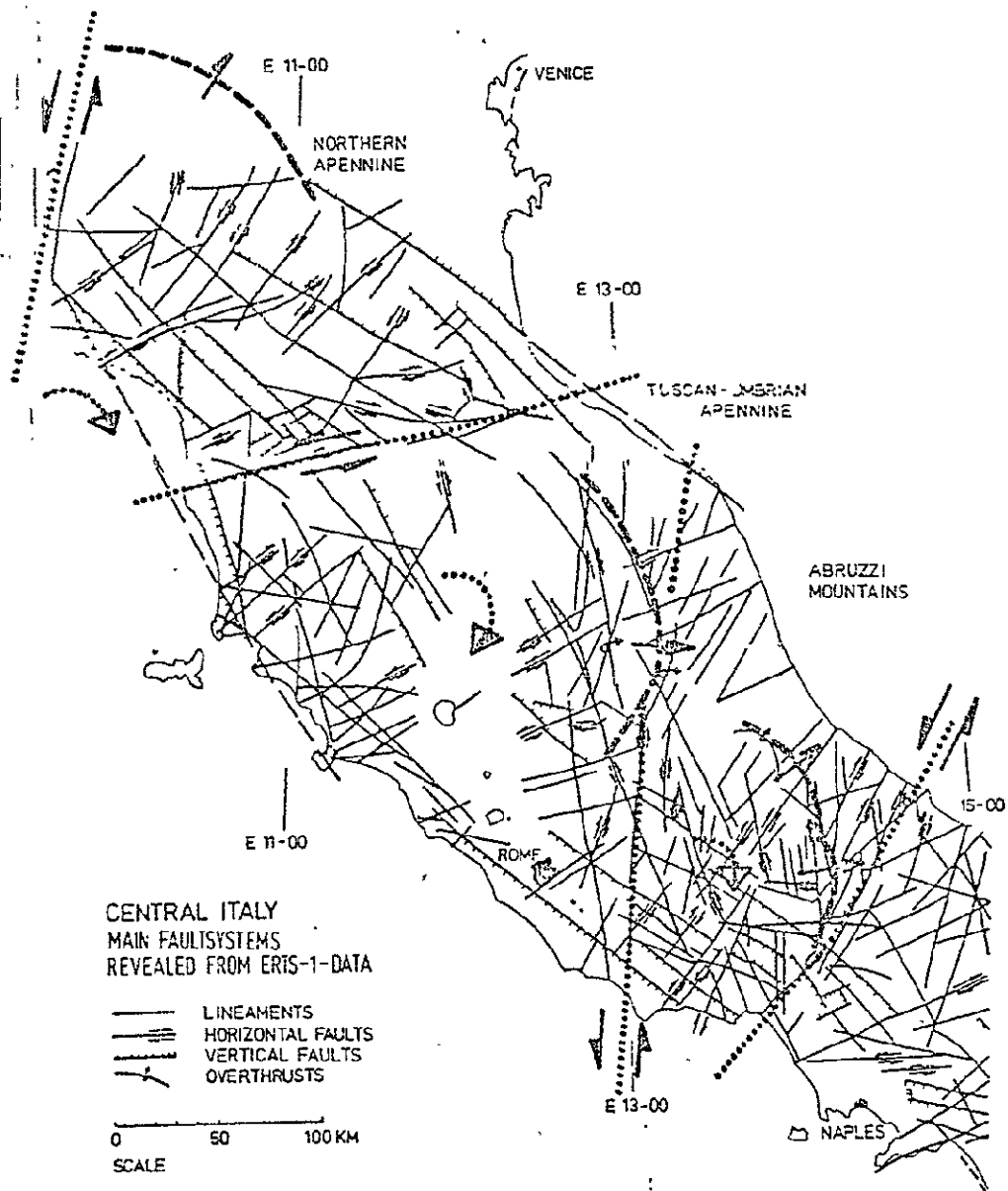


Fig. 11 Main fault systems in Central Italy

4. Relationship between Northern Apennines Po Valley and the Southern Alps

It is understood that the extensive tectonic fractures must have their origin in the deeper crystalline basement. These large scale movements result in a system of fractures revealed only by a subtle lineament pattern in the sedimentary cover, interpretable on the basis of space and aerial images.

However, the exact location of the fracture planes, revealed by the lineaments, is difficult to detect.

But for the geologist, the knowledge of the relative position of the fracture planes, obtainable through evaluation of photolineaments is, especially, of great importance.

In the area of the northern Apennines, SW-NE and NW-SE striking parallel fractures are known and can be traced as lineations through the bordering Po Valley. Some of these lineations even extend into the southern Alpine body.

From geological investigations, it is known that swales and ridges existed during Triassic time. These features resulted from NNE-SSW striking fractures in the crystalline basement (Auboin, 1967; De Jong, 1967; Nithack, 1968).

Furthermore, it is proven that there is a stepwise downward progression from the southern Alps to the Po Valley, created by WNW-ESE stepwise faults.

It can be expected that the above-mentioned prevalent vertical movements within the crystalline basement are present also in the basement of the Po Valley area.

This conclusion is reached on the basis of the lineament evaluation (Figure 13) and the morphology of the Quaternary basin, described by the map of Figure 12 (Bederke & Wunderlich, 1968).

The characteristic morphology of the Quaternary basin in the region of the Po Valley suggests that the large scale lineaments exist throughout the Apennine-Po Valley and

southern Alps and that they are an expression of actual faults.

Based on this conclusion, a schematic block diagram could be constructed for the above-mentioned area (Fig. 1.4).

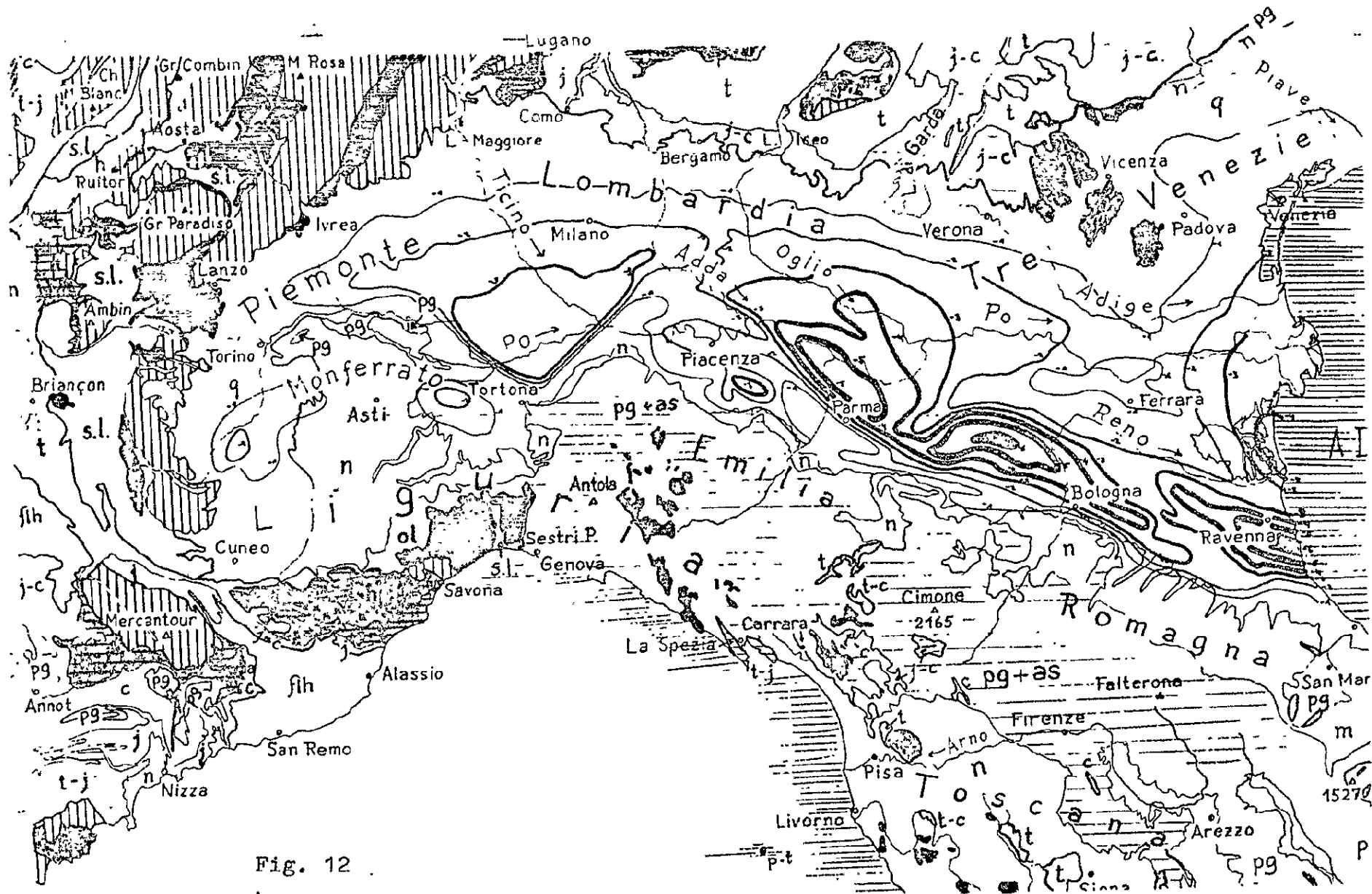


Fig. 12

REPRODUCIBILITY OF THE
ORIGINAL PAGE IS POOR

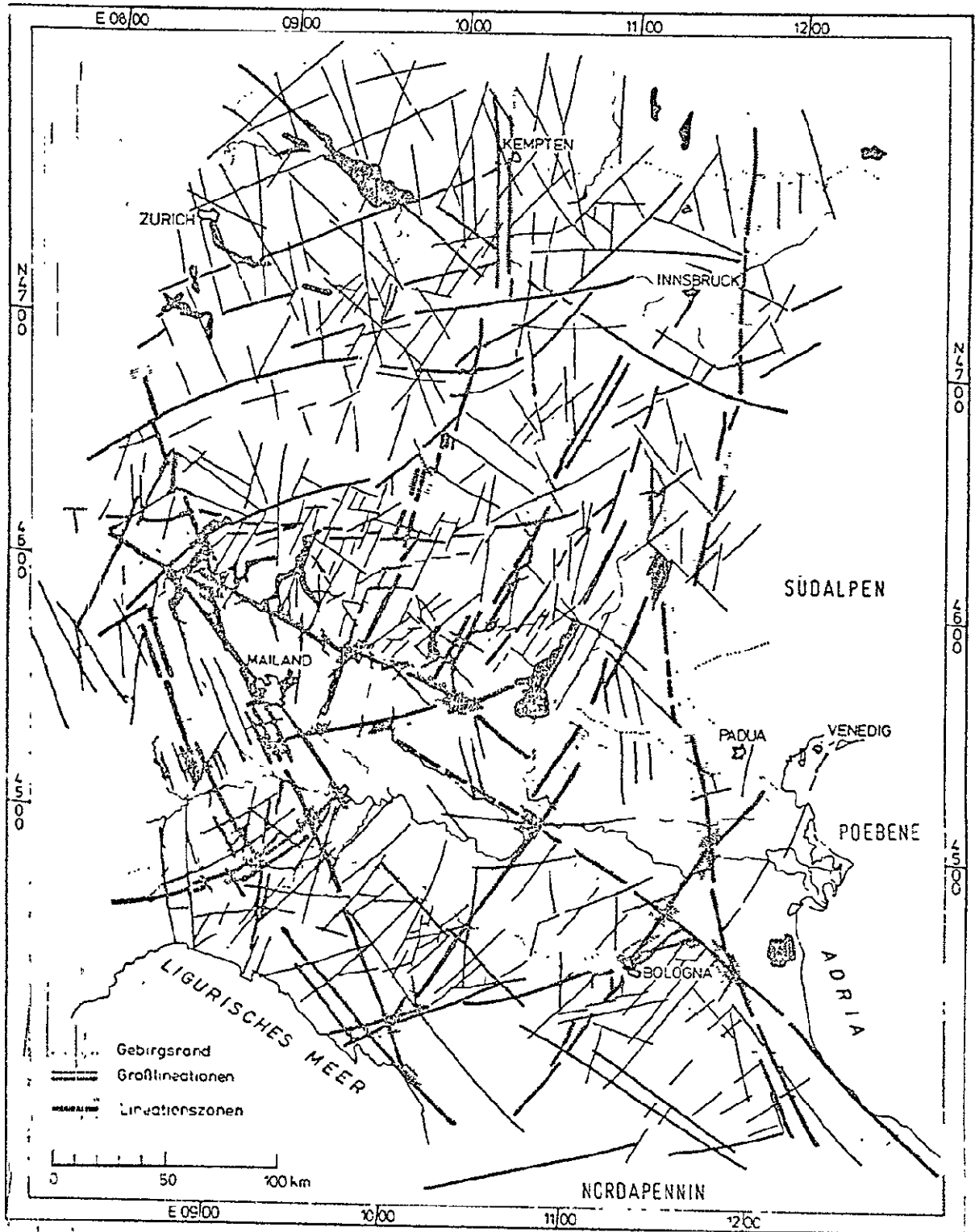


Fig. 13
 Northern Apennines, Po Valley, Southern Alps
 Lineations derived from LANDSAT imagery

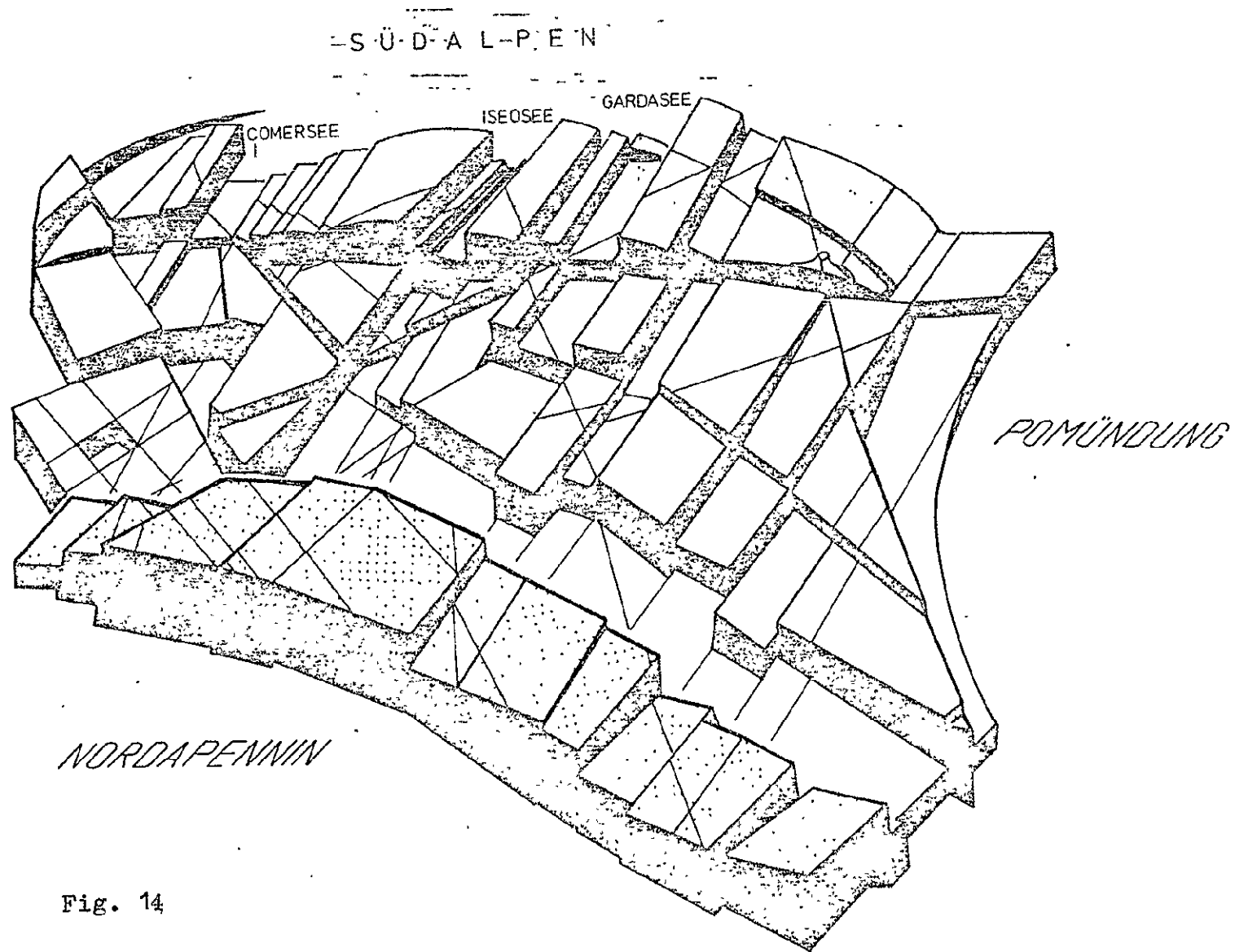


Fig. 14

5. Comparison of Lineament Pattern with Tectonic Ground Truth Measurement

Satellite imagery can be regarded as an optimum base for a large scale lineament and structure analysis. By utilizing the unique synoptic view over large areas, the interpreter is able to delineate linear features and to recognize subtle structural elements on the earth surface, detectable by aircrafts or by ground investigations. Because of the above-mentioned advantages of space imagery, it is not surprising that many scientists, and especially geologists, have concentrated their efforts on preparing detailed lineament maps. This kind of evaluation is of great scientific importance, especially with respect to the understanding of inter-regional structural relationships. In addition to the above-mentioned aspects, a further evaluation procedure is to verify the interpreted structural elements from space imagery by intensive field work. Within this approach a first order task is to assess the influence of interregional structures on the meso-tectonic fabric.

The mesotectonic fabric of rocks is the result of certain tectonic stress conditions. During geological time, stress patterns have changed their orientation and intensities several times. The above-mentioned changed stress conditions often are reflected by typical symmetrical configurations of joints. A careful interpretation of the fabric enables the geologist to draw conclusions on former stress conditions. That is not only of scientific, but also of great economic importance. Quite often a close relationship exists between a specific tectonic situation and the occurrence of ore deposits. In order to investigate the possible influence of lineament features to be seen on LANDSAT data to the meso-fabric, a test site in the southern part of the TUSCANY near SIENA was chosen.



Fig. 15:

Geological Map of the test area and its surroundings

- Signatures in darker grey: Mesozoic rocks
- O Oligocene rocks
- Mp Miocene/pliocene rocks
- Faults

REPRODUCIBILITY OF THE
ORIGINAL PAGE IS POOR

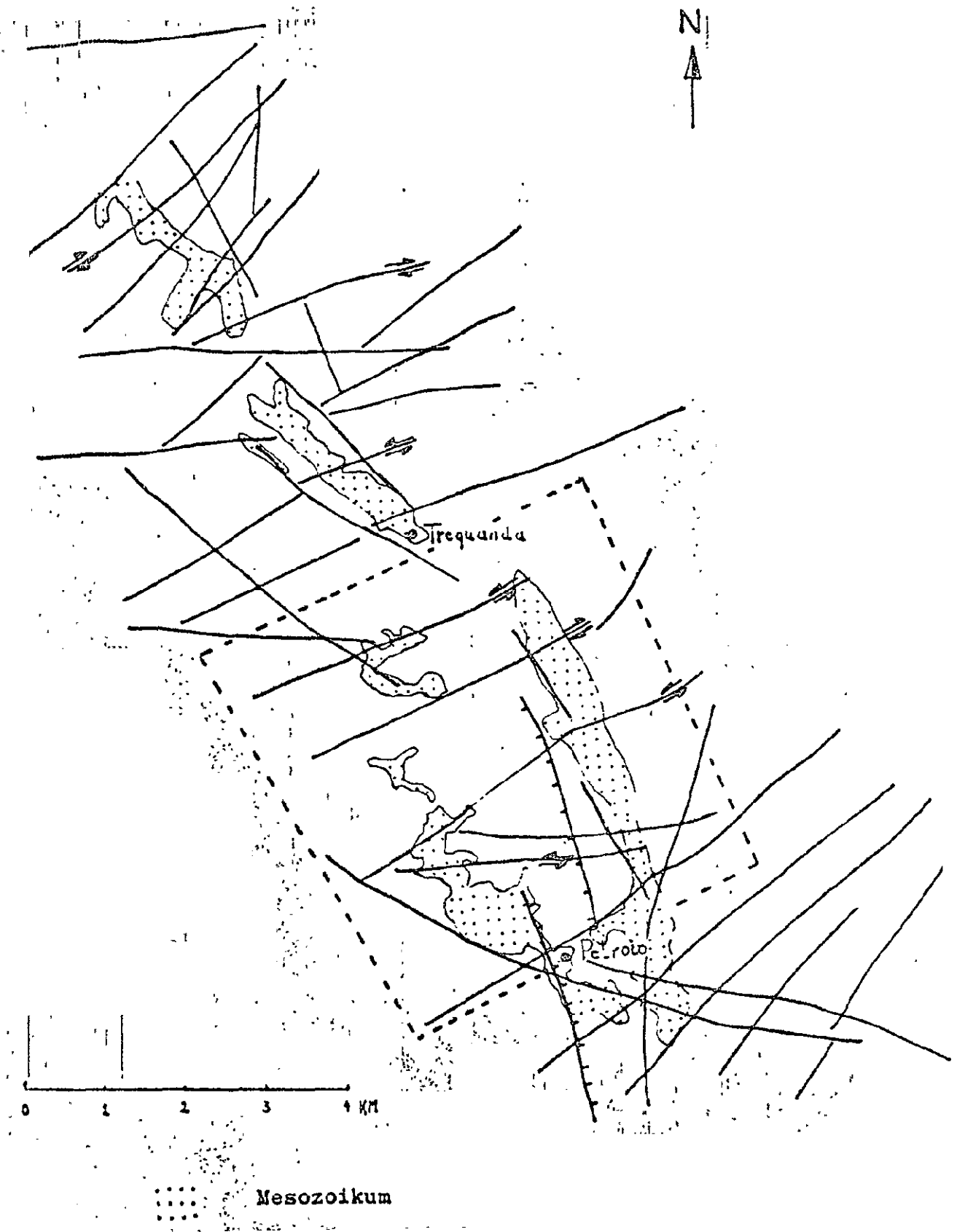


Fig. 16

Photolineations derived from aerial photographs

5.1 Geology at the Test Site

The ground truth area is part of a very important orogenic structure with Apenninic strike direction, whose nature is still open to discussion. This structure is known as Cetona - Orsaro - line (the most suitable name without genetic significance). Morphologically, the Cetona-Orsaro-line forms a 260 km long ridge of variable altitude and extension. In the North of the Arno River, it represents the main crest of the Apennines. With respect to geology, the ridge is built up in its southern part by Mesozoic limestones, dolostones and alternating cherty--calcareous-marly strata and in its central and northern parts mainly by the Macigno sandstones of Oligocene age. (Fig.15) In general, the structure in the mapping area could be explained as a sequence of two overturned anticlines being replaced by thrust faults. The original fold-structures appear now to be disturbed by synkinematic shearing and postkinematic block faulting. Such block-faulting revived the old fracture pattern and created the horst-like uplifting of the ridge as a whole. The ridge is divided by several horizontal faults transverse to the strike of the folds (Fig.16). The largest displacements have taken place on ac-direction, as revealed by satellite images and aerial photographs (Fig.16,17). On the contrary, shear directions are less important with respect to large scale displacements.

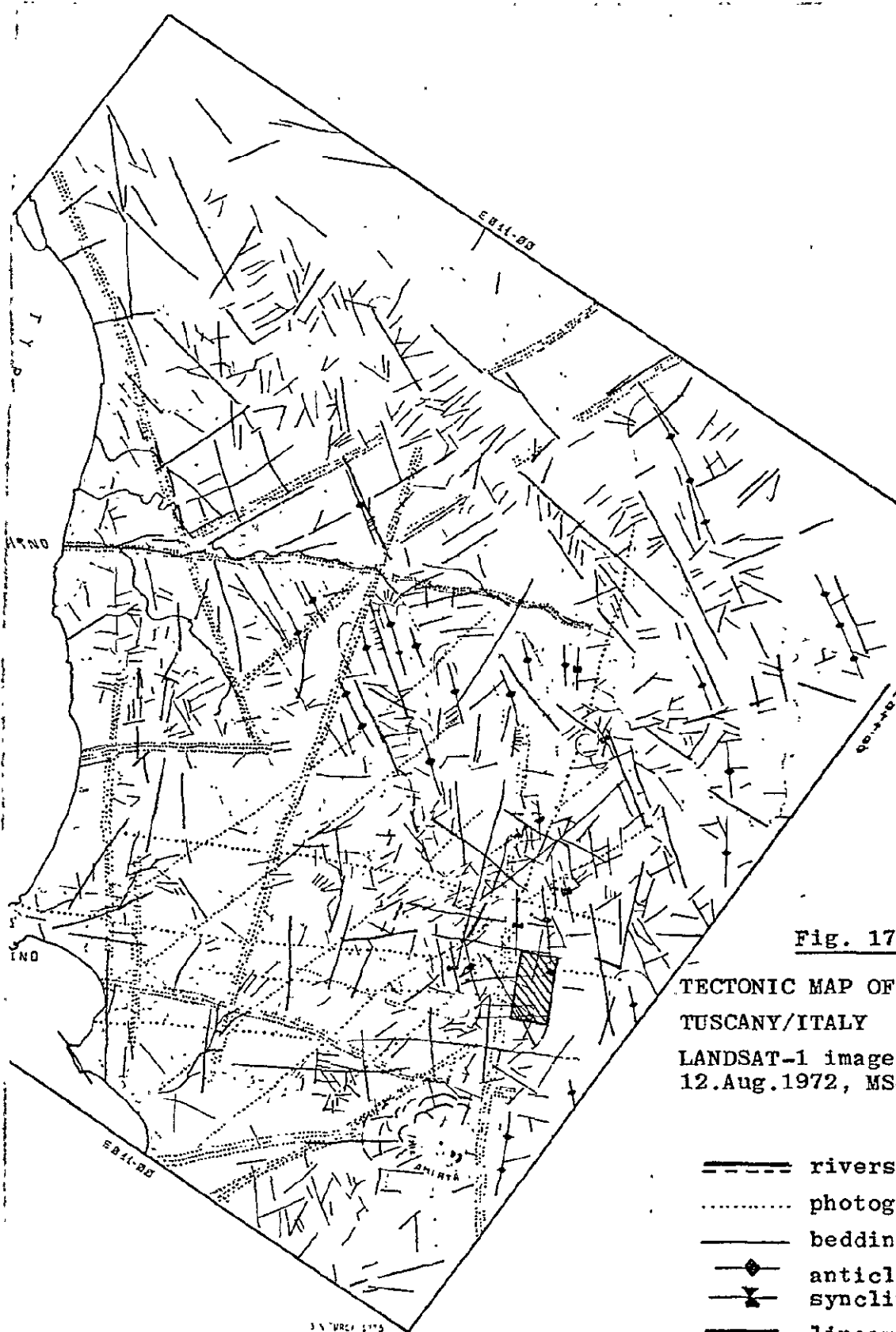







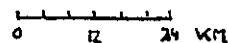


Fig. 17:

TECTONIC MAP OF
TUSCANY/ITALY

LANDSAT-1 image
12.Aug.1972, MSS 5

- | | |
|---|------------------|
|  | rivers |
|  | photogeol. units |
|  | bedding traces |
|  | anticlines, |
|  | synclines |
|  | lineaments |
|  | main lineations |






129UG72 C N43-33/E2-2-SS N 14-34-E2-2-SS S R SUN EL52 RZ:32 E2-2-SS 192-22-4-G-1-N-D-2L NPSR E2-2-SS 222-29232-5 2

Fig. 18

LANDSAT image of Tuscany

 : test area

REPRODUCIBILITY OF THE
ORIGINAL PAGE IS POOR

5.2 Evaluation of a LANDSAT-1 Image of the Tuscany, with Special Regard to the Ground Truth Area

The following Figure 17 is based on a LANDSAT-1 image of the Tuscany taken on August 12, 1972 (Fig.18). The ground truth area is demarcated by dotted lines. The interpretation map (Fig. 17) shows all the large lineaments touching the calcareous ridge situated between Rapolano and Montepulciano. The important ESE-WNW-striking horizontal faults can be followed almost to the Tyrrhenian coast. In the same way, the bc-fault-traces (representing reverse faults) reach far to the North and South. In aerial photographs (Fig. 16), a third important fault direction striking 110° can be recognized which does not appear on the LANDSAT image. This is probably explained by the fact that scan-lines run nearly parallel to this direction. For this reason the recognition of those linears is impossible. In addition, the LANDSAT image indicates some lineaments, unrecognizable by ground truth or by evaluation of aerial photographs. Examples are the lineament W of the ridge, the result of the uplifting of the ridge, and the other one N of Trequanda, the result of the displacement of the ridge by about 400 m transverse to its strike direction. Another one, only in part recognizable on aerial photographs, but well-identified in the satellite image, marks the boundary of the western part of the horst structure. All the large horizontal faults in the ac-direction ("antiapenninic"), seen in the aerial photos, are more difficult to recognize on the LANDSAT image.

The Large Scale Structure

The existence of two different b-axes (see chapter: "Examples of Characteristic Pole Diagrams out of the Test Site") indicates two deformation stages, the first of which, at least, is active still in the upper Triassic, but no longer is active in the Oligocene. A multistage deformation is postulated by several scientists investigating the Geology of the Apennines (Baldacci, et al., 1967, Bortolotti, 1966, Giannini, 1962, Sestini, 1970, Reutter, 1968). A possible explanation for the

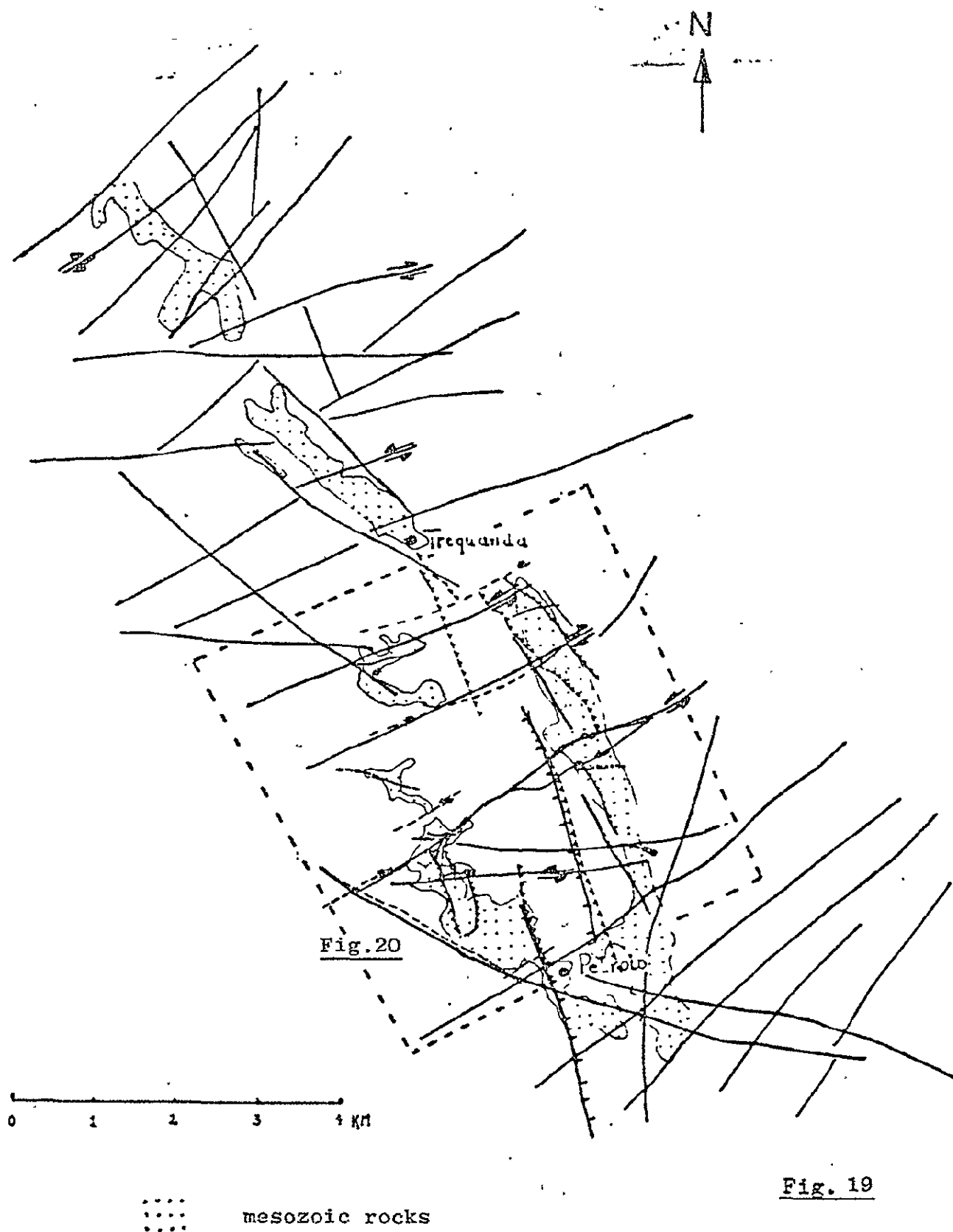


Fig. 19

Fig.19 : Photolineations derived from aerial photographs
 Fig.20 : Faults mapped by field work

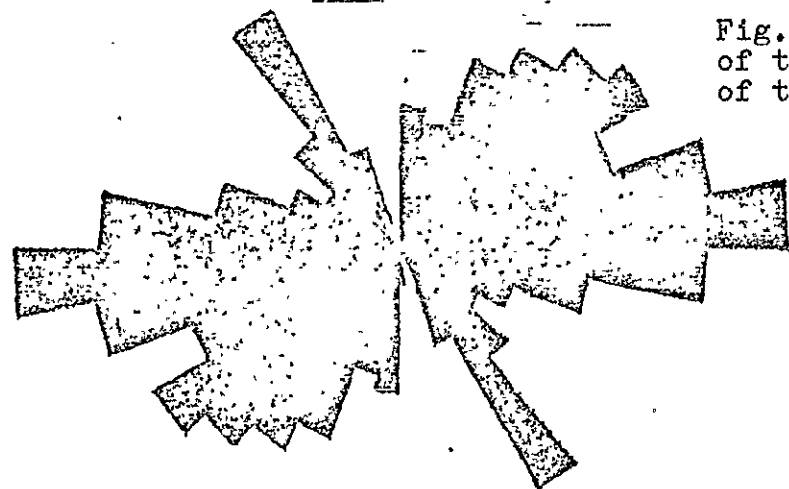
difference of the two b-directions is given by Boccaletti, Guazzone (1968, 1970). They postulate an anti-clockwise rotation of the Italian Peninsula, which brought the axes to their present directions. The structural data reported by these authors (e.g. the E-W stress direction in the Tuscany, corresponding to N-S fold axes) cannot be confirmed in our mapping area. Wunderlich's (1966) opinion that the stress direction rotated counter-clockwise to the WNW-ESE trend on the margin of the Po plain is better suited to the structural facts. A new concept was proposed by our research team: based on the interpretation of LANDSAT-1 images we contend that a clockwise rotation of a block formed Tuscany and part of Umbria. Such a rotation results from a lefthanded horizontal fault following the Arno valley and another N-S striking left handed horizontal fault between the towns Ancona and Latina (see previous part of this report).

5.3 Relation between Field Work and Phototectonic Interpretation of Aerial Photographs

The relations between field work and aerial photointerpretation are demonstrated in figure 19 and 20. Figure 19 shows the main lineaments touching the Mesozoic ridge in the area around Trequanda, as seen on aerial photographs.

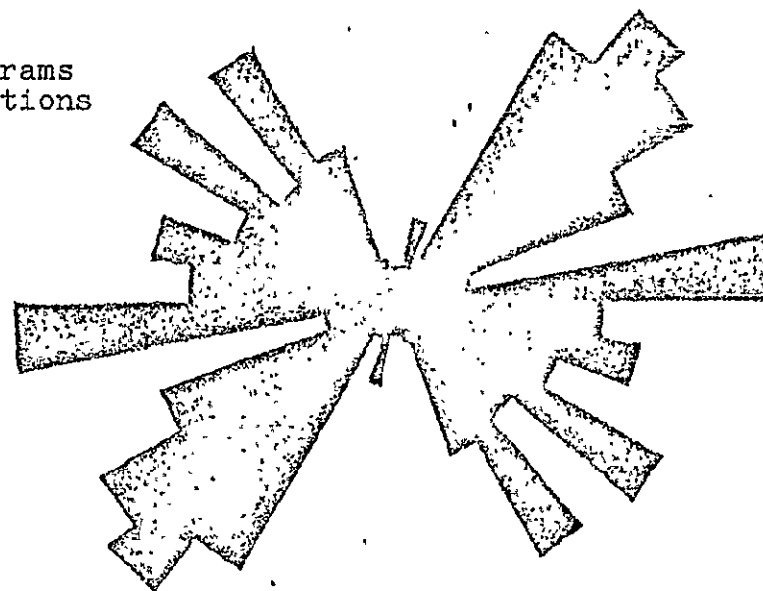
Recognizable displacements are marked as well. Figure 20 is a structure map of the study area S of Trequanda. This map was prepared from data supplied by intensive field investigations which paid special attention to large lineaments visible on aerial and satellite images. Such combined work applied to a small ground area has provided a solid base for the inter-regional interpretation of LANDSAT images (as performed in the previous chapter). The combination of field measurement and lineament analysis indicated the existence of two fabric systems with different orientation and suggested the concept of clockwise rotation of Tuscany-Umbria.

Fig. 21: Rose diagrams
of the photolineations
of the test aerea



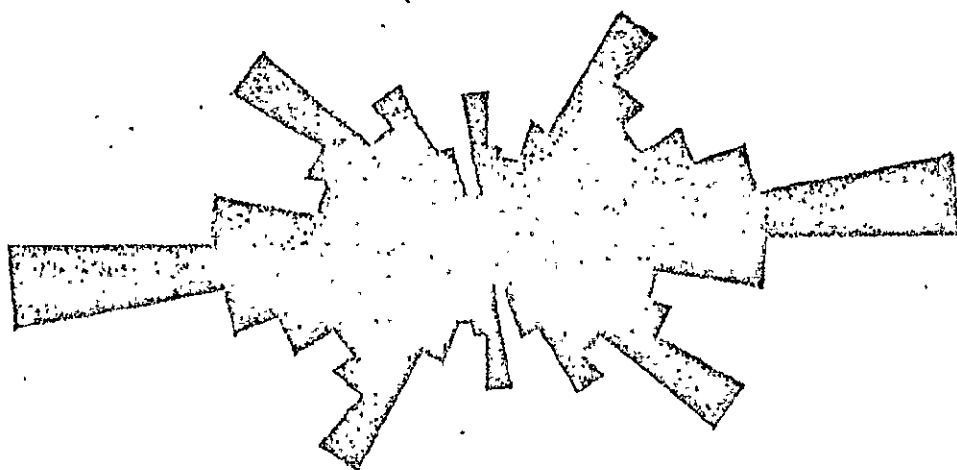
Mesozoikum

19,06 km



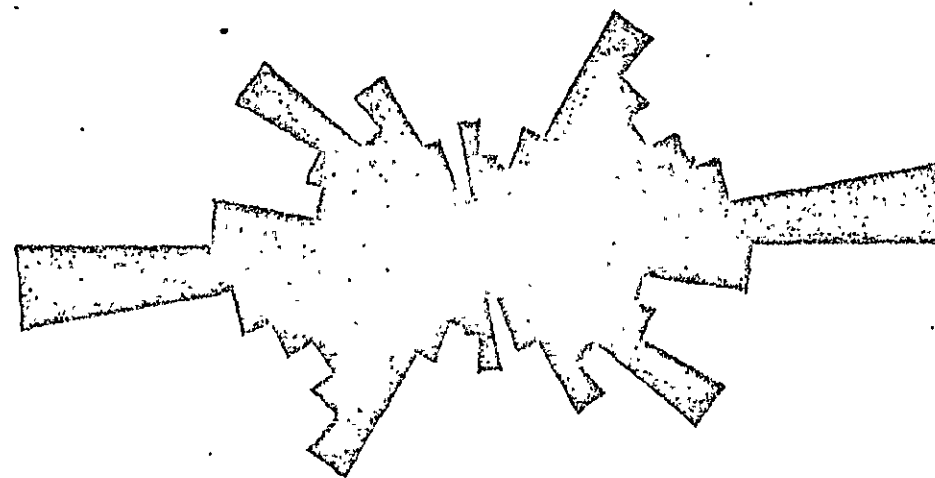
Macigno + Argille

23,16 km



Pliozän

242,2 km



Gesamtgebiet

280,4 km

The Photo Lineaments

The lineament map (Figure 19) has been statistically evaluated in three separate zones:

- zone 1: formed of Pliocene sands
- zone 2: formed of Mesozoic limestones and cherty-calcareous-marly alternating strata
- zone 3: formed of Macigno sandstones and Argille Scagliose

The rose-diagrams show the percentage of all the lineaments for 10° -classes. Looking at the four rose-diagrams (Fig. 21) (one for each specific zone and one for the whole region) the most striking feature is the similarity of the diagrams for the whole region and for the Pliocene. This is caused by the fact that Pliocene in this region covers by far the largest areas. So it has great influence on the percentage of lineaments of the whole region. The evaluation of the three zones agrees with the conclusions reached by the interpretation of equal area projection diagrams of joint poles.

In the Mesozoic limestones the early deformation stage is reflected by lineaments in ac_1 -direction accompanied by hko_1 shear directions. The stratification was nearly horizontal during this early deformation stage. The younger stage (during upfolding) is represented by ac_2 and bc_2 . Very important are E-W-striking hko_2 -lineaments reaching the absolute maximum in this zone. Zone 2 (Argille Scagliose and Macigno) show especially ac_2 , bc_2 and hko_2 formed by the younger deformation stage. The scattering of the maxima can be explained by the different competences of arenaceous and argillaceous beds. A last stage with 125° striking bc -traces seems to have been important in late orogenic block-faulting. In zone 3 (transgressive Pliocene sediments) the fracture traces are not statistically distributed, but the directions of the underlying Mesozoic rocks seem to penetrate through the younger sedimentary covering.

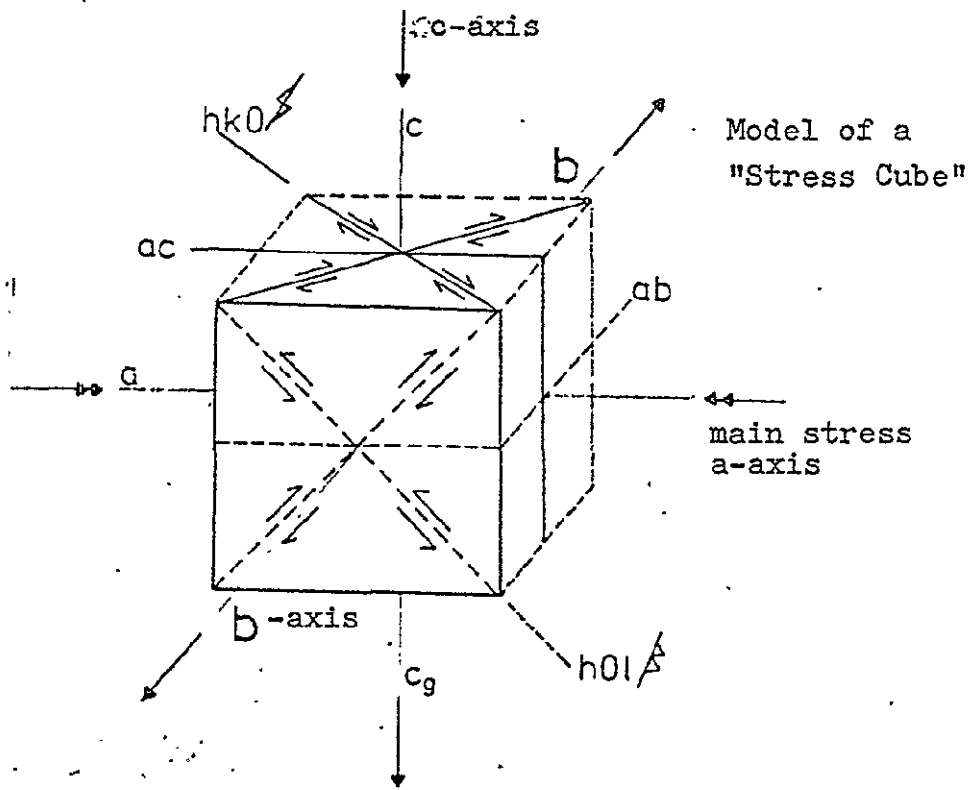


Fig. 22

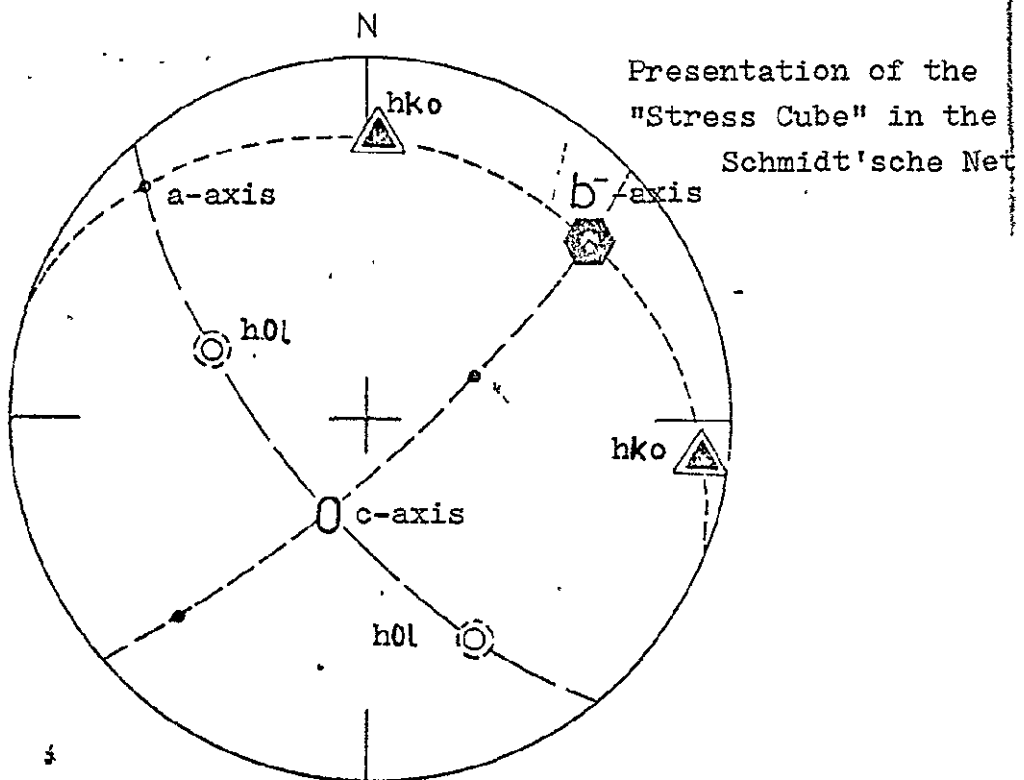



Fig. 23

5.4 Some Methodological Aspects on the Evaluation of Meso-Tectonical Measurements

Aproximately 1500 joints and 500 bedding planes were measured in the field. These measurements were plotted in pole-diagrams (equal area projections). Interpretation of the diagrams is based on theoretical principles developed by R. Adler et al. through intensive research in the coal district of the Ruhr Region, Western Germany. Adler found, by the measurement of several hundred points, that two deformation systems, corresponding to two deformation stages, always existed. In the younger stage, the older joints and faults are only revived, forming suitable angles to the new main stress direction. In the other case, totally new parting planes have originated. In addition to these two systems in most cases a third system is recognizable, caused by a special stress field in the surroundings of large scale faults. One aspect of the field work was to verify the influence of such large lineaments on the tectonic deformation system, as can be seen in LANDSAT-images.

Figure 22 shows an ideal stress-cube with the corresponding positions of the dividing surfaces. Figure 23 illustrates how a surface appears as a great circle in the equal area projection diagram (Schmidt Net). For statistical evaluations the use of the projection poles of the surfaces is more suitable since numerous great circles on a single diagram are disturbing to the interpreter.

The following symbols are used in the pole-diagrams:

	= ac		= hko
	= bc		= hol
	= ab		= ohl

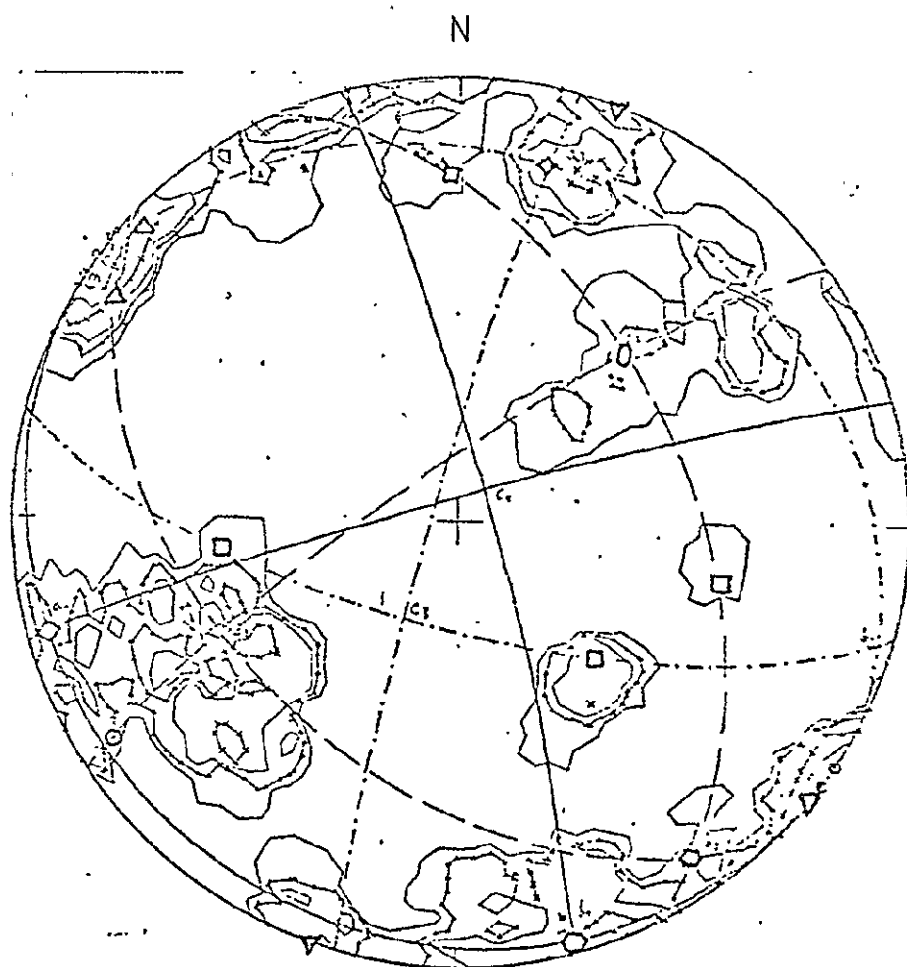


Fig. 24

Piazza di Siena, 166 joint poles

REPRODUCIBILITY OF THE
ORIGINAL PAGE IS POOR

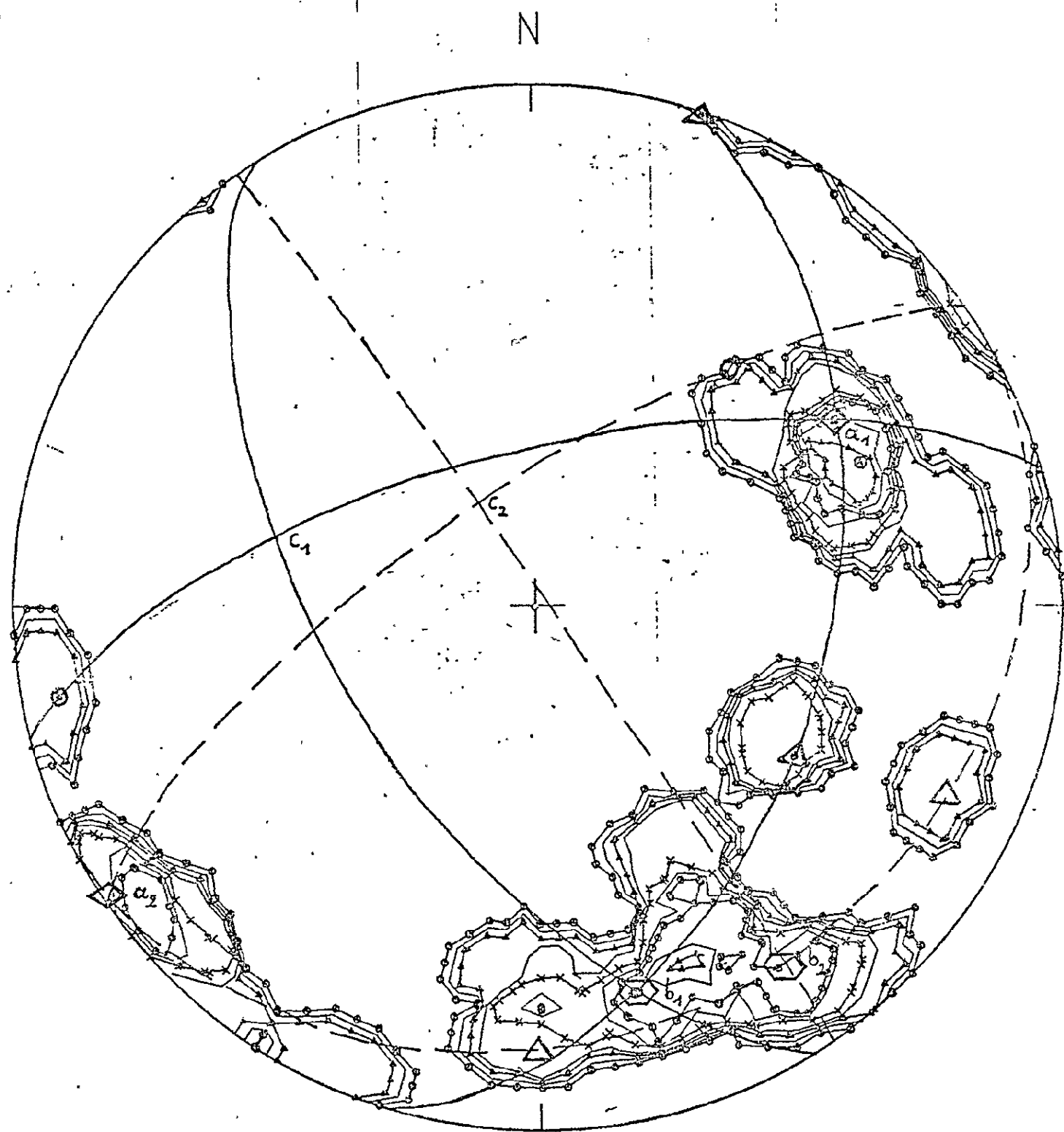


Fig.25

S. Pietro a.M., 44 fault poles

5.5 Tectonic Systems Derived from Pole-Diagrams

The following pole-diagrams (Fig. 24 - 26) are only 3 characteristic examples for the tectonic data, which were taken directly or photogrammetrically.

The joint-pole diagrams (Fig. 24,25) clearly show the existence of two deformation systems, characterized by typical configuration of parting planes, as follows:

System 1 is characterized by well-developed ac-fractures, whereas bc and hko are less important. Furthermore, hol and okl can be seen. The b-axes of the various diagrams have a strike between 166° and 170° . This fabric can surely be attributed to the stratification (ab great-circle representing bedding planes) and for this reason it must have been formed before folding.

On the contrary, the second fabric system is composed mainly of ab-jointing. Ac and hko are represented less or are totally lacking. On the other hand, hol and ab (in the massive Liassic limestones) are well-developed. The b_2 -axes show strike directions of $142-158^{\circ}$. They are identical with the β -axes of the bedding-pole diagrams, (Fig. 25) The above-mentioned characteristics of the b_2 -axes and the significant assembling of joints indicate the origin of the second fabric in a later deformation stage, during upfolding of the strata.

In addition to those two basic deformation systems, a special fabric can be related to important fault structures (thrust faults and horizontal faults). Such systems are defined by secondary shear jointing, as described in the introductory chapter.

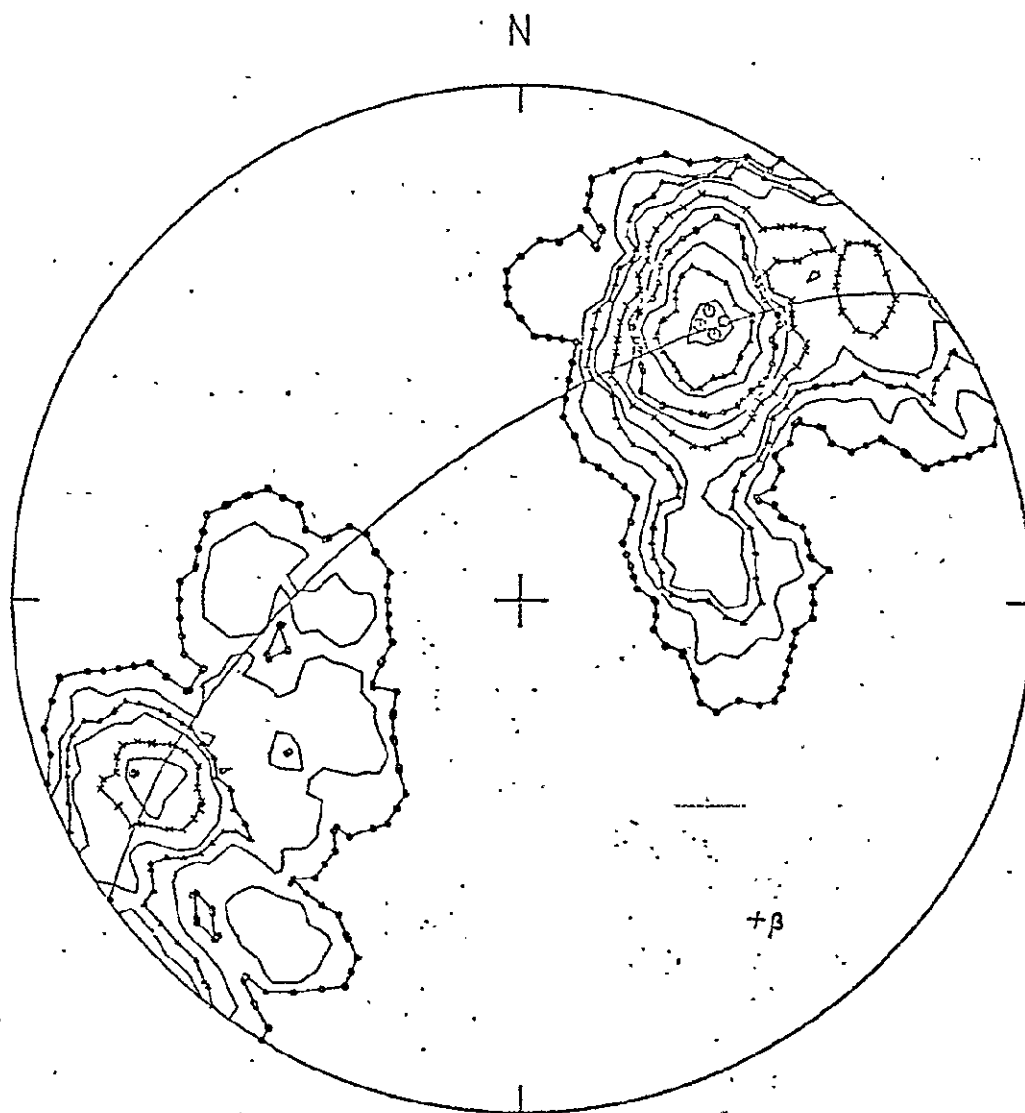


Fig. 26

Piazza di Siena, 160 bedding poles

The evaluation of the tectonics of the Northern and Central Apennines as described in the previous chapters is based on field work, interpretation of aerial photographs and satellite imagery. Aerial photographs and especially field work cover small areas. Therefore only, the synoptic view of the satellite images allowed to gain the results, which partly lead to new ideas on the tectonic systems of the Apennines.

The methods applied during this work are not only of scientific value but also give a basis for the exploration of tectonic controlled mineral deposits by satellite imagery.

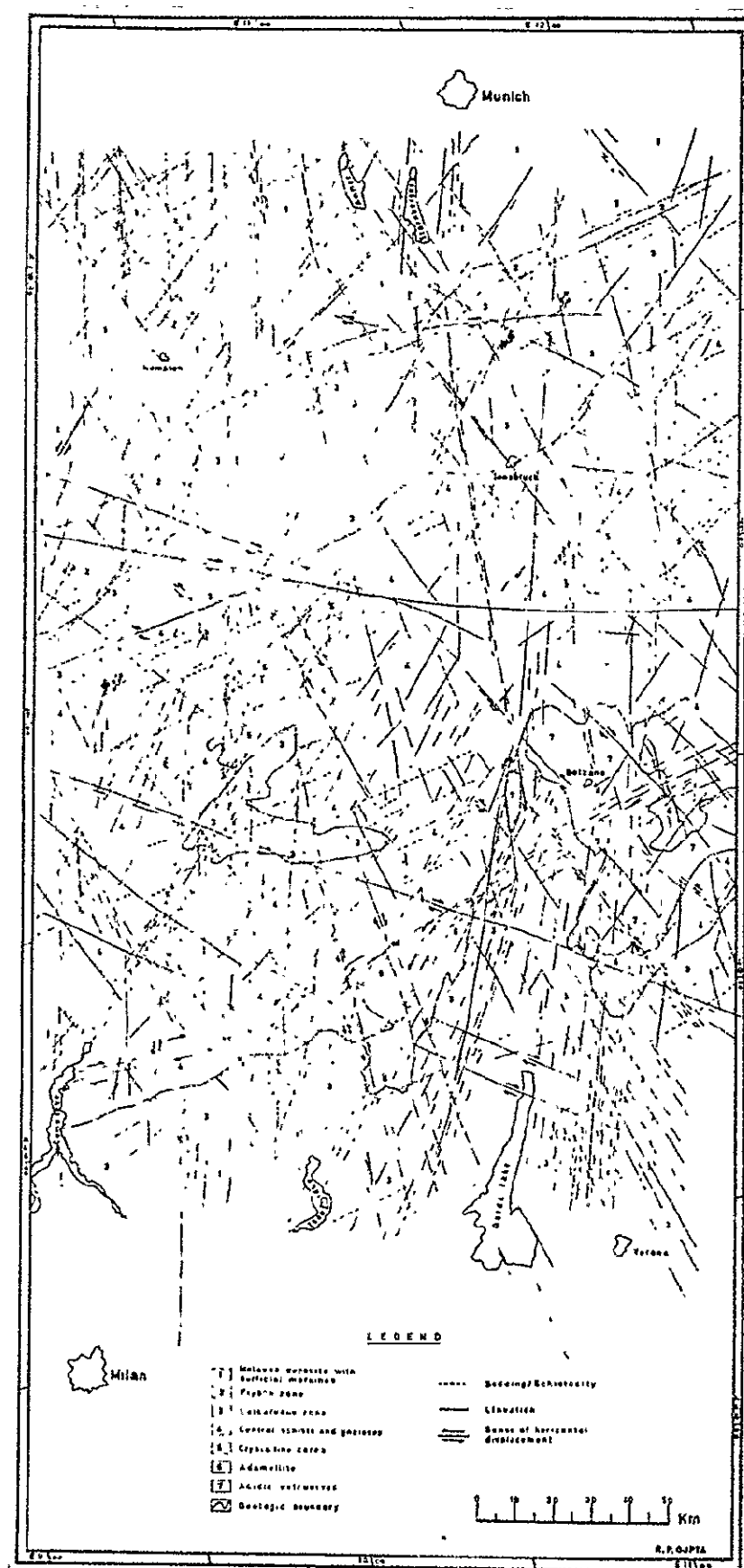
B) GEO-TECTONIC STUDIES IN EASTERN ALPS⁺

INTRODUCTION AND METHOD

A section across the eastern Alps has been analysed using the imagery from the LANDSAT-1 and 2. It has been shown, as a result of the present studies, that a great potential of these satellite images lies in delineating active movement zones of today. Presence of such movement zones along with their sense of movement can be deciphered, on the satellite images, by very accurate and detailed mapping of lineations and study of deformation of landform structures and river courses.

Conventional methods of photo-interpretation utilizing texture, tone and morphology, have been applied to these images for delineating faults and lineaments. ^(Fig. 27, 28) Special attention was paid to the trends and their deformation, if any, of the landform structures and river courses which has helped in deciphering direction of movements along the faults. For example, study of the courses of tributaries of the Adige river in the Bolzano-Merano region has indicated presence of an active fault (sinistral sense of movement) along the river valley. The main Adige river flows NW-SE in this tract. Tributaries on the eastern side of the Adige river turn southwards while approaching the main river, whereas those on the western side turn northwards, thus simulating a typical drag-effect (Fig. 29). The southwards turn of the tributaries on the eastern side may be accounted for also due to general loss of elevation southwards. However, the fact that the tributaries on the western side turn anomalously northwards - towards the region of general higher elevation and against the direction of flow of the main river - brings clearly out the presence of active movements along the Adige river valley in _____.

⁺ This work has been carried out by Dr. R. P. Gupta, guest scientist from the Department of Geology and Geophysics, University of Roorkee, India.



REPRODUCIBILITY OF THE
ORIGINAL PAGE IS 1000

Fig.27: Lineation map of the eastern Alps as interpreted from the LANDSAT-1 and 2 images

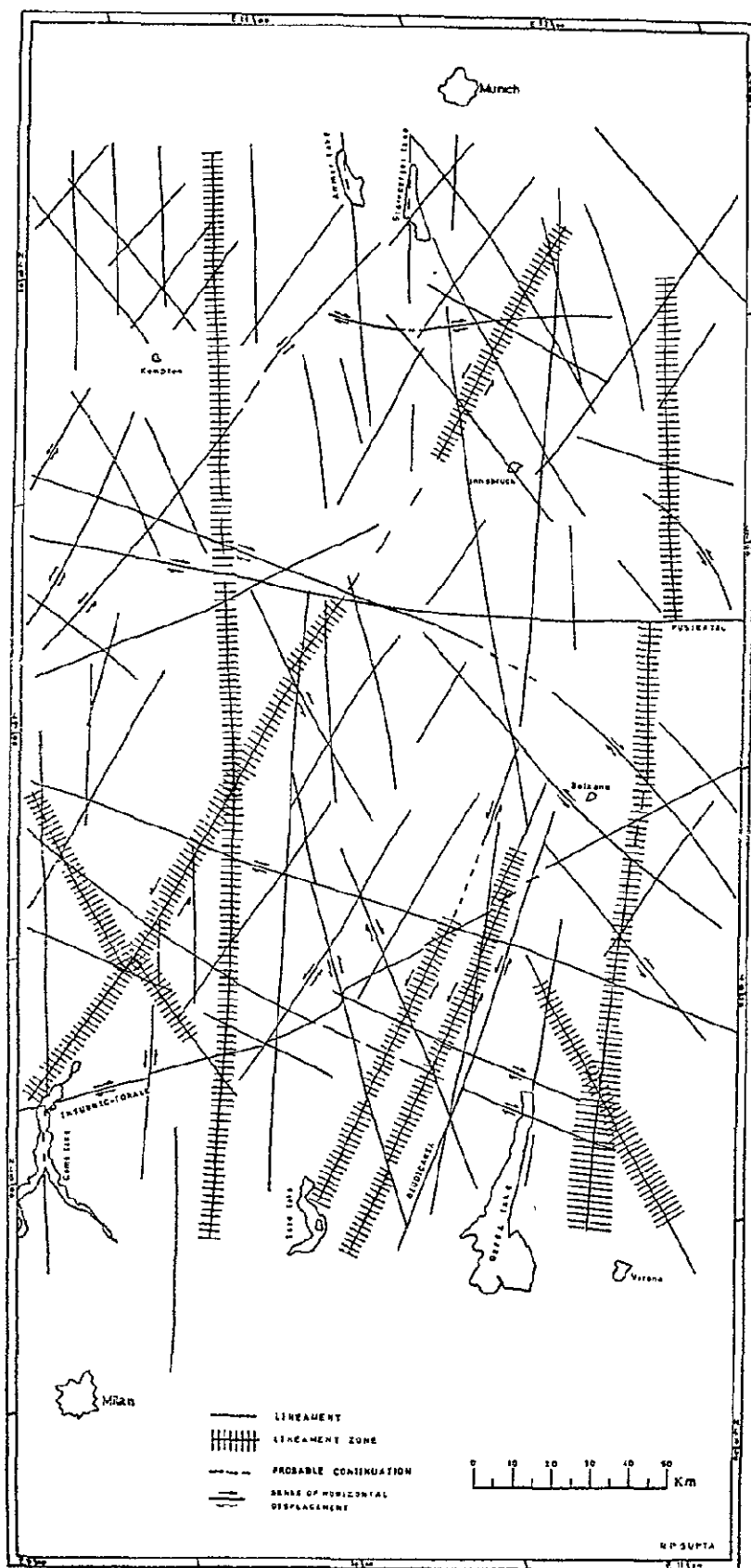


Fig.26 Major tectonic zones and lineaments in the eastern Alps

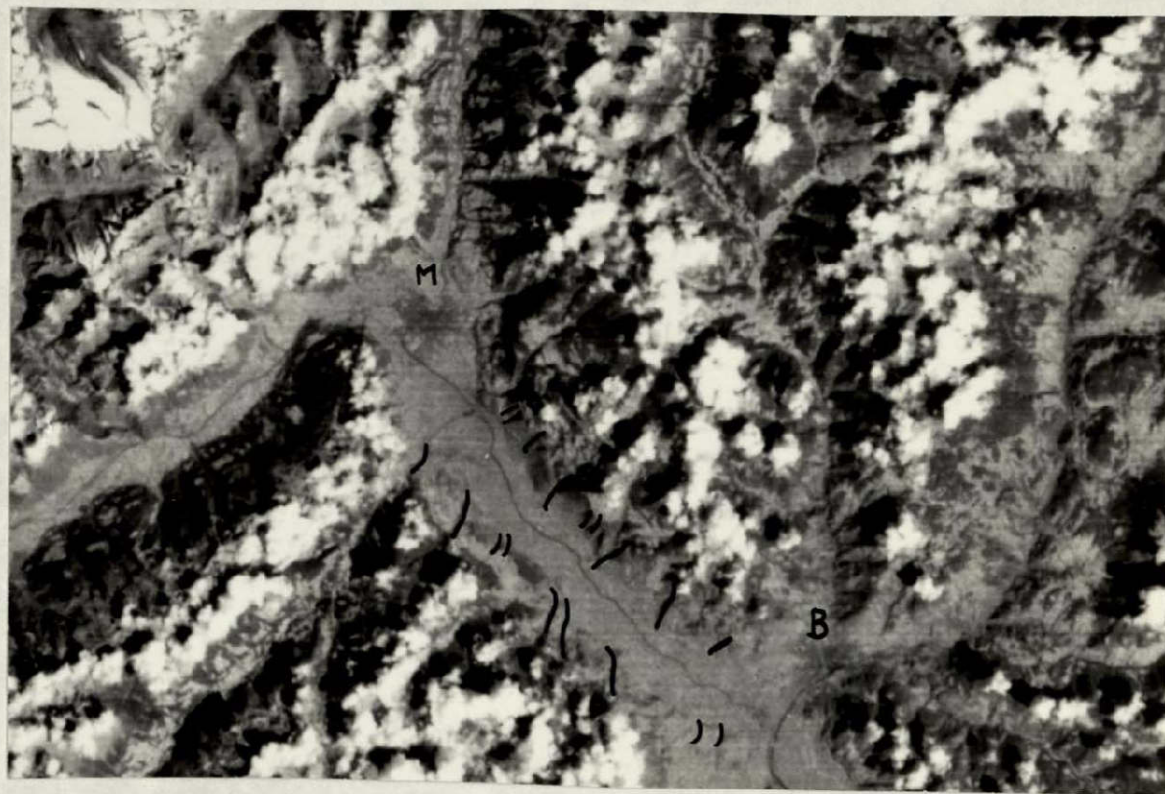


Fig.29:Turning of the tributaries indicating active sinistral faulting along the Adige river valley in the Bolzano (B)-Merano (M) region.
LANDSAT-1, dated 31.8.72, channel 7

this area, the sense of movement being sinistral. The lineament can be traced and extended in the mountainous tract on either side, on the imagery, where also movements with sinistral sense along the lineament are confirmed. It may be added here that as the satellite images provide vertical views, only horizontal movements can be deciphered on the images. However, the swampy areas occurring in the south-western part of the river valley in consideration indicate that the possibility of concurrent vertical movements with western block as downthrow side, is also not ruled out. Similarly, accurate detail mapping of photo-lineations representing geomorphological features has shown the presence of drag-effects pertaining to dextral movements along the Insubric-Tonale Line (Fig.30).



Fig. 30: Drag effects along the Insubric-Tonale Line suggesting movements with dextral sense.

LANDSAT-1, dated 7.10.1972, = 0,8 - 1,1

Interpretations have been made by superimposing observations on multi-time imagery. Images obtained on 13.8.72, 31.8.72 and 7.10.72 by LANDSAT-1 and those on 7.8.75 by LANDSAT-2 have been made use of. This, on the one hand, has helped in removing errors due to illumination conditions, such as position and angle of sun leading to shadows. (Bodechtel and Nithack, 1974), and on the other hand, has strengthened validity of the observations and interpretations therefrom.

RESULTS AND DISCUSSION

It is apparent (Fig. 27) that nearly all lineaments are characterized by several long to small en-echelon minor lineations constituting a zone. So, basically we have to visualize zones rather than planes such that each zone is comprised of numerous small to large parallelly arranged en-echelon minor zones and surfaces. Fig. 28 shows a generalized map with major tectonic zones and lineaments. A few of the lineaments are seen to be very extensive, being traceable from one end to other end of the investigated area and running across the entire section of the Alps. Some of the lineaments have been off-set by others. Besides, as mentioned earlier, several lineaments have been found to be active (Fig. 29, 30, 31). Results obtained in the present investigations render it necessary to make a special mention, among many others, of the Insubric-Tonale Line and Pustertal Line-- the two recognized major geotectonic boundaries in the eastern Alps (Fig. 31).

Insubric-Tonale Line : On the satellite images, this lineament appears to consist of a number of minor overlapping lineations and shows displacements along other intersecting presumably later lineaments (Fig. 27, 28). The present investigations, as shown (Fig. 30, indicate movements (dextral) along this Line. It is worthwhile to recall that Gansser (1968, p. 139) on the basis of field investigations in this region wrote about temptations to postulate lateral displacements and Laubscher (1971) based on palinspastic restorations involving the Dinaride Alps and the

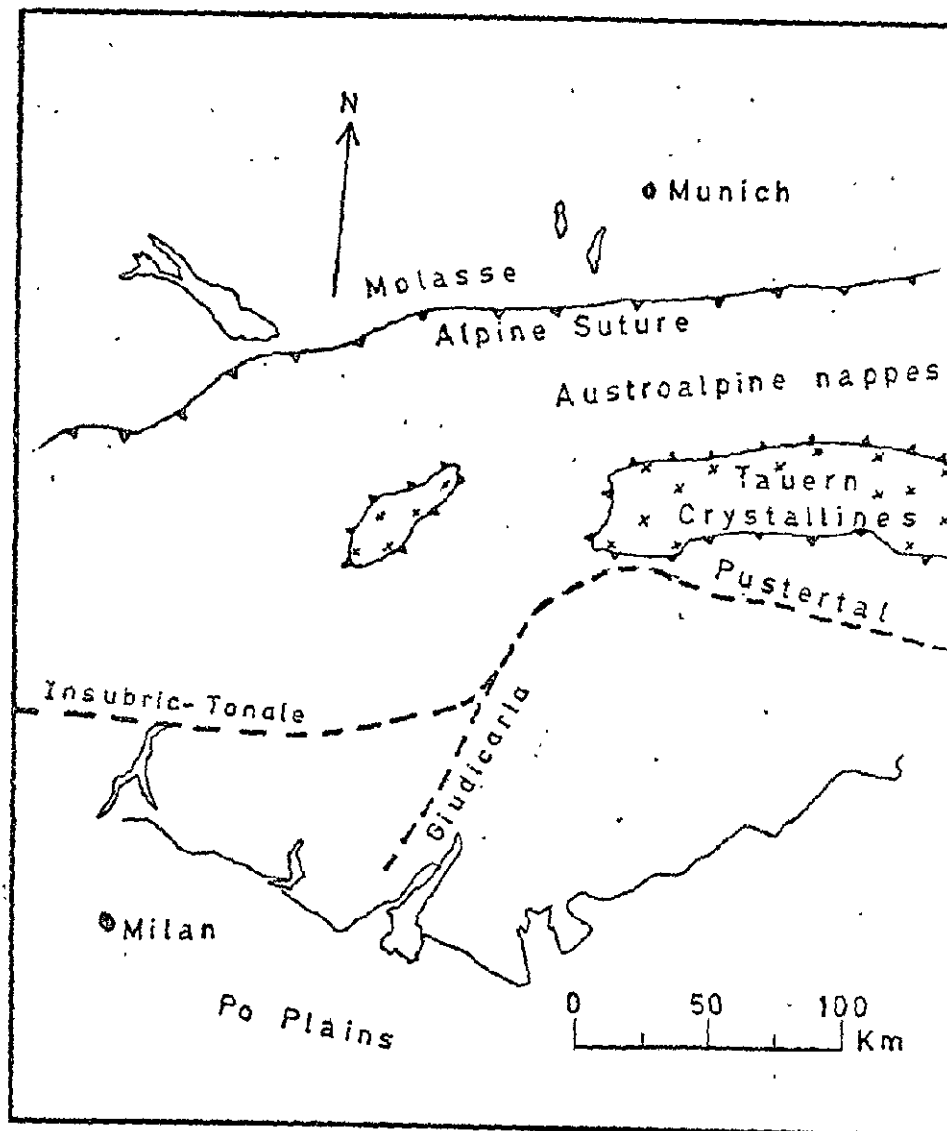


Fig. 31: Regional tectonic map

Apennines inferred 300 km. of post-Oligocene slip, both suggesting similar sense of displacement as deduced above (also c.f. Laubscher, 1973; Ernst, 1975^{a, b}). Further, the Insubric-Tonale Line is commonly shown to be abruptly terminated on the east by the Giudicaria Line (Fig. 31)

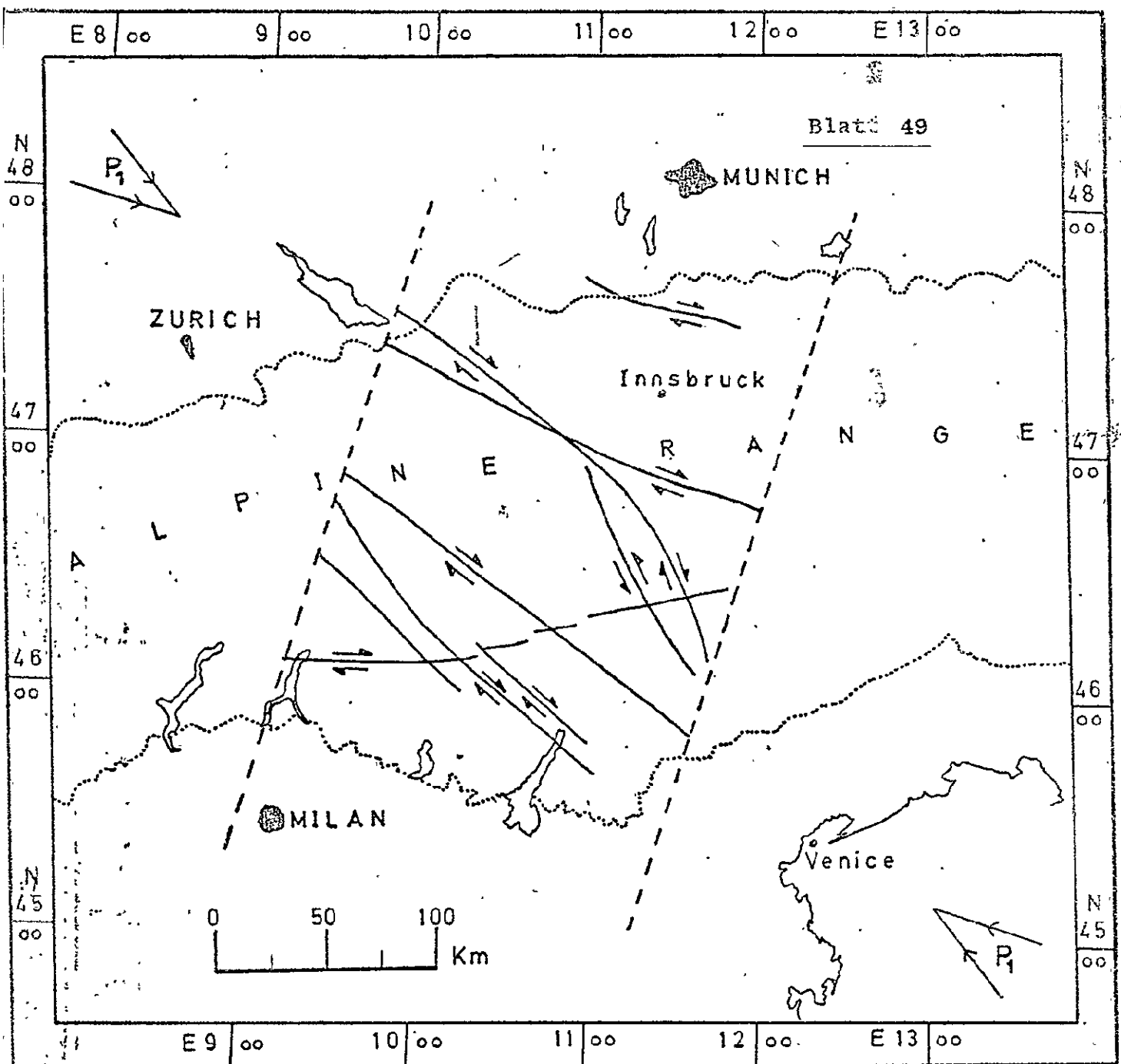
However, the present investigations indicate continuation of this trend in the acidic extrusives lying on the eastern side of the Giudicaria Line and the Adige river (Fig. 27). Though the intensity of development of this lineament in the acidic extrusives is not so pronounced, the mere presence is striking. In the geological past, the Insubric-Tonale Line, of course, seems to have been cut-short (or displaced) by the Giudicaria Line. However, later movements along the Insubric-Tonale must be postulated to explain its eastward continuation in the acidic extrusives. Further, though the seismic investigations have failed to record movements along this Line (in Gansser, 1968), the results of the present investigations that all along this Line the geomorphological features are aligned simulating drag effects, strongly suggest that this geotectonic boundary is still active or at least has been active in the recent past.

Pustertal Line: Similar to the Insubric-Tonale Line, the Pustertal Line is a major geotectonic feature (Fig. 31). The geological field mapping shows no indication of continuation of this Line into the area of present study and therefore it has been, by and large, considered to be abruptly terminated by the Giudicaria Line on the west. Continuation of this Line westwards across the Giudicaria Line was first detected on the ERTS-1 imagery by Bodechtel and Lammerer (1973). In the present study it has been further established that this Line constitutes a zone of active movements as accurate mapping of the geomorphological features adjoining this lineament on the imagery has revealed drag-effects with dextral sense of movement. Its westward continuation across the Giudicaria Line and presence of drag-effects indicate its later rejuvenation and still active nature (dextral). It may be of interest here to mention that on the basis of repetitive precise levelling measurements over time, active vertical movements along this zone at the rate of nearly 1 mm./year have been found by Senftle and Exner (1973).

System of Post-Alpine Faults - Relation to the Present Day Stress Field

An interesting feature is the presence of several W-E to NW-SE trending lineaments some of which have been neither mapped so far, nor could be visualized earlier (Fig. 27, 32). On the satellite imagery, they appear as rather unprominent fine lineaments which failed to make an impression during the first hand study for major lineaments. It was only during detailed analysis that their presence became clear and thenceforth has been confirmed on separate observations on both LANDSAT-1 and 2 images. It is important to note that it is not the case of an isolatory occurrence; on the contrary they appear to form a set and hence certainly demand attention. These lineaments are fine but extensive and cut across all earlier trends and boundaries thus indicating that they are post-Alpine in age. Often along their length they are marked with geomorphological evidences, in the form of drag-effects, indicating movements of evidently recent nature. Some of these lineaments partly follow the old major tectonic zones, like the Insubric-Tonale Line and the Pustertal Line, apparently extending and rejuvenating them. Further, a relation between these lineaments and the stress field leading to folding and uplift of the Alps (maximum principal stress at N 15-20, in this area, see page 51-53) is difficult to arrive at. On the other hand, it is easy to link these lineaments to the stress field of the present times. On the basis of in-situ stress measurements and fault plane studies of earthquakes, maximum principal stress of the present day stress field in central Europe has been found to be W-E to WNW-ESE (Ritsema, 1969; Illies, 1974, 1975; Ranalli and Chandler, 1975), which taking the intermediate principal stress to be vertical, would fairly well explain the development of these post-Alpine seemingly active zones of movements (Fig. 32).

REPRODUCIBILITY OF THE
ORIGINAL PAGE IS POOR



I N D E X

Section studied

Post-Alpine movement zones with
sense of horizontal displacement

Direction of the maximum principal
stress of the present day stress field
in Central Europe

Fig.: 32: Relation between post-Alpine movement zones
and the present day stress field

Predominant Lineation Trends - Relation to Stress Field

A trend diagram depicting relative predominance of various lineation trends observed on the satellite images of the area, is shown in Fig. 33. Clearly three major directions stand out: (i) N 45-225, (S_1); (ii) N 15-195, (T); and (iii) N 345-165, (S_2).

Out of these three lineation groups, the two S_1 and S_2 oriented at N 45° and N 345°, respectively are considered to be of shear origin and the third, T, trending N 15°, to be of tensile origin (all the three being of cogenetic nature) on the basis of following arguments:

(i) A number of movements planes are observed, oriented at nearly N 45° (fig. 27) and hence the lineation group S_1 is of shear origin.

(ii) The lineation groups S_1 and S_2 appear to form a conjugate set. Here a few additional remarks seem warranted. The pile of rocks involved here range from rather incompetent sedimentary deposits with surficial loose moraines to low to high grade metamorphics and crystallines (Fig. 27). Regional geology after Carte tectonique internationale de l'Europe, 1:2,500,000). Evidently, they have wide diversity in their failure characteristics. However, a corollary to the Coulomb-Navier criterion for shear failure widely applied to rocks (c.f. Anderson, 1951; Farmer, 1968; Price, 1959, 1966) states that under normal stress conditions the dihedral angle of the shear fractures (2θ) is related to the coefficient of internal friction (μ) as follows:

$$\tan 2\theta = \pm \frac{1}{\mu}$$

$$\text{or: } \theta = \pm \frac{\pi}{4} \pm \frac{\phi}{2} \quad \text{where } \phi = \tan^{-1} \mu$$

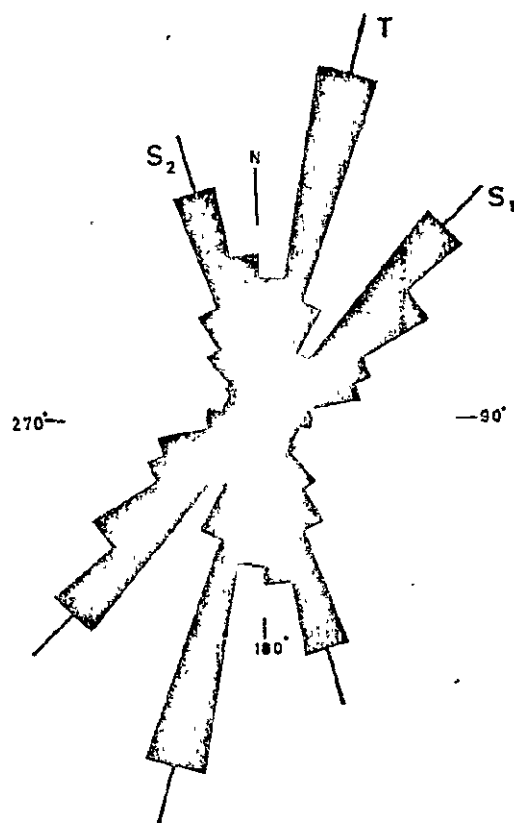


Fig. 23: Trend diagram of lineations

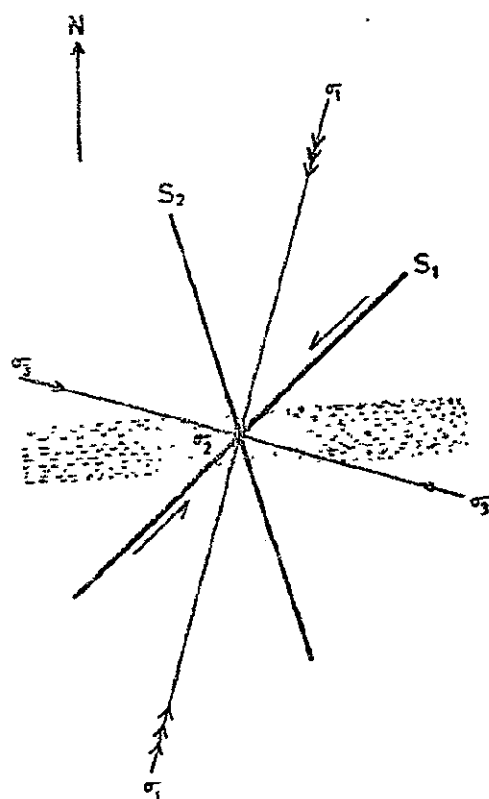


Fig. 34: Preferential sinistral movements
on the NE-SW trending lineaments

REPRODUCIBILITY OF THE
ORIGINAL PAGE IS POOR.

For most natural rock substances the angle of coefficient of internal friction (ϕ) being around $30-45^\circ$, the dihedral angle (2θ) ranges around $45-60^\circ$, which is in conformity to the angle between S_1 and S_2 (taking intermediate principal stress to be vertical). Further, the above relation between the dihedral angle and the coefficient of internal friction implies that the dihedral angle increases with decreasing frictional resistance. This feature seems to be corroborated in the present study as the S_1 and S_2 lineations seem to widen out towards the northern tract from the central parts of the Alps (fig. 27). This "refraction" observed in this area, is attributable to the decreasing competency of the medium, as the northern tract is underlain by largely molasse and surficial moraine deposits and the central mountainous range is underlain by competent sedimentary and crystalline rocks.

(iii) A third set of lineament (T) is oriented at $N 15^\circ$. Few displacements are noted parallel to this set. On the other hand, many of the larger lakes are observed to lie along this set of lineament, for example, Starnberger Lake and Ammer Lake in the North and Garda Lake (?) and Como Lake in the South (fig. 27). Further, this trend ($N 15^\circ$) coincides with the direction of maximum principal stress as derived from the orientation of S_1 and S_2 conjugate shear sets. Therefore, it seems logical to conclude that the lineament set T has cogenetically developed as a result of tensile failure.

Hence, the above interpretations that the S_1 , S_2 and T groups of lineaments have cogenetically developed and that S_1 and S_2 are of shear origin and T of tensile origin, are well-interknit and appear to be logical. It is interesting to find how the direction of maximum principal stress deduced as above from the lineament analysis of Alpine section compares with that independently inferred for the adjoining areas by other workers. A major geotectonic

feature adjoining the Alps is the Rhinegraben system, considered to be more or less contemporaneous with the Alpine orogeny. The Rhinegraben trending NNE-SSW, evidences crustal dilation normal to the graben axis, of about 4.8 km. and an average direction of maximum principal stress of about $N 20^{\circ}$ (NNE) must be concluded for the beginning of rifting in Middle Eocene times (Illies, 1974, 1975). This is in striking conformity to the direction deduced as $N 15^{\circ}$ from the above lineament analysis for the Alpine section. Further, the above inferences regarding average direction of maximum principal stress in late Mesozoic - early Tertiary times from the macrotectonic observations are corroborated by the results of statistical evaluation of field measurements on horizontal stylolites in unfolded Mesozoic platform sediments, made all over Central Europe (Beiersdorf, Wagner, Wunderlich and Plessmann, in Illies, op.cit.)

The presently concluded situation that the then prevalent maximum principal stress seems to have been not perpendicular (and hence the minimum principal stress not parallel) to the general trend of the rocks in this Alpine section needs explanation. It seems that this abnormality ^{has} been caused by the presence of a hindering block on the south-east. The alternative possibility is by postulating two different phases of deformation, the first phase (with average maximum principal stress trending $N 35^{\circ}$) bringing about the regional folding and uplift of the Alps, followed by a second phase (with average maximum principal stress oriented at $N 15-20^{\circ}$) causing largely translational movements, shearing and faulting but retaining the pre-existing strike trends. The author tends to favour the first possibility as separate phases of folding and faulting are difficult to visualize. Often the two phenomena are found to be concurrent and closely associated with each other. If the main phase of deformation had maximum principal stress at $N 35^{\circ}$, the related tectonic impressions which would have been of the same degree of magnitude and intensity, should have been visible and thus borne evidence to that. Further, uplift of the Alps associated with northwards movement of the Adriatic block

has been long postulated (for example, Aubouin, 1964) and the same block, which lies to the south-east of the area, could have also provided the hindering resistance referred to above. Besides, the presence of such a block would be further in conformity to the observed predominance of NE-SW (S_1) lineations with sinistral sense of horizontal displacement, described below.

S_1 Lineations and the Giudicaria Line

A striking feature is the large number of NE-SW trending lineations (S_1) with predominantly sinistral sense of movement, observed throughout the region of study (Fig.27). They are developed with varying intensity in the area and are more prominently developed in the vicinity of Giudicaria Line. From field investigations Trevisan (in Laubscher, 1973) reported the large system of NE-SW trending sinistral faults in Giudicaria. Evidently , intense development of S_1 set of shear planes and zones seems to have controlled the development of Giudicaria Line.

The reasons why movements have taken place largely on the S_1 -set of shear surfaces and not on the S_2 -set and that too with predominantly sinistral sense are also clear. The general strike of rocks is N 75-80° (Fig.27). The maximum principal stress has been concluded to be directed at N 15°, giving the conjugate set of shear surfaces at N 45° (S_1) and N 345° (S_2). Thus, the shear surfaces S_2 trend nearly perpendicular to the general strike of rocks whereas those of S_1 -set make acute angle (30-35°) with the latter (Fig.34). In such a state, movements on the S_1 -group of surfaces, with sinistral sense, would be evidently preferred.

CONCLUSIONS

On the basis of above studies on LANDSAT-1 and 2 images of eastern Alps, the following broad conclusions may be drawn :

- (a) A number of W-E to NW-SE trending post-Alpine active lineaments are present, These lineaments can be logically related to the present-day stress field.
- (b) There are three dominant lineation-sets in the eastern Alps. They have co-genetically developed as a result of shear and tensile failures, due to stresses with maximum principal stress averagely trending N 15°.
- (c) The Giudicaria Line seems to have been controlled by the NE-SW trending lineaments over which movements with sinistral sense have been preferred.

It goes without saying that as the satellite images provide very accurate map of ground features, a great potential of these images lies in their detailed and accurate mapping. This can unearth valuable information of local and regional importance, unobtainable from any other source.

C APPLICATION OF LANDSAT DATA FOR LAND USE MAPPING BY CONVENTIONAL INTERPRETATION TECHNIQUES

For many earth scientific activities; land use maps form the basis for further planning and inventory preparation. Very often the existing land use maps are more than 20 to 40 years old and do not correspond any longer to the existing situation.

In order to prepare a land use map on a conventional basis, many man-years are necessary to conduct intensive field work and supporting aerial photointerpretation. The Italian authorities are faced with the problem of producing new land use maps of the mountainous regions on a scale of 1 : 500'000. Especially in mountainous regions, the cost factor has always been a severe constraint, hampering completion of this project. Preliminary evaluations of LANDSAT-data, has indicated the high potential of multi-spectral satellite data and its suitability for land use mapping. On the basis of our background experience in aerial photointerpretation and satellite data evaluation techniques, we approached this problem by determining the feasibility of vegetation mapping through application of conventional interpretation techniques to LANDSAT-data. The tasks seem to be solvable with respect to the small scale and the few main or level one categories that have to be determined. The different categories of interest are:

1. barren land (rocks, gravel)
2. permanent snow cover, glaciers
3. urban areas (including industrial areas and larger transportation patterns - streets)
4. pastureland (areas covered by grass)
5. agricultural areas (including plantations)

6. forested areas

7. water bodies, rivers and lakes

1. Data Source

LANDSAT-1 MSS images taken during '72 and '73 were used as the data source. The nine inch negatives (scale 1:1.000.000) were photographically enlarged on a scale of 1:250.000. For most of the areas the information loss acquired through repeated photographic processing of the images did not interfere with the detection of level 1 categories. For some key-areas a direct production of images from tape were carried out by PRAKLA-Company. These images, showing maximum information of the MSS data, were generated on a scale of 1:200.000. Furthermore for some middle Italian and Sicilian areas Skylab photographic data in panchromatic and false colour were produced. By this means a total cloud-free-coverage of the areas of interest was obtained.

2. Evaluation Techniques

2. 1. Background Information

The basis of any photointerpretation is not only the experience of the interpreter, but also detailed background information. The background information for our project consisted of:

- a) existing land use maps on a scale of 1:200.000, produced 20 - 40 years before
- b) existing field data obtained through intensive field investigations of the last ten years
- c) detailed vegetation profiles.

Information gained through field work proved to be the most actual information and could be utilized with high confidence.

2.2. Interpretation Key

2.2.1 LANDSAT-1 multispectral scanner data

For conventional photointerpretation there are no significant differences of information between MSS 4 and 5 and between MSS 6 and 7.

On the other hand MSS 5 and 7 show the best contrast of grey tones in vegetated and non-vegetated areas. Therefore images of these two bands were chosen for the land-use mapping.

From an earth scientific point of view, the utilization of data representing different vegetation cycles would be the optimum.

This requirement could not be fulfilled over all areas because of insufficient continuous data. It turned out that for the production of a preliminary base map, channel 5 was optimally suited. Band 7 was utilized in order to obtain additional information for discriminating various types of surface features. So, for example, the use of band 7 allows for the separation of coniferous forest from mixed forest, the better delineation of agricultural areas and the clear identification of barren land. For the level 1 classification the sensitivity of band 7 to soil moisture has been somewhat disadvantageous.

The diagrams of figure 35 represent a qualitative comparison of grey tone classes obtained from band 7 and 5. In the coordinate-system the land use categories were plotted as a function of their grey tone in both channels. It is evident, that such schematic representations only gives a very rough idea about the principles of evaluation. Of course such diagrams do not reflect the experience of the interpreter, his ability to differentiate subtle grey tones or his analytic ability under various environmental conditions. Furthermore both diagrams do not express important criteria such as texture and morphology and also the synoptic knowledge of the geological conditions. An interpretative decision can be made by a combined analysis of all criteria, as shown for grass in figure 36 .

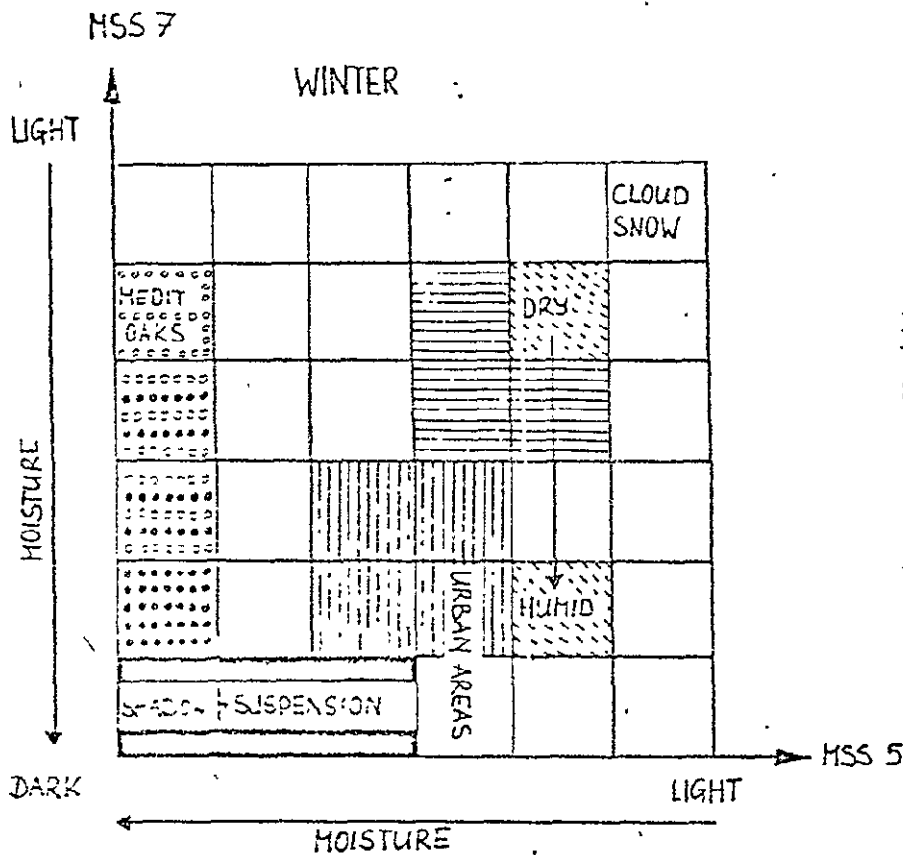
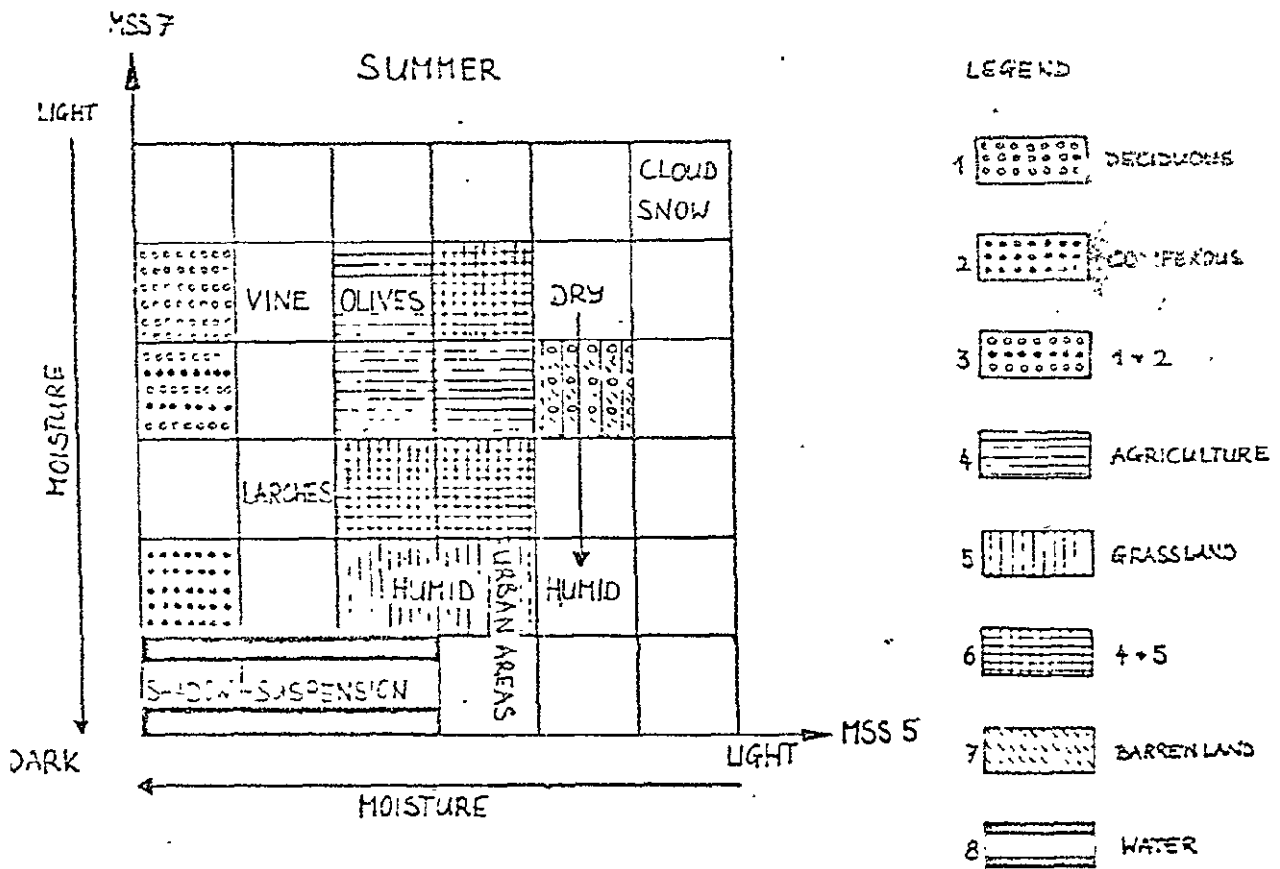


Fig. 35

Schematic position of land use categories in a coordinate system based on the grey tone in images of MSS 7 and MSS 5

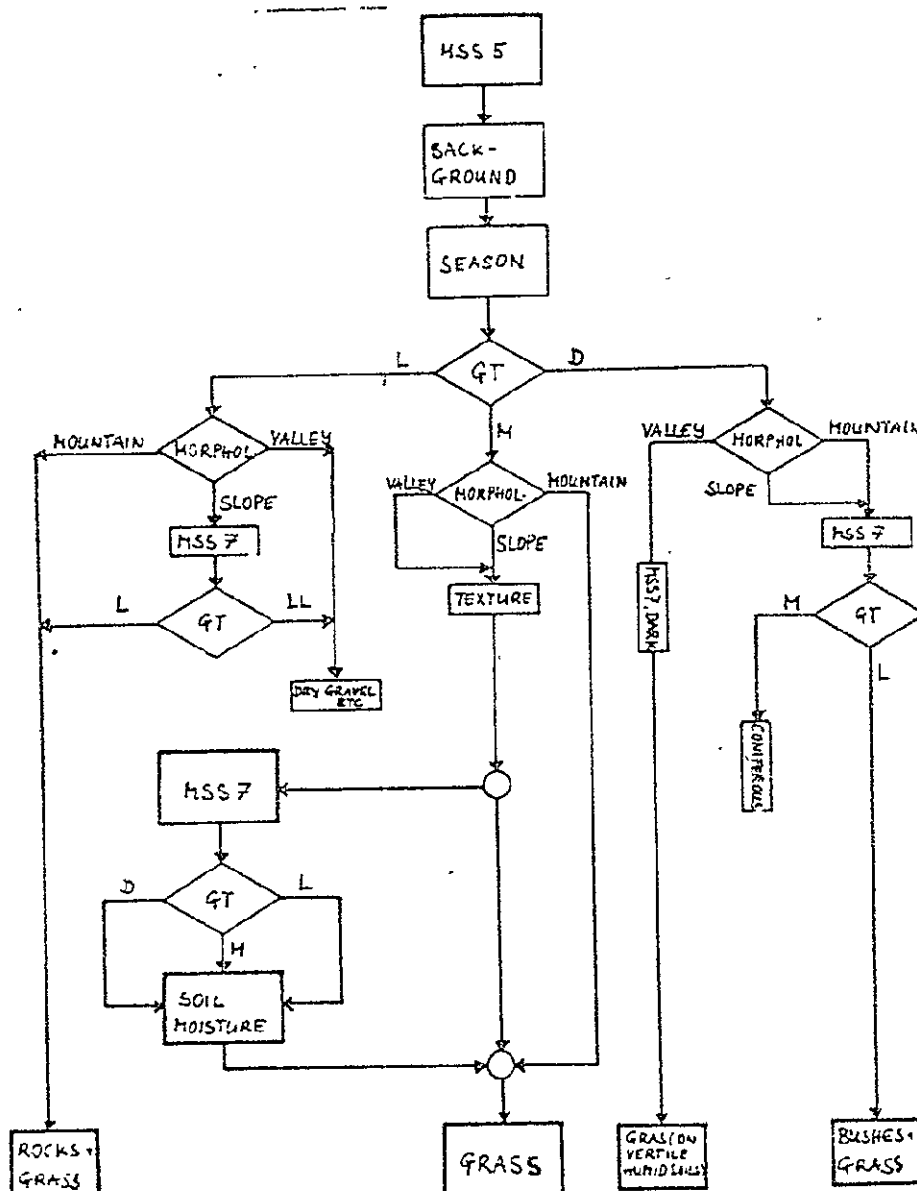


Fig. 36

Identification of grass land

Schematic diagram for the interpretation of LANDSAT MSS-data

(Legend: GT = grey tone, L = light, LL = very light,

M = medium, D = dark)

2.2.2 Skylab data (colour and false colour images)

Colour photographs of Skylab (for example 190 a, taken in September 1973), were projected on a scale of 250.000. Due to the outstanding colour quality of these images, the following surface features could be clearly identified: forested areas, agriculturally used areas, grassland and barren land. False colour composites of Skylab data and also of LANDSAT-1 MSS data served as basic information for differentiation areas with grassland from agricultural use regions. The determination of borders between those two features has been very difficult with black and white images taken during late autumn, summer or winter. During these seasons, the fields are not planted or are already harvested. In relatively dry areas grassland and agricultural areas appear in relatively unidentifiable grey tones when the field patterns are far below the resolution capabilities of the sensor system. The only reliable criterion for differentiation is a distinct red colour represented in false colour images.

2.3 Gray Tone and Colour Tone

In respect to the physical properties, various surface features reflect incoming radiation in different intensity levels. The reflection intensity is translated on photographic data into a gray or coloured tone. Therefore the photographic density is one of the most important interpretative criterion. In addition, the density is very sensitive to uncontrollable factors, caused by natural phenomena or by photographic processing techniques.

2.3.1. The Impact of Natural Parameters on the Photographic Density

In general pictorial representations of our earth surface are a combination of all possible factors of which the image density only plays one part. Problems arise concerning the identification of surface features, regarded to be homogeneous from any earth scientific point of view. This is due to the fact that such a homogeneity does not necessarily correspond to a homogeneous distribution of gray tones. Therefore in order to decide whether to deal with category a or b, further decision-making criteria have to be introduced. So for example, a well cultivated fertilized medium humid meadow may have a darker grey tone than an uncultivated grassland under the same environmental conditions. Grassland in an Alpine valley, for example, has a different grey value from grassland in a south Italian Apennine valley. Grass growing on clay has a different dark grey tone than grass on limestone. The grey tone, the intensity of reflections, is mainly dependent on natural factors such as soil moisture, soil type, climatic zone and local climate. The image, figure 37, represents some of the basic relationships between environmental parameters and grey values. Another important factor, not taken into account, is the exposure of the surface to an illumination source - the Sun. In areas with great relief the identification of surface features is extremely difficult, not only due to the shadows themselves, but also to the change of the relative sunangle. Another important factor is the changing state of vegetation during the year, i.e. the change of reflectance depending on the seasons. Therefore multitime imagery allows better identification and further differentiation of land-use categories.

2.3.2. Impact of Technical Factors on the Photographic Density

The main technical factors influencing the density of images are related to the image generation itself.

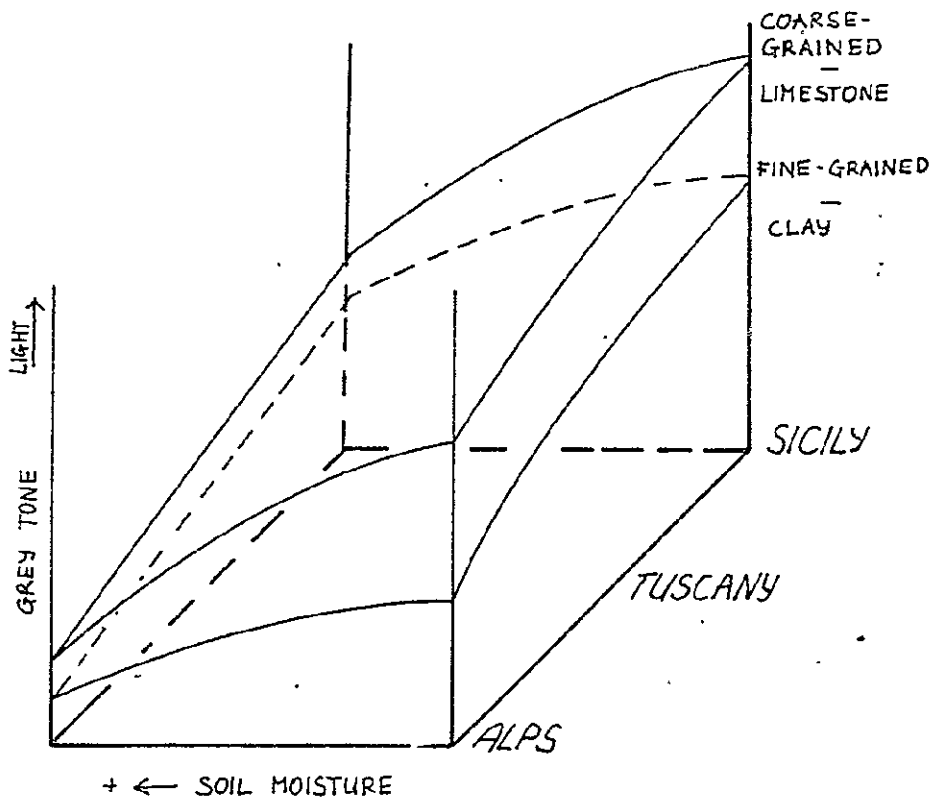


Fig. 37 Grey-tone levels of grass

Schematic representation for the factors soil,
soil-moisture and climatic zone

Concerning the generation of images from a digital tape, restrictions result from the dynamic range of the output device. The equipment used for data generation has an overall dynamic range of 16 grey levels. In comparison with the theoretical performance of the MSS scanner, with a dynamic range of 128 (MSS 5) and 64 (MSS 7) grey levels, the applied generated images represent reduced information. In order to minimize this effect the available interval of 16 grey tones was adapted to the actual sensitivity range of the scenes. In order to obtain maximum grey resolution for the areas of interest, the adaption was carried out on scenes that did not show maximum reflective contrasts, such as snow and water, in infrared images. A second important parameter which influences the quality of the film material is the degradation effect resulting from photolab processings

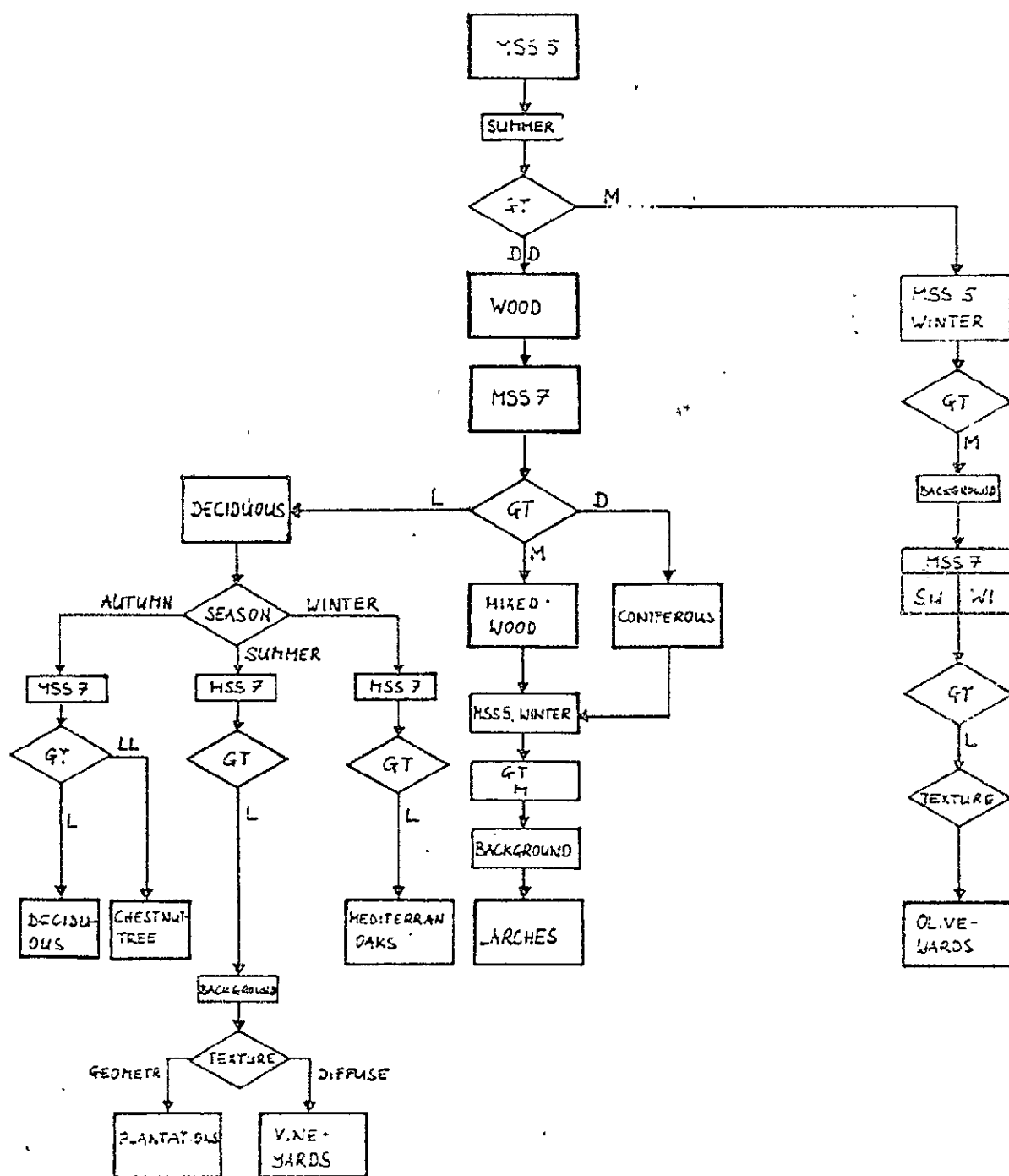


Fig. 38

Identification of wooded areas

Schematic diagram for the interpretation of LANDSAT MSS-data

(Legend: GT = grey tone, L = light, LL = very light,
M = medium, D = dark, DD = very dark)

such as enlarging etc. During these processes the grey tones are influenced by the various film emulsions, by various exposure times and by the state of the chemical ingredients.

Another degradation effect which occurs mainly in channel 7 is caused by the high contrast between water and land masses. The extreme dark water areas interfere in such a way that the coastal areas always appear in darker grey tones. The above-mentioned photographic factors may especially degrade the possibilities and the accuracy of conventional photointerpretation techniques. In other words the interpreter has to revise his interpretation results not only from image to image but also within the evaluation of one scene.

3. Possibilities and Limitations of the Conventional Classification

The possibilities of identifying surface features is extremely dependant on the resolution capabilities of the sensor and on the target size. Figure 38 demonstrates to what degree under optimum conditions, the differentiation of trees can be made. With regard to trees or tree-cones, two points have to be taken into consideration. With respect to the resolving power to the multispectral scanner, larger areas with a dense tree population can be identified as uniform reflecting areas. It is understood that with a dense population of trees there is no interfering reflection from the ground. Furthermore because of the poor resolution of the satellite data, the differentiation between bushes and forests, can not be made.

Furthermore conventional definition based on the percentage of trees within a certain area can not be made.

To a certain degree, grey tone and background information enable the interpreter to map areas with different densi-

ties of wood. But the geometric resolution of LANDSAT-1 images does not allow to map woods by quantitative measurements of percentage of trees per area. Therefore areas with for example 10 % trees, which are conventionally defined as wood do not appear on the evaluated land-use map.

Further difficulties arise when comparing forsts and plantations. Densely planted hazels agrumenplantages and vineyards have the same reflection characteristic as deciduous forest, at least for the eye. A basic local knowledge and the experience in examining textural information may sometimes help to overcome above-mentioned difficulties.

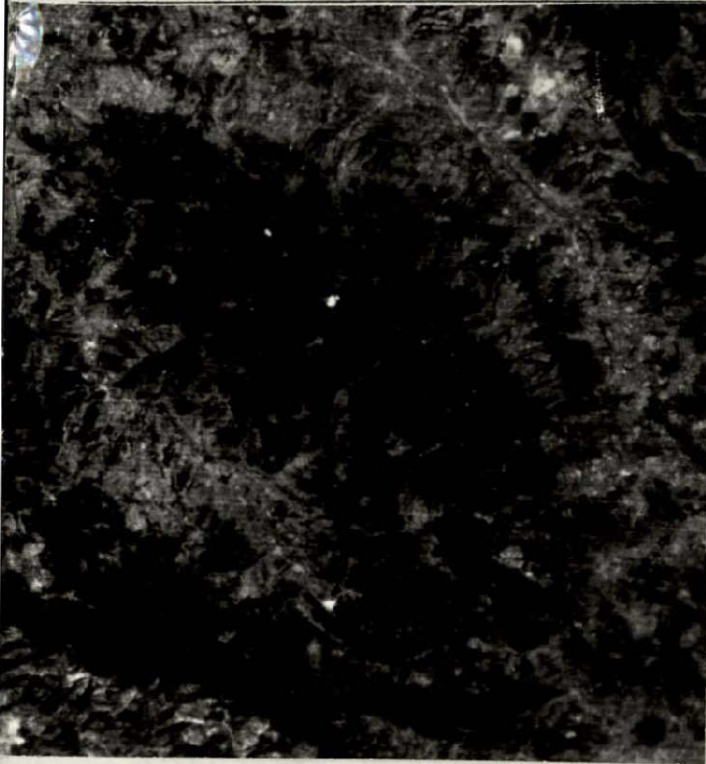
Plantations, for example, are very often characterized by geometric borders, and in contrast, vineyards often show a kind of chaotic texture.

Cultivations with clearly separated rows of plants such as oliveyards are characterized by a uniform medium grey value. These grey values are originated by intensities reflected from the ground coverage and the foliage of the trees. The following images demonstrate areas with plant units which have characteristic signatures. Figure 39 shows coniferous and deciduous forest near Pratomagno, mountains south east of Florence, figure 40 mediterranean oaks in the Apennine west of Rieti, figure 41 oliveyards of the Tuscany, figure 42 an area with bush and grassland near Valle Taleggio (Bemgasc Alps).

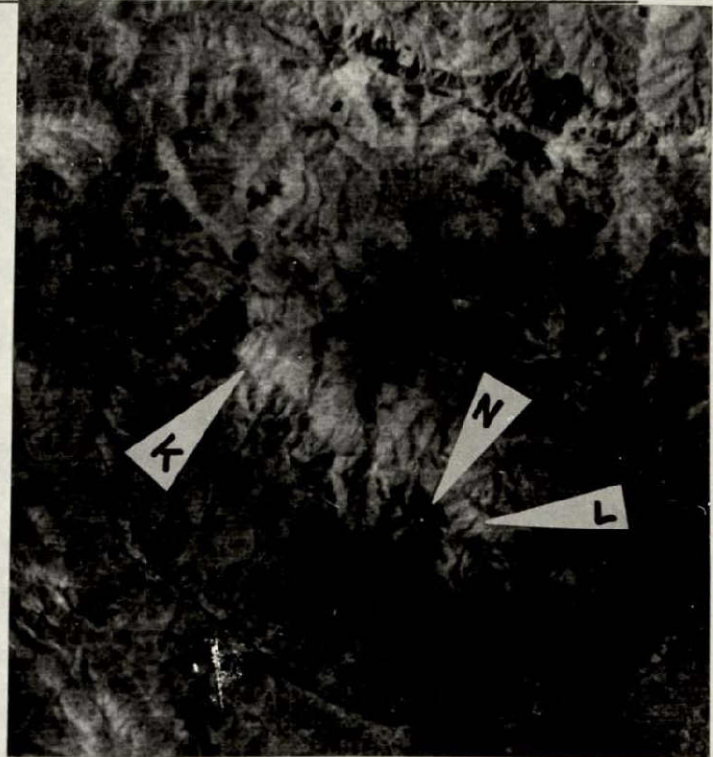
Especially the last example (fig. 39) indicates the difficulties which result from the poor geometric and spectral resolution of LANDSAT-1-images.

Areas with mixed reflections are very difficult to classify without knowledge of the local conditions. Normally in such cases textures can not be detected any more and the surfaces

appear rather uniform. The limitations of differentiating between various surface features becomes evident if we are looking at interface regions between meadows and areas with dried-out grass and barren rocks. Barren rocks are clearly detectable but a distinct tracing of the border between the grass land and areas without vegetation is impossible.



a)



b)



REPRODUCIBILITY OF THE
ORIGINAL PAGE IS POOR

c)

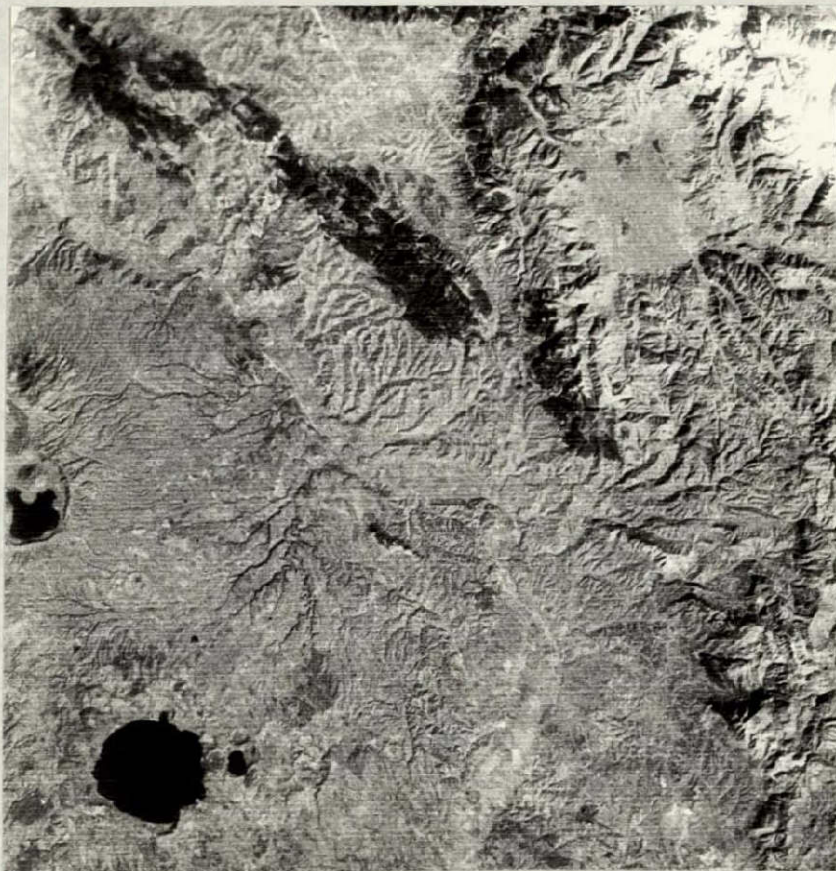
Fig. 39

Pratomagno Mountains (detail from LANDSAT-1 image of 12. Aug. 1972)

a) MSS 5 (dark = wooded areas)

b) MSS 7; light = deciduous wood (L = in general, K = chestnut)
dark = coniferous (N)

c) Ground truth photograph, showing coniferous (dark) surrounded
by deciduous wood



a)



b)

Fig. 40:

Mountain ranges west of Rieti (detail from LANDSAT-1 image of 6.Feb. 1972)

a) MSS 5 (dark = mediterranean oaks)

b) Ground truth photograph taken in June 1973 near Amelia.

Dark = mediterranean oaks



Fig. 41:

Lower valley of the Cornia
River, east of Piombino
(detail from LANDSAT-1 image
of 12 Aug. 1972)

MSS 5: dark = woods
middle grey = olive yard
(arrow)

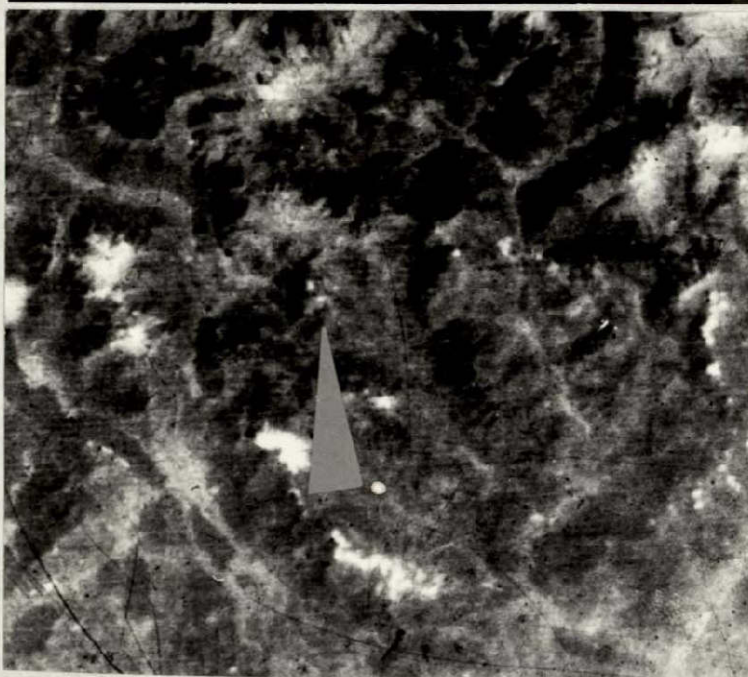


Fig. 42:

Valle Taleggio (Bergamasco
Alps)

LANDSAT-1, MSS 5, 7.Oct.1972

(a) does not show the distinct
vegetation pattern as the
ground truth photograph (b)

a)

b)



REPRODUCIBILITY OF THE
ORIGINAL PAGE IS POOR

Discussion of the Results

The possibilities of conventional interpretation mentioned above base on extreme situations. With respect to the 7 level I categories the results are good.

Mapping of Land-Use Categories

The land-use classification followed the USGS-system which ANDERSON, HARDY & ROACH (1972)* established for the interpretation of remote sensing data.

For our special problems there was introduced the level I category "grassland", which in the USGS-system belongs to "agricultural land", if it is pasture, and to "range land" if it is uncultivated.

The following table (Fig. 43) shows to which degree LANDSAT and SKYLAB images can be used for mapping land-use categories of level I and II. The table is based on our experiences during this work and therefore is valuable for European mountainous regions.

Good satellite data and good background information enable the interpreter to subdivide the level I categories no. 2, 4, 5 and 6 in level III and IV categories. The following schemes show these subdivisions, which are not included in the above USGS-system.

* J.R. ANDERSON, E.E. HARDY & J. T. ROACH: A Land-Use Classification System for Use with Remote Sensing Data. - Geol. Surv. Circular, 671, 1-16, Washington 1972

LEVEL I	LEVEL II	LANDSAT MULTISPECTRAL	SKYLAB IMAGERY
1) BUILT UP LAND		++ o	++
	Residential	+	+
	Commercial	+	+
	Industrial	+	+
	Communications	+	+
2) AGRICULTURAL LAND		+++ o	+++
	Fields	+++ o CIR	+++ HP/A
	Plantations	++ o CIR	+++ HP/A
3) GRASSLAND		+++ o CIR	+++ CN/CIR/A
	Pasture	+ o CIR	++ HP/CN/CIR/A
	Uncultivated	+ o CIR	++ HP/CN/CIR/A
4) WOODS		+++ S	+++ S/A
	Deciduous	+++ S	+++ CIR
	Coniferous	+++ o	+++ CIR
5) WATER		+++	+++
	Streams, Waterways	+++ (o)	+++
	Lakes	+++	+++
	Reservoirs	+++	+++
6) BARREN LAND		+++	+++
	Beach	+++	+++
	Sand	+	+
	Rocks	+	+
7) PERMANENT SNOW/GLACIERS		+++	+++

Fig. 43: Quality of Landsat- and Skylab-imagery for land-use mapping if level I and II categories are wanted (Legend see fig. 22 a)

Fig. 43. a

LEGEND for fig. 43

+++	Identification \geq 90%
++	Identification \leq 90%
+	Identification only in special cases
o	sequential imagery
S	Images taken in Summer
A	Images taken in Autumn
HP	High Precision Photograph
CN	Natural Colours
CIR	False Colours

+ Ground truth knowledge

LEVEL I	LEVEL II	LEVEL III	LEVEL IV
2. agricultural land	acres	— grain	— wheat
			rice
	plantations	— truck crop	
		— vineyards	
		orchards	
		oliveyards	
		citrous	
		nut-plantations	
4. woods	deciduous	— deciduous	— deciduous
		evergreen	— mediterranean-
		deciduous	oak
			Macchia
	coniferous	— spruce	
		— pines, stone	
		— pines	
		larches	
5. water	lakes	natural	shallow
		artificial	deep
			+ suspension
	rivers		
	channels		
6. barren land	barren rock	— volcanic	
		— sedimentary	— limestone
			sandstone
			marles,
			shales

Many categories, however, are not sharply bordered because of a gradual change of grey tones; i.e. a zone of mixed vegetation. Even if the categories can be identified, such cases produce a great uncertainty and mistake in bordering different land-use categories, especially if the scale is large.

4. 2. Cartographic Accuracy

Besides methodological problems and their solution it is important to calculate the cartographic accuracy.

If the geometric accuracy in the scale of 1:1'000'000 there is regarded mostly no important differences between LANDSAT-1 images and topographic maps. During mapping the enlargements squares of 10 cm x 10 cm were rectified by using exact topographic features identical in the images and in the topographic maps.

Finally the geometric accuracy was as good as it is required for maps of a scale of 1: 250'000. Areas of 1 mm x 1 mm, i.e. 250 m x 250 m, were mapped, so that the geometric resolution of topographic maps, too was obtained.

4. 3. Comparison with other Methods of Mapping

The quality of new methods are generally compared with the results of former, "conventional" Techniques.

Especially with respect to woods the borders taken from satellite images were more accurate than those of existing land-use maps. This can be explained by this reasons: Those areas which were mapped from aerial photographs lost their initial accuracy by the generalization necessary for a scale of 1:250'000. If the map is based on field work the borders can only be drawn roughly.

4. 4. Comparison with Automatic Digital Classification

Because of the difficulties described in the above chapters and because of the digital original MSS-data there must be asked whether an automatic digital classification would not be preferred to the conventional methods of photointerpretation. Only a time-cost-calculation can answer this question.

At first, there are two important facts:

- A European mountainous region of ca 200'000 km² was mapped. This area would be covered by 6 LANDSAT-frames.
- Level I categories were mapped. They include a great lot of sub categories which had to be combined. The subcategories result from differences of vegetation and soils.

Next we must have a look at the time needed for the conventional interpretation.

2 months	mapping	5 photogeologists
1 month	photographic laboratory work	1 photographer
1 month	ground truth	2 geologists

Because of the overlapping of processes the whole map was done in 3,5 months.

Furthermore, at the recent state of automatic digital classification there must be done some premises:

- All necessary computer programs must be established - i.e. programs for the statistics and programs for the correction of grey tones, which is very important especially in mountainous areas with an intensive relief and with a small scale pattern of different soils.
- The computer must be capable to combine the level I categories from the very great number of subcategories often very similar to one another.

Although automatic digital classification is already done for small European areas and just because of the intensive experiments on this field, it is obvious without an exact calculation:

1. The computer will probably classify much quicker than a interpreter.

2. The classification pixel by pixel will be much more exact than a conventional interpretation.
3. The costs for computer time will be much higher than the costs for interpreters, materials and field work.

Furthermore the high degree of resolution is not necessary because areas of 80 m x 80 m can not be figured out in a scale of 1:250'000 or less.

In spite of the possibilities offered by statistics and by computers the automatic digital classification must solve the same problems as the conventional photointerpretation. A computer needs background information as well as the human interpreter. But it is very difficult to code all important background informations in a way that a computer can work with them.

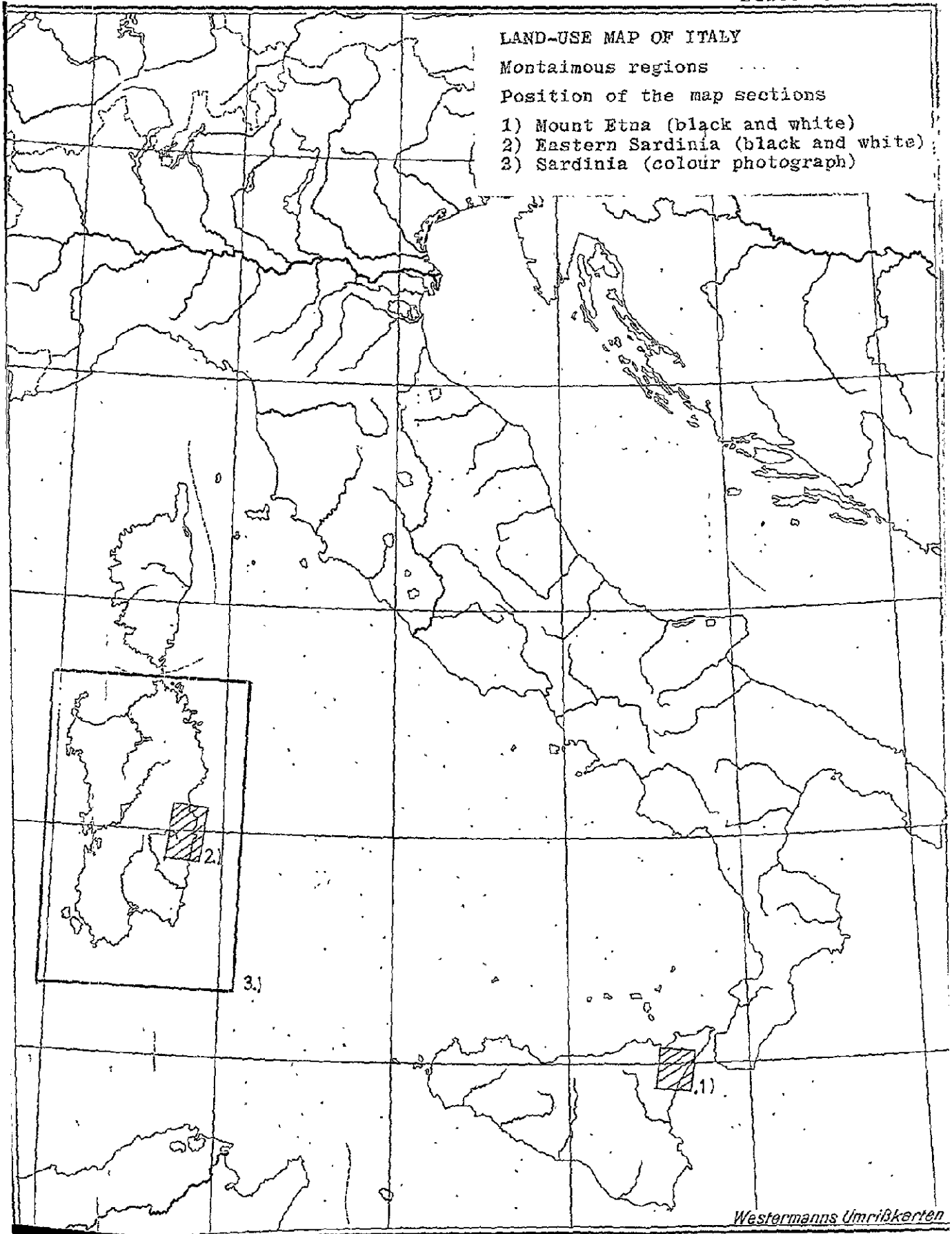
This short discussion shows that, at least for large mountainous areas in Europe, the conventional photointerpretation is and, for the near future, will be the only operational method for land-use mapping.

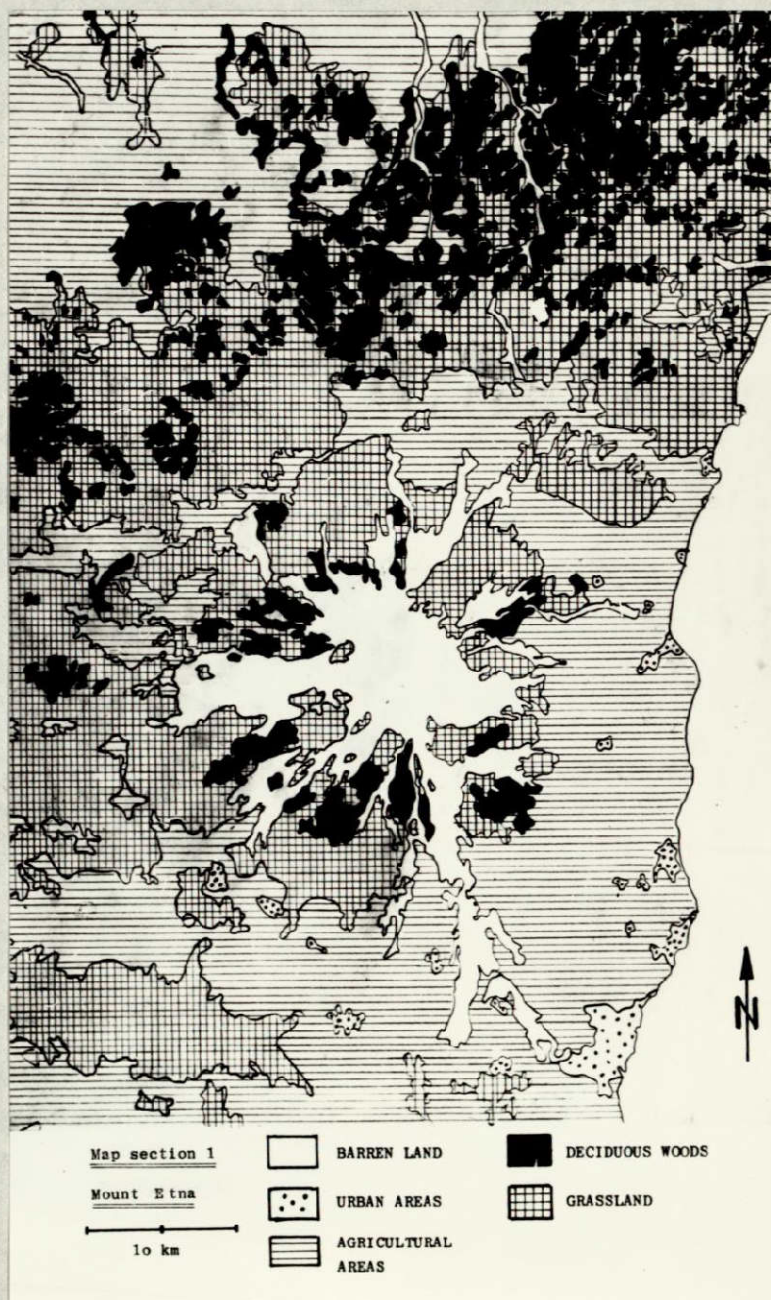
LAND-USE MAP OF ITALY

Mountainous regions

Position of the map sections

- 1) Mount Etna (black and white)
- 2) Eastern Sardinia (black and white)
- 3) Sardinia (colour photograph)





REPRODUCIBILITY OF THE
ORIGINAL PAGE IS POOR



REPRODUCIBILITY OF THE
ORIGINAL PAGE IS POOR

PART II

METHODOLOGICAL INVESTIGATIONS
(DIGITAL ANALOG INVESTIGATIONS)

Methodological investigations concerning the various techniques of processing multispectral data have been emphasized during the last two years.

Within the scope of this activities the following methods have been applied:

- 1) Digital treatment of MSS data including the development of software programs
- 2) Combined digital analog treatment of multispectral data
- 3) Analog electronic data processing
- 4) Fourier analytical evaluation of LANDSAT data by an optical computer

A Digital Image Data Processing

Due to the relatively late delivery of LANDSAT CCT's we went into the field of digital data processing only towards the end of 1973.

The digital treatment of multispectral data involved not only data processing in terms of automatic classification but also all data handling and preprocessing techniques for a more quantitative evaluation of spectral information.

The required soft-ware development for above mentioned approach has been carried out at our institution without adapting existing programs.

Today the ZGF is in a position not only to have a reliable program package for data pre-processing but also classification algorithms are implemented.

The flow-diagram for data processing and the applied systems is shown in Fig. 44

1. Image data processing package -IMAGIN-

1.1 Preparation of data for digital evaluation

At the beginning of the evaluation activities no computer programs and arithmetic models were available to the ZGF. For these reasons, it was necessary to create data files on types which could easily be handled by computers of different producers. The tapes could have been read in the original format, but this would have required the creation of ASSEMBLER-Routines for each type of computer used. On the other hand evaluation programs in ASSEMBLER seemed useless for this user-oriented application. Therefore a conversion routine for the data conversion from the original 8-bit-format to a universal FORTRAN-executable 13-Format was implemented.

During the whole activities of digital data evaluation the following computer types have been used:

- Siemens 4004/151
- CDC 6400
- CDC 1700 (for type conversion from 9 to 7 track and vice versa)
- IBM 360/90
- TR 440 (which will be used in the future)

Although the utilisation of different computers for the evaluation activity was anything but economical, it had the advantage that all programs have been tested and were executed on either one of these. Therefore program caused discrepancies between different systems and compilers are very unlikely. In fact, discrepancies never did occur once the programming work terminated.

The advantages of the FORTRAN programming, although in execution a little slower than ASSEMBLER routines, became evident once the programs are given to users, or are integrated to different data service system.

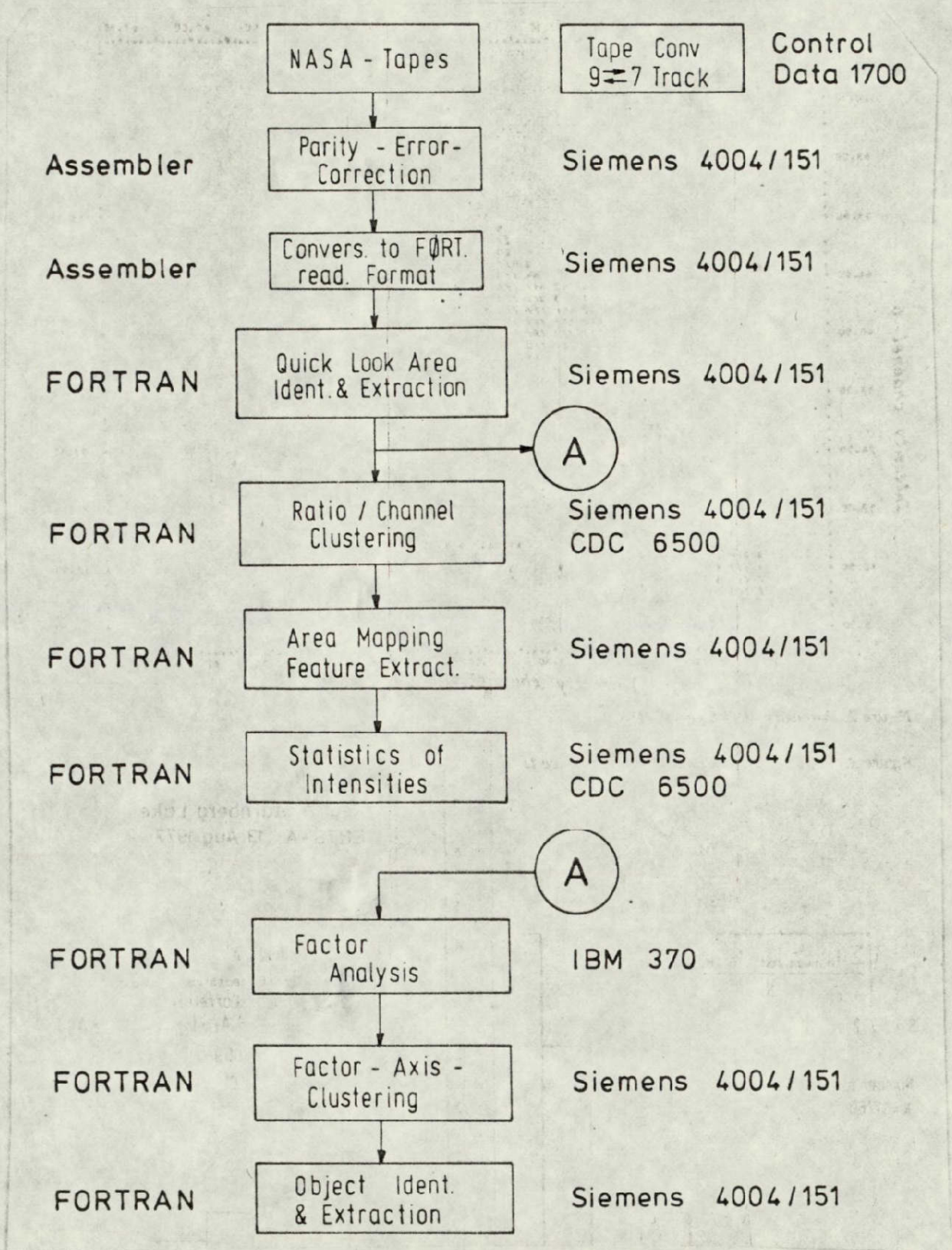


Fig. 44 Flow diagram of data processing

1.2 Check of Data Quality

LANDSAT CCT'S have been the only multispectral information in digital form. Therefore until now, all activities towards the development of a data processing software have necessarily been based on this data.

At the beginning we had to face problems concerning the data quality.

One principal failure which eventually occurred were parity errors on the original data tapes. The maximum number of events that occurred were about 1200 parity disturbed records in the 2340 records of tape data file. In order to correct these data, a parity correction routine was created. All parity errors up to now proved correctable.

An analog display of either one of the multispectral bands showed a systematically increased intensity value for each sixth scan line. This effect became particularly evident for low level intensities as for example for water bodies.

For analog processing such as density slicing, the sixth scan line effect was very disturbing.

For the automatic classification it did not result in the expected reduction of quality because of its high correlation to all spectral bands.

Therefore no special processes for eliminating the sixth scan line effect were applied.

1.3 Description of IMAGIN Routines (see Appendix 1)

The software routines developed can be separated into 4 groups representing

- descriptive statistics
- data manipulation
- classification periodicity analysis
- support routines.

The full program check is listed in Appendix 1.

The programs involved are:

1. Category: Descriptive statistics

- 1.1 HDAR Calculation of mean, standard deviation, and variance for a set of multispectral data including graphic display
- 1.2 KORR Calculation of correlation, covariance matrix
- 1.3 REGR Determination of the regression function for one or several sets of data in linear, quadratic or cubic dependence and graphical display of the clusters and the regression function

2. Category: Data Manipulation

- 2.1 WIFU Weighting of spectral intensities for contrast enhancement and illumination (for graphical presentation)
- 2.2 HAKAN Principal Component Analysis for the selection of those axes with the high variance and the controlled illumination of those containing with the highest degree of systematic errors
- 2.3 FAKTR Factor analysis -Principal components
- FAZEN Factor analysis -Centroid method
- VARMX Varimax rotation

3. Category: Classification

- 3.1 DISK Discriminant analysis for the supervised classification of multispectral signatures
- 3.2 AUKLA Clustering for the unsupervised classification of multispectral signatures

4. Category: Periodicity analysis

- 4.1 FORAN Fourier analysis for the determination of one or two dimensional periodicities within an image (of only one spectral region)

5. Category: Support routines

Supporting subroutines for matrix inversion, the generation of gray scale maps, matrix multiplication etc.

On the basis of above described software package, LANDSAT data were processed under the following aspects.

- 1) Statistical evaluation with respect to the information content of MSS bands
- 2) Data Reduction
- 3) Automatic classification

2. Selection of Data Material and Test Sites

Concerning our activities on digital data processing during the last year, we were mainly involved in learning about the significance of the spectral information gathered by the MSS scanner and in developing and updating software programs. For this basic research and software development the selection of test sites has not been carried out with special regard to our LANDSAT test area in Italy, but more under the following requirements.

- they should all be very close to the location of ZGF (not more than 150 km). Thus it would be possible to visit them regularly. Then only a short time would be needed for comparison of results obtained by the computer evaluation to the real situation;
- they should show significant features for the central European user;
- to obtain results concerning the resolution to be obtained by a pixel-by-pixel selection, areas were chosen which contain features of high neighbouring contrast.

All test areas were chosen of the same size and the same geometry: 98 lines and 120 pixels per line = 11760 pixels per test area. This geometry of the frame has been selected simply for particular reasons of computer display, not for any other purpose.

The areas in particular are as follows (fig.45,46)

Scene Nr.	Name of area	Data taken
1.	Ostersee Area	
2.	Ammersee-North	
3.	Hofolding Forest	ERTS 1021-09380
4.	Landsberg Fields	Date: 13 Aug. 72
5.	Valli di Comacchio	ERTS 1218-09341
6.	Marina di Carrara	Date: 26 Feb. 73

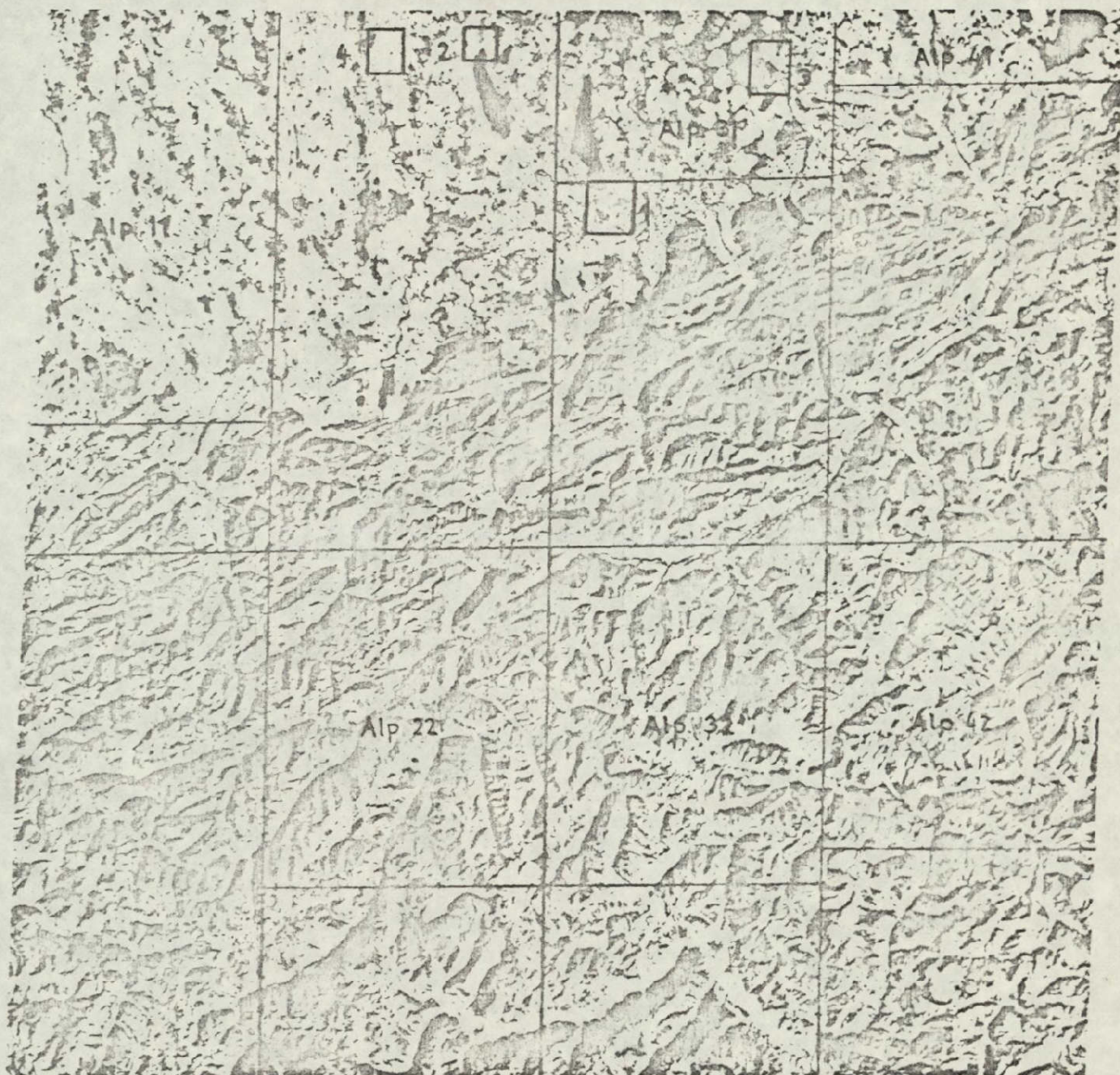


Fig. 45 LANDSAT-scene ID 1021-09380 with test areas
for the statistical evaluation

REPRODUCIBILITY OF THE
ORIGINAL PAGE IS POOR

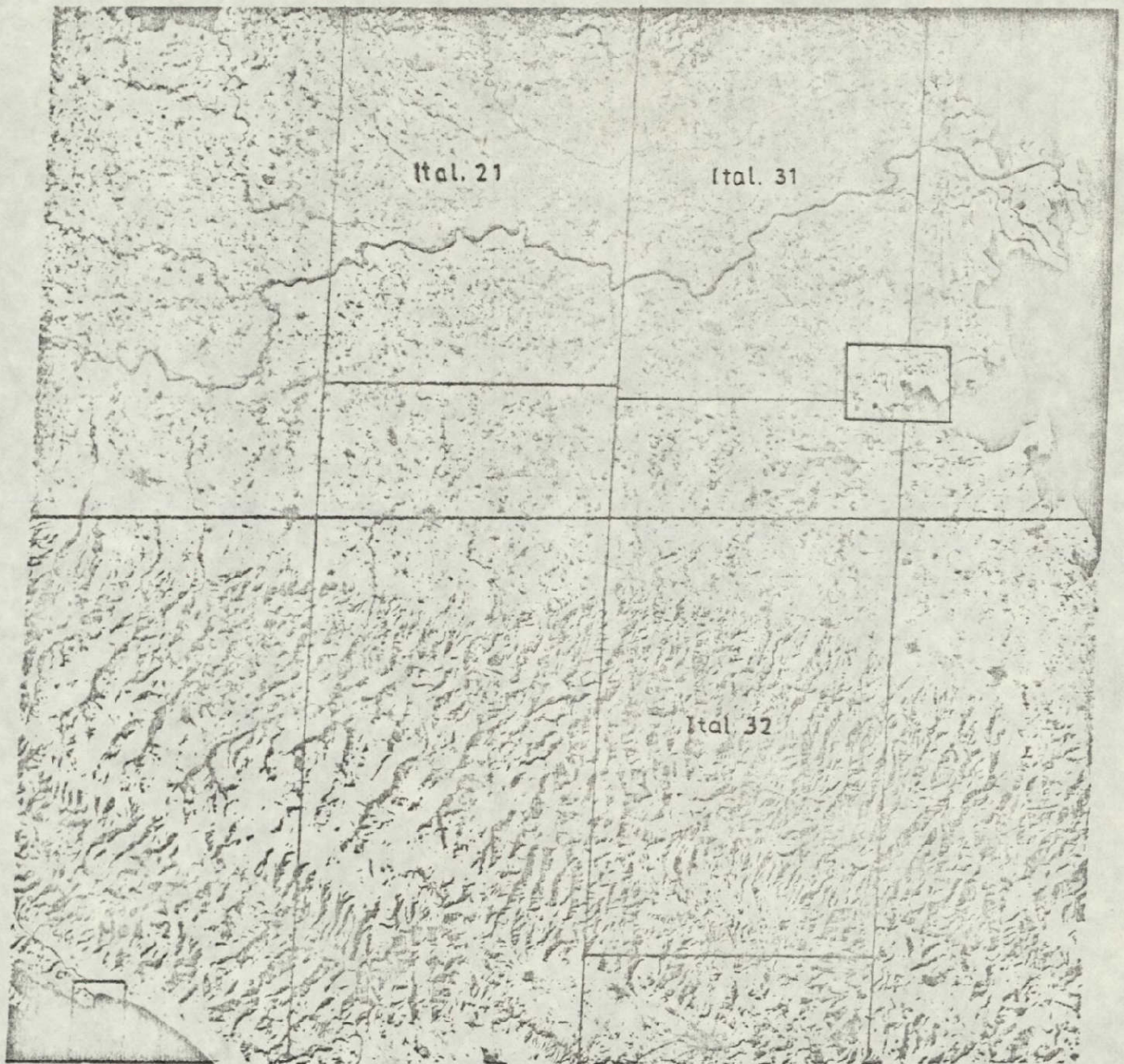


Fig. 46 LANDSAT-scene ID 1218-09341 with test areas
for the statistical evaluation

REPRODUCIBILITY OF THE
ORIGINAL PAGE IS POOR

Scene Nr.	Area Features
1.	Lakes, Marsh land, Coniferous forest, Pastures, Agricultural Areas
2.	Lakes, Reed Grass, Coniferous Forests, Leaf Tree Areas
3.	Agricultural Areas, Meadows, Mixed Forest Types
4.	Mixed Forest Type, Agricultural Areas
5.	Rice fields
6.	Coast area

In order to look at the statistics of the multispectral scanner data additional larger areas out of above LANDSAT scenes were selected (Fig. 46- ALP)

3. Statistical Evaluation.

The statistical evaluation began with an intensity (dynamic range) comparison of different data channels to obtain some idea of the intensity population of a typical Central European scene, represented by the Starnberg Lake area. By plotting these data for two MSS channels in a Cartesian coordinate system, a distinct linear relationship between the intensities of ERTS infrared channels MSS 6 and MSS 7 became evident (Fig. 47).

Assuming a straight line as the best correlation curve for the data set, the constants A_1 and A_2 in the linear equation for channels 6 and 7

$$I_6 = A_1 + (A_2 * I_7)$$

were found to be 5.3059 and 1.5101, respectively, for this particular region.

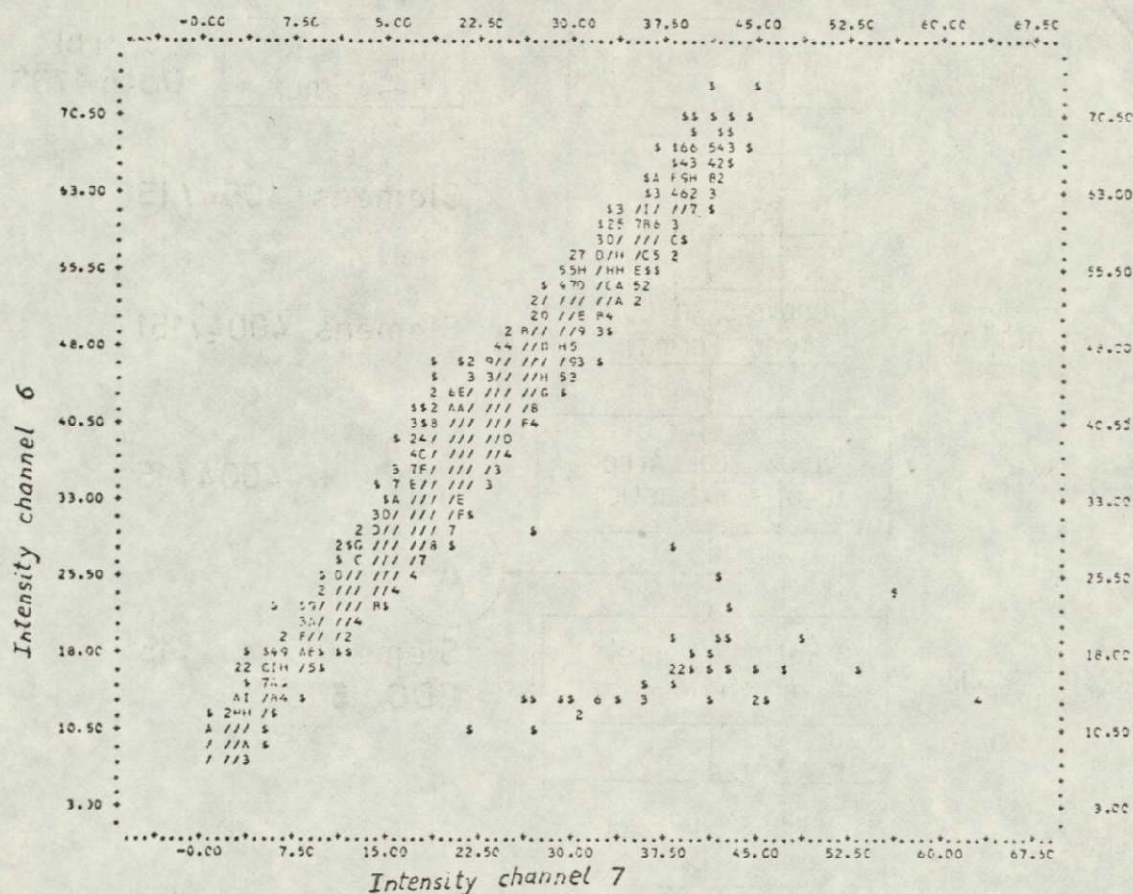


Fig. 47 Intensity Plot, MSS 6 versus MSS 7

These constants were obtained by a least-squares method on the basis of the following relations:

$$A_1 = \frac{(\sum I_6)(\sum I_7^2) - (\sum I_6)(\sum I_6 I_7)}{N \sum I_6^2 - (\sum I_6)^2}$$

$$A_2 = \frac{N \sum I_6 I_7 - (\sum I_6)(\sum I_7)}{N \sum I_6 - (\sum I_6)^2}$$

The deviation in the measured intensity values and those calculated with the above formula as a function of the measured values of channel 7 is shown in Figure 48. The mean deviation was found to be 2,2 for a scale of 128 intensity values for LANDSAT MSS data.

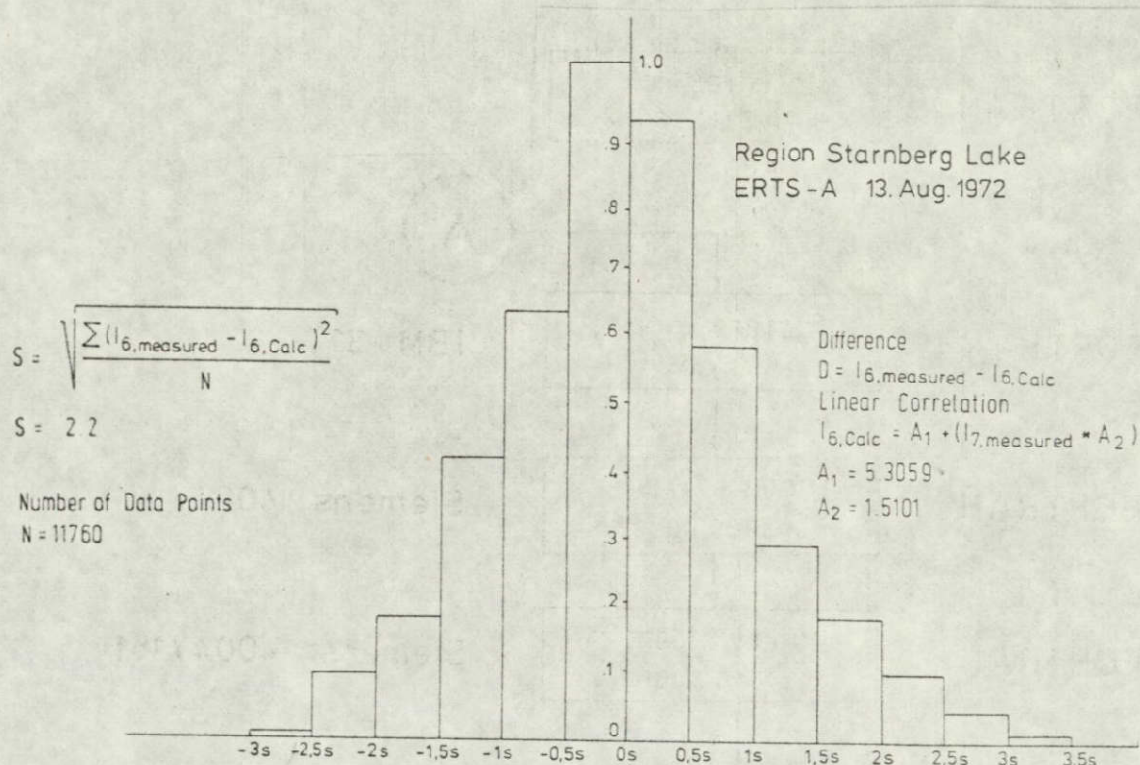


Fig 48 Population as a function of difference D

The graphical presentation shows very good agreement with a normal distribution, with populations of:

- 68 % in the region of $0 \pm 1 S$
- 93 % in the region of $0 \pm 2 S$
- 98 % in the region of $0 \pm 3 S$

with

$$S = \sqrt{\frac{\sum (I_{61, \text{measured}} - I_{61, \text{calc}})^2}{N}}$$

A histogram of the measured data of channel 6 and those derived mathematically from the experimental values of channel 7 shows almost an equivalent population distribution to that presented in Figure 49 for the Starnberg Lake area and the Italian Mediterranean scene.

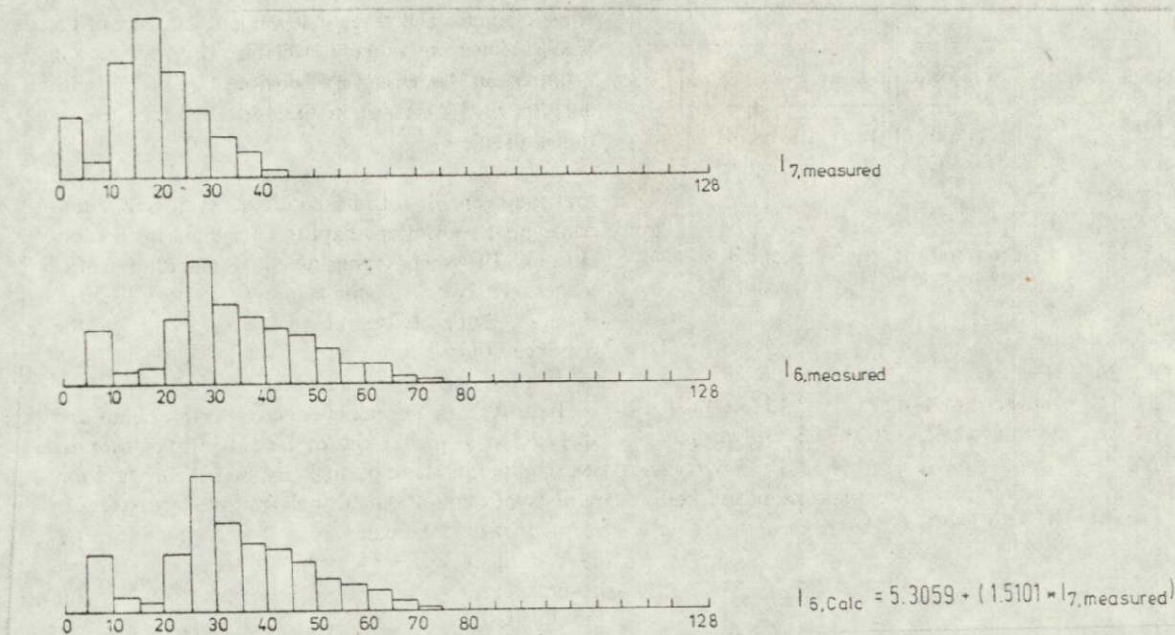


Fig.49 Histogram of the population of experimental and calculated values of $I_6 = f(I_7)$

Based on these results, the analysis was subsequently extended to complete Central European and Italian scenes indicated in Tables 1 and 2. Evaluation of these data shows almost equivalent constants A_1 and A_2 for the same type of landscape and landform.

Table 1.

Scene	Number of pixels	Channel 6		Channel 7		Linear equation		
		\bar{I}_6	S_6	\bar{I}_7	S_7	A_1	A_2	S
ALP 11	974400	35.75	10.83	18.79	6.8	0.28	1.84	10.35
ALP 31	324800	36.98	13.64	20.44	8.72	0.3	1.75	
ALP 41	97080	44.23	13.70	25.19	9.07	3.40	1.17	3.71
ALP 22	950040	38.21	16.55	20.03	9.22	0.3	1.85	26.55
ALP 32	950040	40.73	21.08	20.62	9.89	0.12	1.95	26.55
ALP 42	946533	37.71	16.57	20.26	9.54	3.54	1.11	10.18
ITAL 21	936767	22.96	6.55	12.18	3.95	0.13	1.84	12.1
ITAL 31	943467	24.12	3.86	11.82	2.45	0.11	2.0	17.57
ITAL 32	943879	25.41	4.16	13.08	2.88	0.14	1.91	16.19
MED 12	40000					5.01	0.0678	5.5

Table 2.

Scene	Identification
ALP 11 ALP 31 ALP 41	Northern half of strips 1, 3 and 4 of ERTS 1021-09380, 13 August 1973
ALP 22 ALP 32 ALP 42	Southern half of strips 2, 3 and 4, ERTS 1021-09380, 13 August 1973
ITAL 21 ITAL 31 ITAL 32	Northern half of strip 2 } ERTS Northern half of strip 3 } 1218-09341 Southern half of strip 3 } 26 February 1973
MED 21	Mediterranean water surface of southern strip of ERTS 1218-09341, 26 February 1973

Linearity alone, however, is not a sufficient identity criterion. Much more important is the average deviation between the measured intensities of channel 6 and those derived mathematically from the experimental values of channel 7. The data obtained show that the average deviation for the equivalent landscape and land-use scenes are almost identical. This is valid not only for the Central European summer scene, but also for the Italian winter scene. The additive and multiplicative constants for the linear equation show a strong deviation for equivalent scenes only in those cases where the test area considered largely contains a single uniform feature. This was the case for scene ALP 41 (water surface of the Chiemsee Lake), scene ALP 42 (mostly cloud covered), and MED 12 (uniform water surface of the Mediterranean). Applying these results to a scene of the same type, but containing several different features, results in a very wide deviation between the measured and mathematically derived values of channel 6.

From these results, it can apparently be concluded that a strong correlation, and therefore redundancy, occurs between the intensity values of channels 6 and 7 for each

REPRODUCIBILITY OF THE
ORIGINAL PAGE IS POOR

individual data point. Such strong dependence has further consequences which find their impact in the mathematical procedures for feature recognition and identification. The idea was to present the data from the four MSS channels in four-dimensional mathematical space and, by identification of particular characteristics to recognise the presence of certain features in the scene.

The fact that there is a strong correlation between the two infrared channels means that one set of data does not really give new information, so that only three channels and three independent data sets of the four assumed are actually available. This reduction in information became very obvious for the factor analysis and is evident in the correlation matrix obtained (Table 3).

Although these results could be interpreted such that the channels 6 and 7 could be considered redundant, great restrictions have to be applied to this conclusions. The scenes considered were either winter scenes (Italy) or mid-summer scenes (Central Europe). Both landscapes are characterised by the presence of highly uniform land-use patterns, containing features of the harvest or post-harvest period.

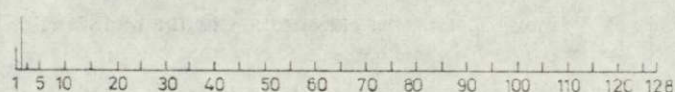
To arrive at a definite conclusion, extension of this analysis to a greater set of land-use types over all seasonal periods, and particularly over the maturation periods of certain agricultural fruits, is necessary. It seems that in these cases, as well as for such features as waters of different turbidity, cloud and snow cover, there is no redundancy between the two infrared channels, and therefore one of them cannot be dispensed with.

REPRODUCIBILITY OF THE
ORIGINAL PAGE IS POOR

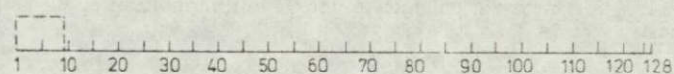
Table 3 Correlation coefficients LANDSAT MSS bands

	MSS-4	MSS-5	MSS-6	MSS-7
MSS-4	1.000	0,762	0,218	0,141
MSS-5	0,762	1,000	0,471	0,388
MSS-6	0,218	0,471	1,000	0,987
MSS-7	0,141	0,388	0,987	1,000

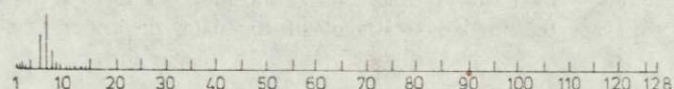
While working on the statistical evaluation of the Central European and Italian scenes, an interesting feature concerning only the water bodies became evident. While the intensity level of European lakes ranged from 0 to 9 in channel 7, the dynamic range for the Mediterranean water body was 0 to 2 (Fig. 50.)



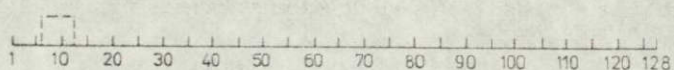
17 Bocca di Magra (ERTS-A 26 Febr 1973)



17 Starnberg Lake (ERTS-A 13 Aug 1972)



16 Bocca di Magra (ERTS-A 26 Febr 1973)



16 Starnberg Lake (ERTS-A 13 Aug 1972)

Fig 50 Comparison of dynamic ranges

REPRODUCIBILITY OF THE
ORIGINAL PAGE IS POOR

4. Data Reduction

Above described phenomenon of the correlative property of MSS bands led to a more detailed evaluation on the basis of special selected surface features. Furthermore this approach led us to discussions about the possibilities of taking advantage of the correlative property by reducing the redundant information for data compression purposes. The selection of test areas has been directed at large homogeneous objects such as coniferous forest, water and large homogeneous vegetated areas. Furthermore, surface areas composed of different sub-categories of earth scientific interest such as agricultural field pattern, were also selected (Fig. 51). The graphical representation, Fig. 51 illustrates the correlation of the LANDSAT bands with the above-mentioned surface features.

Based on this comparison, the following conclusions can be reached:

- A very high redundancy exists between the infrared bands, expressed by a correlation factor above 0,9.
The degree of correlation is approaching a uniform value for all samples except for the mixed forest.
- The visible channels are also characterized by a relatively high redundancy. The absolute degree of correlation is more dependent on the various surface features.
- Low redundancy exists between the visible and infrared channels. The variations in correlation are strongly influenced by the selected samples. So minimum correlation can partly be observed between MSS 5 and MSS 7.

Correlation
Coefficient



REPRODUCIBILITY OF THE
ORIGINAL PAGE IS POOR

fig. 51 Correlation of different ERTS-1 bands with respect
to selected surface features

These examples show very clearly that, at least on the basis of LANDSAT, the significance of spectral bands is strongly dependent on the surface feature, or more generally, on the earth scientific problem in question.

With respect to the relationship described above in general, it is not possible to satisfy different earth scientific requirements with only a limited number of spectral bands.

The result would be the implementation of a multispectral scanner operating a high number of spectral bands. This requirement leads to non-manageable data rates, especially with respect to operational systems. On the other hand, the more or less high degree of redundancy between multispectral data enables the application of redundancy suppression techniques. The strong relationship between correlation factor and surface feature calls for a suppression technique that is carried out in relation to the corresponding user oriented problem and that can be performed after data acquisition and before data transmission.

4.1 Data Compression by Principal Components Transformation

A well known data compression technique is the so called Principal Components Transformation. This statistical method defines a new coordinate system describing maximum dispersion of the input data. The new coordinates or principle components represent a linear combination of the original coordinates or spectral channels.

Application of this technique on multispectral information indicates, that the same information, described by the entire range of spectral bands, can be expressed by a very limited number of principal components. This effect is primarily based on the correlative property of multispectral data. With respect to the number (n) of available

variables represented by the spectral bands, the Principal Components Transformation operates in an n-dimensional space.

From a statistical point of view, the definition of the new axis is based on the dispersion created by the chance occurrence of N categories or data populations. Therefore the dispersion or information content of a single population and of under-represented populations of earth scientific interest cannot be described in an optimum way. Due to this effect, data reduction on the basis of the Principal Components Transformation is of necessity a compromise between the information content of the total input data and the information content of minor populations.

4.2 Application Oriented Data Compression

The effect described above becomes crucial if the Principal Components Transformation is considered as an in-flight data compression technique for operational satellite systems. Furthermore as a statistical method, it requires elaborate computer hardware.

In reality an operational system evidently cannot satisfy the entire multi-disciplinary user community, at least not at the same time. It will be able, however, to cover a limited number of relevant applications. For these reasons in defining earth scientific problems, it is necessary to have optimum information in terms of application oriented low data rates. This requirement can be partly fulfilled on the basis of a so-called Supervised Principal Components Transformation.

The basic idea of this method is, to define a priori (the principal components of only a single- or a group of features which is of interest) and to transform (reduce) the incoming multispectral information with respect to these defined components.

By means of this supervised reduction above-mentioned "compromise-effect" of the Principal Components Transformation is minimized with respect to the dispersion of single or minor data populations. Furthermore, the supervised transformation does not require elaborate on-board computer facilities. Therefore, from a technical point of view, it offers a high potential as an in-flight data compression technique.

In order to demonstrate this kind of supervised transformation, as a first step, the loadings of the principal axis of an inhomogeneous agricultural area and of a homogeneous coniferous forest, were calculated.

Principal Components Factor Loadings

	Agricultural area:			Coniferous forest:	
	I	II	III	I	II
MSS 4	0.815	-0.558	-0.158	0.898	-0.369
MSS 5	0.646	-0.749	-0.150	0.927	-0.437
MSS 6	0.845	0.528	0.016	0.448	0.311
MSS 7	0.754	0.652	0.024	0.273	0.486

As calculated above, the three principal components for the agricultural area contain 99,7 % of the total information represented by the 4 MSS-bands. Because of the homogeneous signature of the coniferous forest, 96,3 % of the total information can be described by only two factors (Fig. 52).

REPRODUCIBILITY OF THE
ORIGINAL PAGE IS POOR

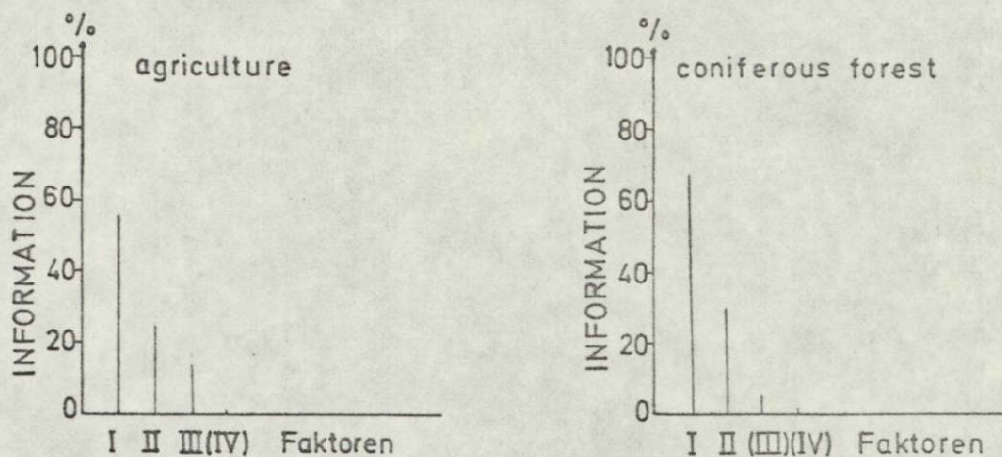


Fig. 52 Distribution of information on principal components for agriculture and coniferous forest

In a second step the MSS data of the test area (Fig. 53), characterized basically by a coniferous- and mixed forest cover and also by an agricultural area, was translated.



Fig. 53 Representation of the test-site (LANDSAT-MSS 7)

The quantized grey step image of fig. 54 represents a transformation due to the first principal component of the agricultural training set.

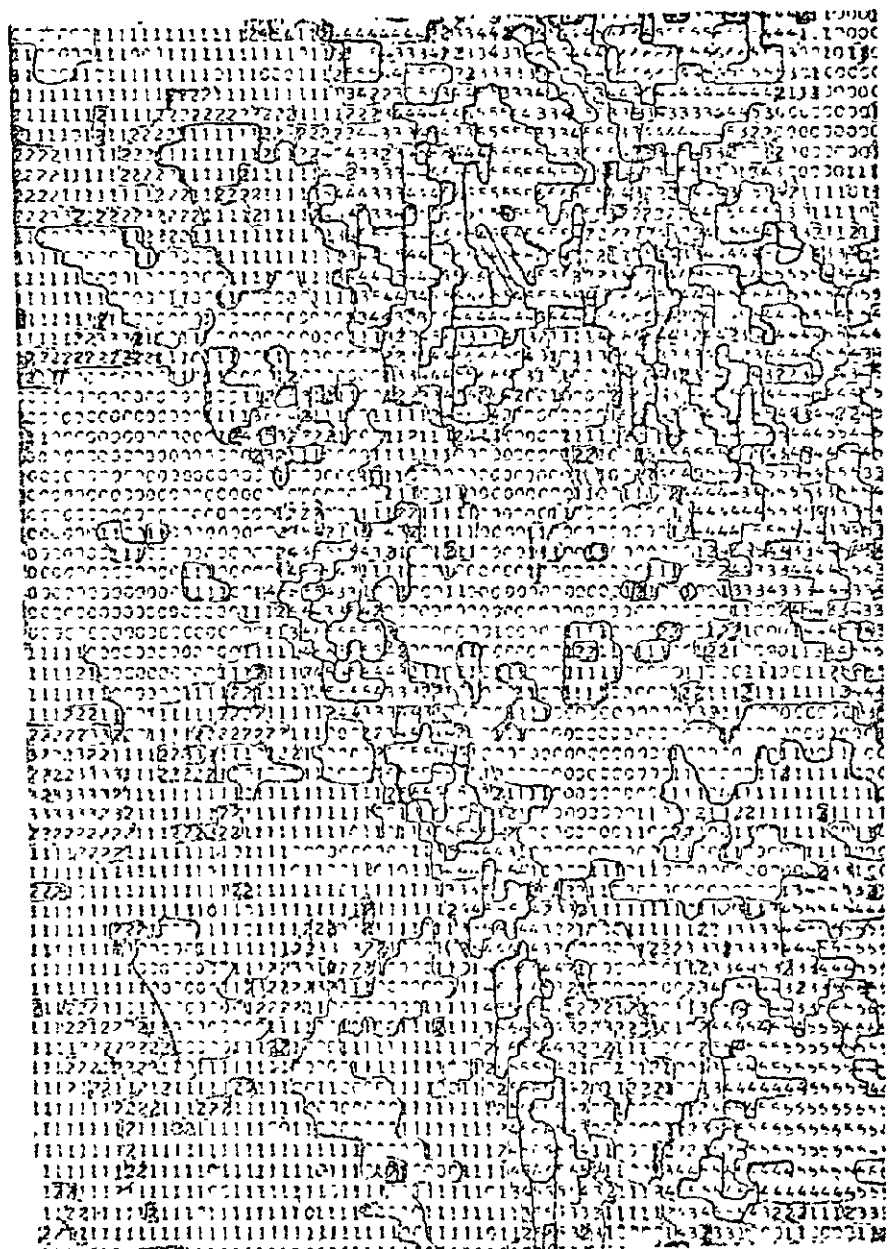


Fig. 54 Principal component image optimized for agricultural used areas

REPRODUCIBILITY OF THE
ORIGINAL PAGE IS POOR

This transformation shows very detailed information on field patterns; whereas, it is not possible to define the homogeneity of the coniferous forest.

A transformation of the same original data with the loadings of the first factor representing coniferous samples (fig. 55) was also carried out.

This time the forest cover appears very well defined and the lack of information on agricultural areas is evident.



Fig. 55 Principal component image optimized for forested areas

By means of corresponding transformations of the original data through available supervised factors, the new set of data can be regarded as compressed input data with optimum information content for specific applications.

Furthermore, by applying the remaining set of data (components), a reduction of computer time in the ratio of 9:16 could be maintained with no reduction in classification accuracy as the processing time required is a quadratic function of the number of spectral bands.

Another type of data reduction can be obtained through application of factor analysis (FAKTR), in order to select those spectral channels with the highest degree of significance for the identification of certain surface features. Using this method for LANDSAT-data, it was found, that only three out of the 4 bands showed sufficient and linear independent information. The high degree of linear dependence, as pointed out already above, between MSS 6 and MSS 7 should be restated.

REPRODUCIBILITY OF THE
ORIGINAL PAGE IS POOR

REPRODUCIBILITY OF THE
ORIGINAL PAGE IS POOR

5. Automatic Classification

Multispectral data require by its nature of representing multivariate information advanced processing techniques. Furthermore this data can be regarded as an optimum premise to apply fully automated evaluation and classification algorithms.

On the basis of data representing Italian and South German scenes, both supervised and unsupervised algorithms were programmed and applied.

5.1 Supervised classification

In order to test and evaluate the supervised classification programs (Appendix 1) a test site near Munich (Fig. 45 Scene 1) was selected. The classification was started with objects easily identifiable by their areal extension and spectral characteristics such as water bodies, coniferous forest, urban areas, and pastures. The result of such a supervised classification is demonstrated by fig. 56

In order to prove the reliability of above classification intensive ground checks and comparative studies based on aerial photographs were carried out.

From this it turned out, that some classes which are uniform from an earth scientific point of view could not be fully recognized by the automatic classifier. Marsh land for example, which is composed by different vegetated and non vegetated surface features could not be separated. Training the computer with data, representing the unhomogeneous category "marsh" interference with other surface features such as coniferous forest occurred.

Dividing the cluster of marshland into more subclusters it has not been possible to map the true areal extension of the marsh itself in spite of a high statistical accuracy in terms of separability. Such difficulties in defining special

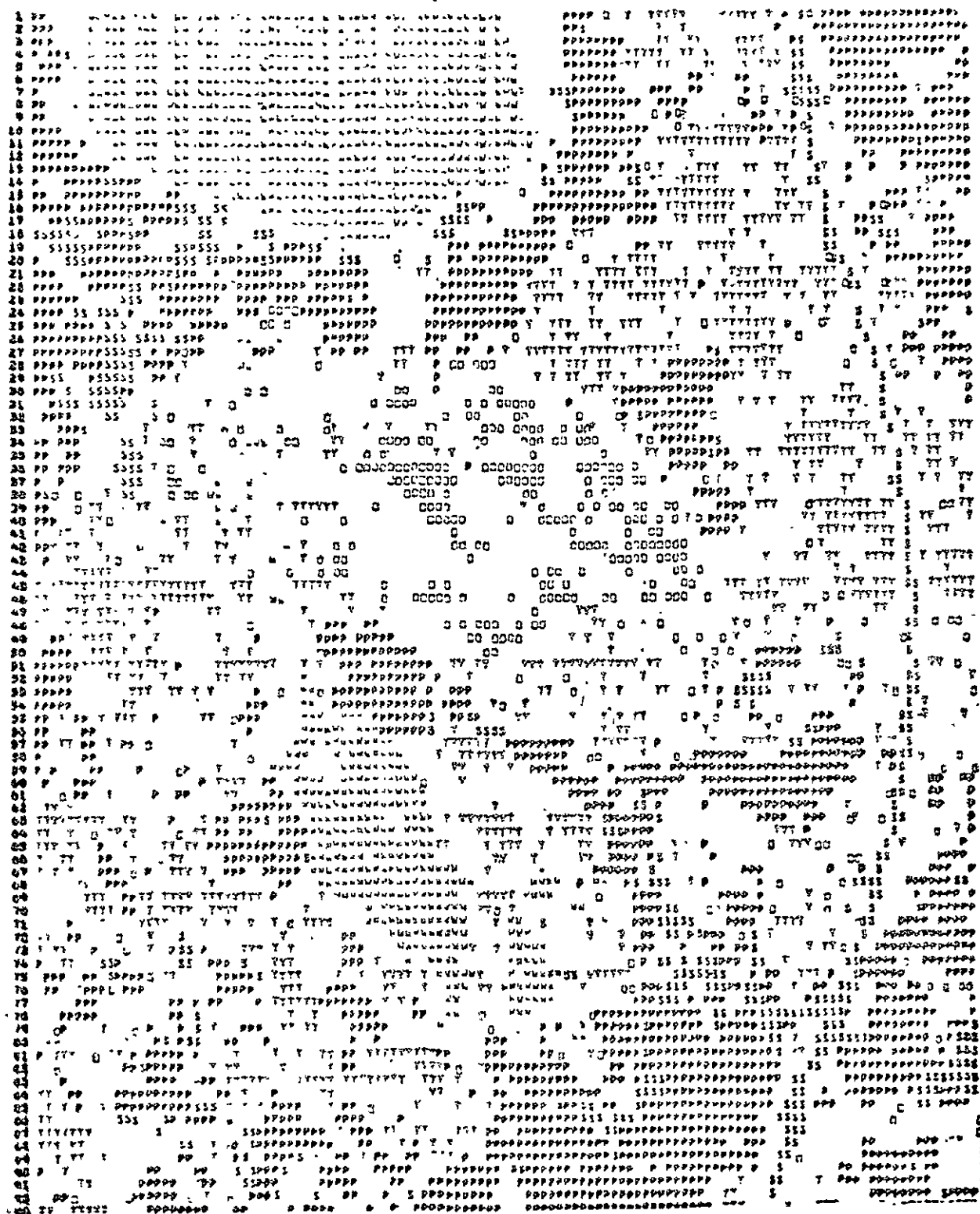


Fig. 56 supervised classification: water=blue, urban=black
pastures=red, coniferous forest=green and
marshland=grey

REPRODUCIBILITY OF THE
ORIGINAL PAGE IS POOR

surface features are not caused by the algorithms used. Rather the reason for classification errors is the significance of the available spectral information for solving a particular task.

Further difficulties arise especially with respect to the resolution capabilities of the MS-scanner and the typical pattern of agricultural used areas in Europe.

In contrast to the extensive land use, characteristic of North America, we are faced with an intensive management of our agricultural areas. This has resulted in very small and unhomogeneous field pattern.

Due to this situation, it is necessary to make a very careful selection of the picture elements for training the computer with certain test features. A further problem is, that the test site very often is much smaller than the dimension of a resolution element leading to a mixture of different spectral significances for one cluster. Furthermore this results in a very poor separability crucial for automatic classification purposes.

The same problem of gathering unhomogeneous spectral information occurs at the borders of two significant surface features. The degree of misclassification for this case can be minimized by comparing neighbouring picture elements.

Due to above mentioned problem in classifying phenomena "below the resolution" other approaches of automatic information extraction techniques should be taken into consideration.

To carry out a spectral-statistical inventory of agricultural used areas over one vegetation cycle in combination with detailed ground truth reports may result in correlation which allow a further use of Landsat data in terms of a pure numerical evaluation. A premise for this approach has to be a maximum repetitive LANDSAT coverage.

REPRODUCIBILITY OF THE
ORIGINAL PAGE IS POOR

5.2 Non supervised Classification

For carrying out a non supervised classification two routines were implemented.

The first routine stores all data necessary for an automatic classification in core. As the numbers of storage elements necessary for the classification depend on the number of picture elements by $n(n-1)/2$, its execution requires much storage, but, on the other hand, is very fast.

The second routine has in core only the information of the clusters found, and the information of the actual data points. It is as fast as the first routine, but does not need as much storage.

With these routines a separation of those clusters with a very high degree of agreement has been obtained. It soon became evident, however, that it was not meaningful to use all data elements for the classification, because of the great computer time necessary for these procedures. Therefore the decision was made to use only a very small number of preselected pixels of a specific significance or to select the data points from a certain land-scape type by random number access.

For classification purposes the Laguna die Comachio south of the Po-delta was chosen (Fig. 46, Scene 1)

The area covers water bodies, large agricultural fields with uniform plant soil association characterized by extreme changes in soil moisture and shallow water in irrigated rice cultures.

By applying AUKLA and AUKLB it was possible to separate four typical categories. The computer print out of the evaluated area (Fig. 57) shows the following categories: deep water, shallow water, channels, water covered fields or areas with extremely high soil moisture, fields with fresh vegetation, dry area with vegetation.



Fig. 57

REPRODUCIBILITY OF THE
ORIGINAL PAGE IS POOR

REPRODUCIBILITY OF THE
ORIGINAL PAGE IS POOR

5.3 The "Slope Method"

With respect to the computer time consuming classification operations the possible information gain has to be carefully examined. Even for a pure scientific data handling computer time often becomes a critical factor which calls for operating may be less complex processing software or analog equipment.

A very easy and still effectful possibility of digital evaluation of multispectral data is, taking into account the reflection properties of some dominant surface features within the spectral range covered by the ERTS-MSS scanner.

Some basic spectral properties are the reflection capabilities of plants and water in the near region of the infrared spectrum. In general, reflection characteristics depend on the spectral range or wavelength of the surface considered. For the particular case of the LANDSAT-data the slope has been defined as

$$\alpha = f \quad (\text{contribution of visible} - \text{contribution of infrared part of the spectrum})$$

$$\alpha = \frac{I_4 + I_5}{2} - \frac{I_6 + I_7}{2}$$

This technique is not based on a statistical approach. Each picture point, represented by 4 Variables - the 4 spectral measurements - is classified with respect to say an certain angle intervalls, and assigned with a corresponding symbol and printed into the maps. This simple decision making program, does not require large amounts of computer time, and storage and can be regarded as a kind of digital quick look operation (fig. 58).

The idea of the slope technique is not to imitate density slicing techniques but to have the possibility to perform a certain kind of preselection of surface features.

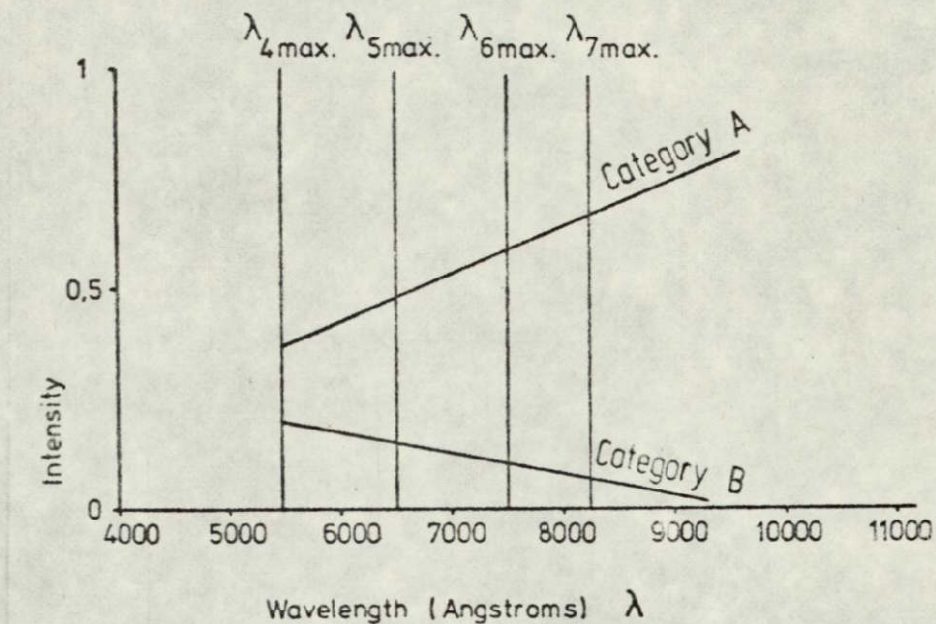


Fig. 58. Spectral slope method

Under this aspect, it is possible to get a distribution display of different water bodies but no idea about its relative degree of pollution.

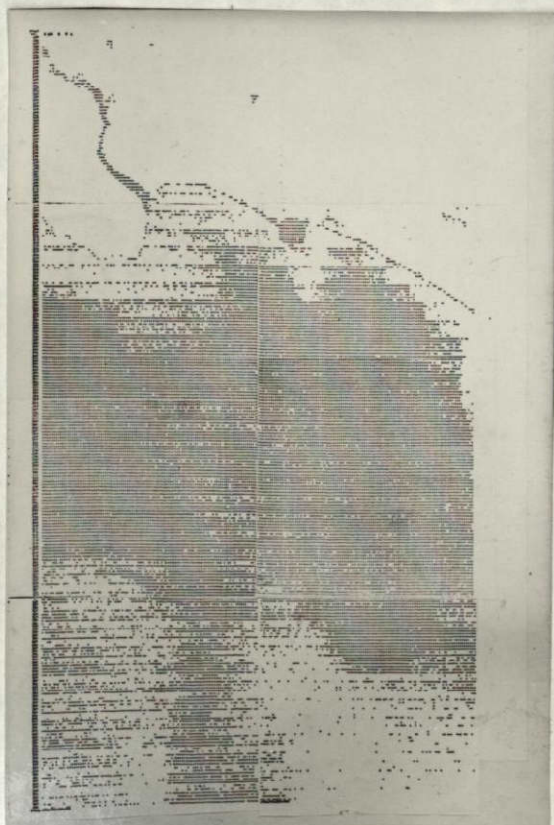


Fig. 59 Color composite representing 3 classes of turbid water

REPRODUCIBILITY OF THE
ORIGINAL PAGE IS POOR

In Fig. 59 the Versilian coast is evaluated using this method. Three different classes of turbid water bodies are distinguished. Main pollution surces SE of the harbour basin of Marina di Carrara, the distribution, transportation and degree of pollution in Thyrrenian Sea can be recorded in relation to different slope angles. Decreasing slope is a function of the reflection and absorption properties within the visible and near infrared portion of the spectrum.

REPRODUCIBILITY OF THE
ORIGINAL PAGE IS POOR

B Analog/Digital Treatment of Multispectral Data

The results of fully automated classification procedures are data in maplike form which consists of averaged information with respect to the information content of the original data. By this the user is confronted with a final data product which does not permit anymore any further interpretations.

Taking into account, the interference and complexity of earth-scientific phenomena and the difficulties described above for many applications the researchers know how is indispensable.

Especially in an experimental phase it is of utmost importance of being able to evaluate multispectral data by combining the advantages of statistical techniques and the interpreters know how.

From an earth scientific point of view a possible solution to take advantage of both can be achieved via the following steps.

- a) statistical enhancement of class separability
- b) combination of transformed data by operating in color space
- c) interpretation

By this technique decision making algorithms which actually result in an averaging of data is left to the interpreters interaction.

1. a) Enhancement of class separability

This preprocessing technique represents a necessary first evaluation step for both the fully automated classification and the combined digital and analog treatment of multispectral data.

REPRODUCIBILITY OF THE
ORIGINAL PAGE IS POOR

The separability of surface classes represented by data clusters in an N dimensional space is commonly increased by applying the principal component transformation. Since a linear transformation of all data points considers the weighted intensities of the original bands, new dimensions or components can be determined. Due to the enhanced separability of the clusters, the pictorial representation of the new components offers enhanced maximum contrast. In order to obtain principal component images which show maximum information for selected phenomena or applications, the transformation must be optimized. The optimization is carried out by applying this technique on selected training areas (as it is demonstrated on page).

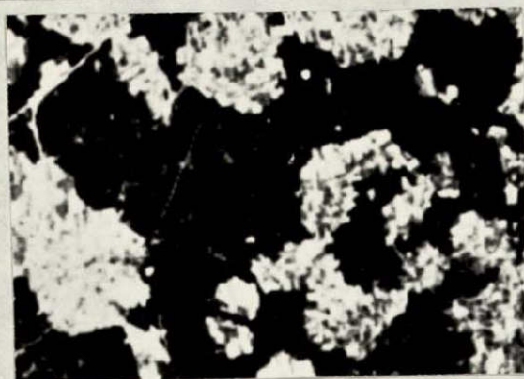
The image of fig.61 represents a weighted transformation of the original bands (fig. 60). It is evident that none of the original bands (MSS 4,5,6 and 7) have a comparable contrast in the region of field patterns.

With respect to the various application-dependent requirements, it should be possible to define standard transformation by taking into account also changing environmental parameters. Therefore this approach has to be based on along term experimental remote sensing measurement program.

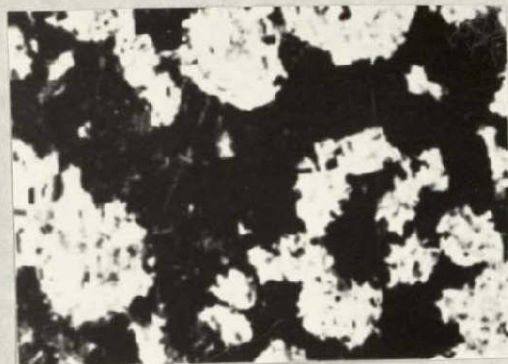


Fig.60 LANDSAT-MSS 4

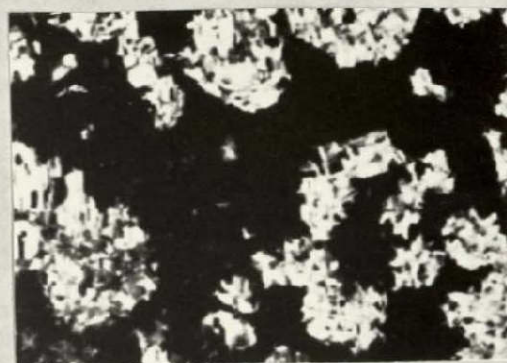
REPRODUCIBILITY OF THE
ORIGINAL PAGE IS POOR



a
(MSS 5)



b
(MSS 6)



c
(MSS 7)

Fig. 60 a,b,c LANDSAT-MSS 5,6 and 7

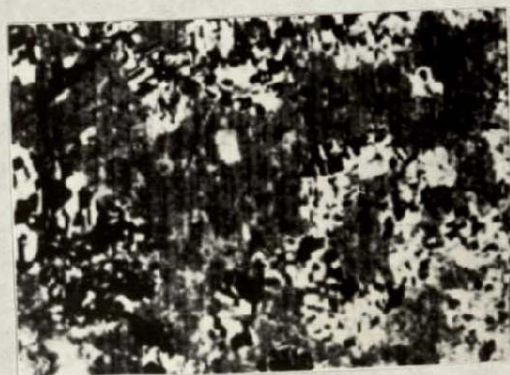


Fig. 61 Transformed image (first principal component)

2. Color Coding by operating in the three-dimensional color space

The transformed spectral information now can be used as a basis for a further automatic classification. With respect to a further analog treatment, a selection of three transformed images (either the first three principal components or a selection of optimized transformations) can be used for the generation of color composites. With respect to the expanded information content of the black and white input images the resulting perceptable color differences are very indicative of the distribution of characteristic surface signatures.

For demonstration some areas out of an ERTS-frame showing the Alps between Munich and Bozen were selected (fig. 62, frame 1 and 2). The image of fig. 63 illustrates the enlarged region of the Murnauer Moos. The image is composed from MSS band 4 (blue), 5 (green) and 7 (red). This false color image shows a relatively low degree of differentiation. Two main categories, grassland (light red) and bog areas can be separated.



REPRODUCIBILITY OF THE
ORIGINAL PAGE IS POOR

Fig. 62

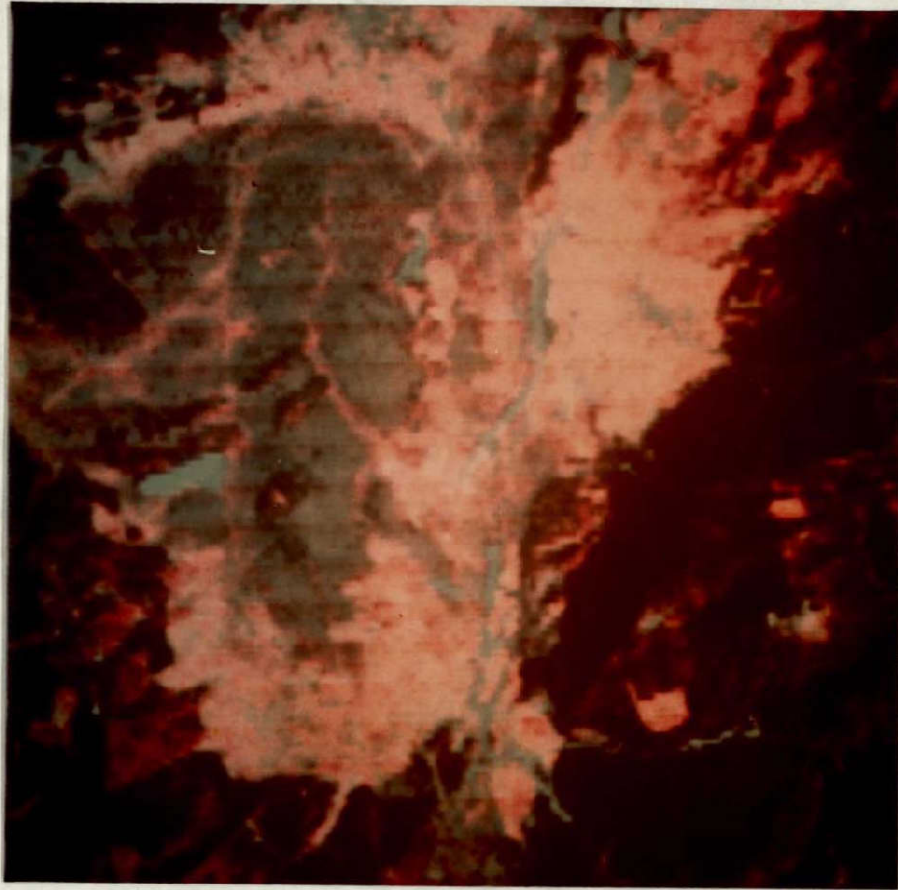


Fig. 63 False color composite "Murnauer Moos"

The color composite (fig. 64) derived from statistically transformed data is characterized by a much higher contrast and an enlarged "spectrum" of colors.

Plant ecologists could derive from the transformed image very good information on the areal distribution of raised-bog (blueish) and transition bog (brown). A differentiation which could not be obtained on the false-color presentation. Furthermore two types of meadows, light brown and green can be separated.

REPRODUCIBILITY OF THE
ORIGINAL PAGE IS POOR



Fig.64 Color transformation on the basis of statistically preprocessed data

Due to the momentaneous experimental status, it would be desirable to quantify and standardize color coding of optimized information on the basis of 3 dimensional color space. The term standardization means a transformation into perceptable color differences.

Quantification means a reproducible relationship between a distinct phenomena and color. Such relationships are for example red color tones indicating vegetation if false color images are interpreted.

Such "quantified data" can be obtained if the input data are derived from statistically optimized preprocesses. For demonstration the data of test area 2 (Fig.62) were selected.

The following color transformations show enhanced information due to different surface phenomena (Fig. 65,66,67)



Fig. 65



Fig. 66

REPRODUCIBILITY OF THE
ORIGINAL PAGE IS POOR



Fig. 67



Fig. 68 Aerial photograph exhibiting the same scene

REPRODUCIBILITY OF THE
ORIGINAL PAGE IS POOR

On the basis of above processed information the user would be provided with optimum data. In comparison to the computerized classification technique, the transformation into the color space procedure, results in data still "untouched" by decision making errors or averaging effects.

The decision making aspect still left to the interpreter could be carried out via isochrome mapping techniques or even by an interpretation based on the earth scientific know how.

REPRODUCIBILITY OF THE
ORIGINAL PAGE IS POOR.

3. Analog Electronic Data Evaluation

The increased interest of scientists in Landsat data and their requirements towards easy to operate and interactive data processing possibilities led to the implementation of an analog data processing system (Phase I, completed July 1975), which will be interfaced to a minicomputer (Phase II, completed beginning of 1976).

By means of the interface combination, the system offers hybrid capabilities. For quick look data evaluation based on photographic LANDSAT-data-products it is possible to operate the analog electronic circuits separately. The System has the following standard evaluation functions:

I Analog Electronics

- point-wise density reading
- density slicing
- line by line intensity level analysis of the whole image including selection of particular features
- combination of multispectral and sequential data with respect to following algorithms
 - ratios; products, sums, differences

- color space operations with original or preprocessed data
- electronic representation of scatter diagrams of any two data sets.

The digital operating circuits will be supported by problem oriented software routines covering the following function.

- CCT input capabilities
- geometric correction of LANDSAT data
- classification statistics
- basic image enhancement.

The results obtained by a pure digital treatment of data can be displayed on a line printer or via the analog electronic circuits.

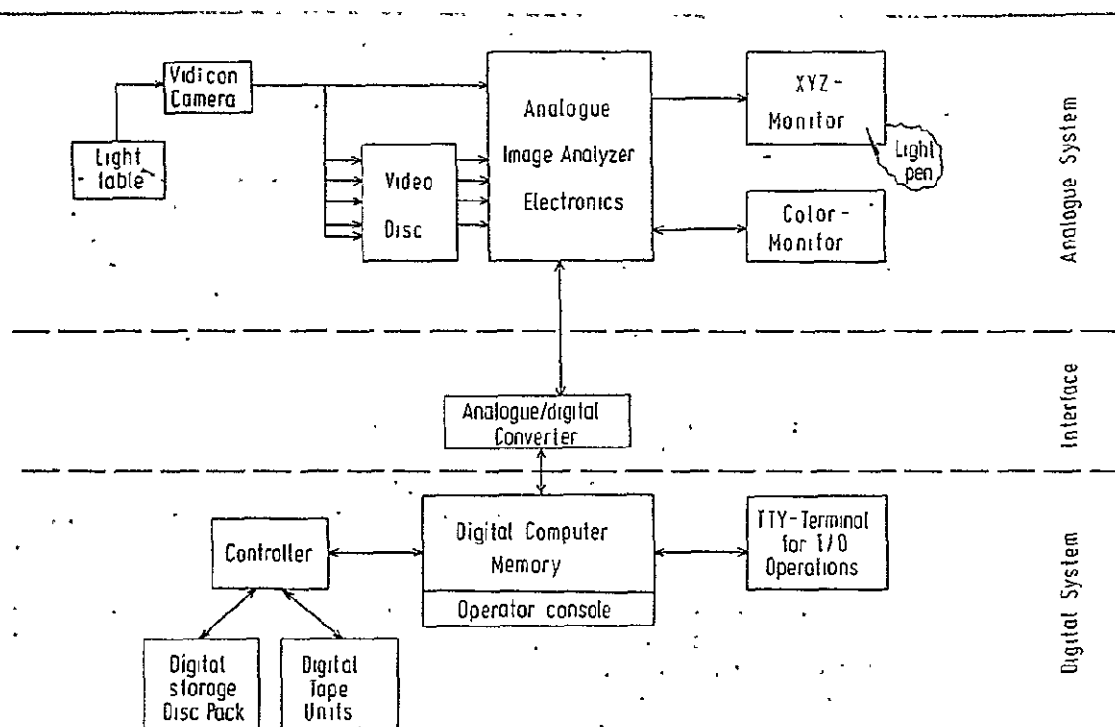


Fig. 69 Scheme of an analog/digital data processing system

C Fourier analytical evaluation of LANDSAT data by
an optical computer

During the last year coherent optical processing techniques were applied on LANDSAT-data under various aspects. The optical bench used is available at the Institut für Nachrichtentechnik at the Technical University of Munich.

Optical processing was carried out for the following purposes:

- image manipulation
- quantitative measurement of spectra

1. Image manipulation

Image manipulations were done with an experimental system\$ exhibited by Fig. 7o

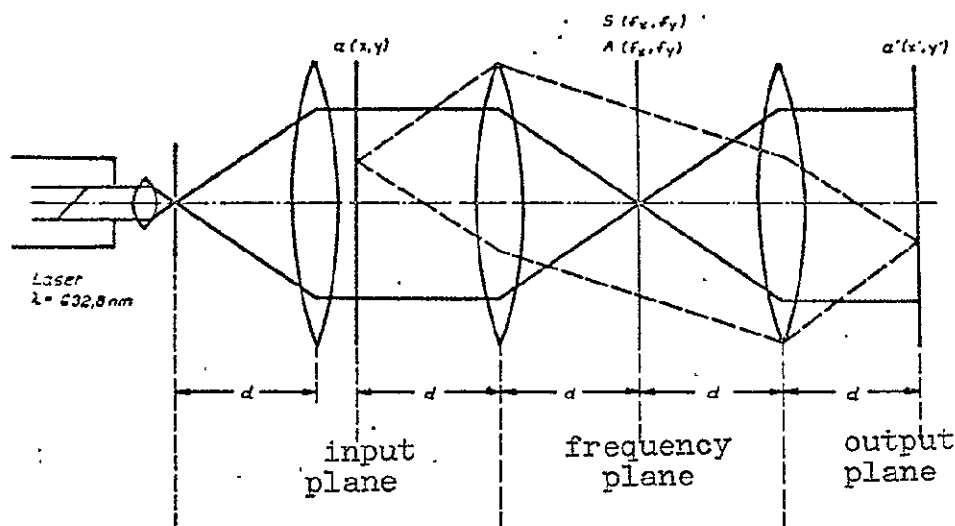


Fig.7o Schematic representation of optical bench

Using a coherent light source and a corresponding lens - system, the two-dimensional pattern (Image) of the input plane is transformed into the Fourier transform (frequency plane). Now it is possible to remove spatial frequencies from the Fourier spectrum by applying optical filters.

Afterwards the filtered image can be optically rebuilt (output plane) which again requires a corresponding lens.

By applying high- or low pass filters image enhancement in terms of contrast manipulations can be carried out.

More interesting for geological applications is the so called directioneal filtering.

For this purposes a 10^0 wedge filter was used to remove those directions which are easily detectable by the eye and which may camouflage minor directions.

By using an S 190 A enlargement representing the Apenine foreland between Pascara and Ancona (Fig. 71a), an attempt was made to remove especially those directions that are not necessarily of tectonic origin in terms of fracture control. The orientation indicated is due primarily to the drainage system directed perpendicular to the Adriatic coast (Fig. 71a). The reconstruction (Fig. 71b) shows very distinctly the prolongations of the main lineations which cut the Apenines in an ENE and an ESE direction (Fig. 71c). Furthermore, a secondary system accompanying the main structures can be detected, especially in the northern part of the area selected.

REPRODUCIBILITY OF THE
ORIGINAL PAGE IS POOR

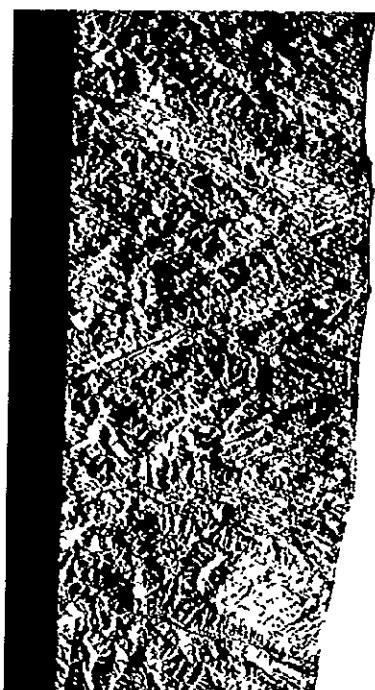


Ancona

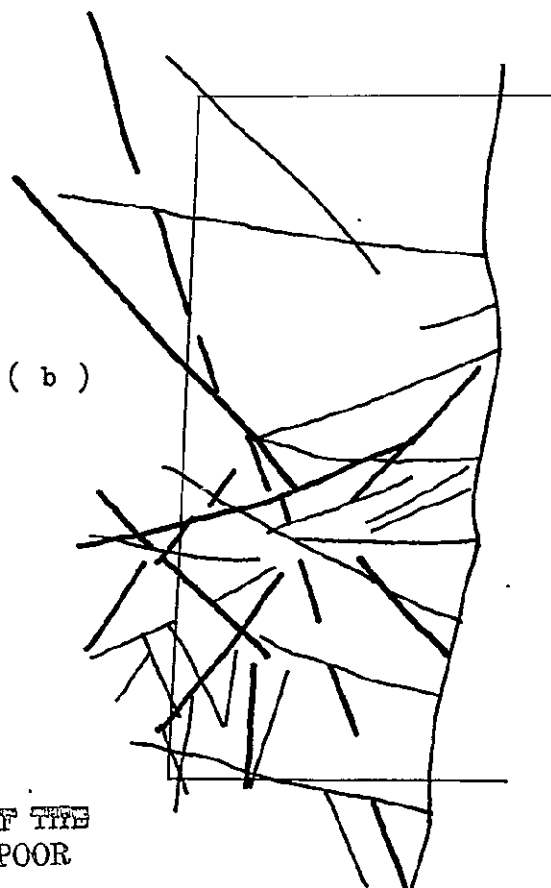
Adriatic
sea

Eastern Apennine foreland
between Ancona and
Pescara
SKYLAB S 190 A, Sept. 73
(Detail)
Reconstruction from an
optical Fourier trans-
form

(a)



Pescara



(b)

(c)

REPRODUCIBILITY OF THE
ORIGINAL PAGE IS POOR

2. Quantitative measurementsREPRODUCIBILITY OF THE
ORIGINAL PAGE IS POOR

Of special interest for tectonical applications is to obtain a quantitative measure of the directional distribution of linear features.

The conventional way of obtaining such information requires time consuming evaluations and measurements of length and direction of each single lineament. The results are then statistically plotted in form of rose diagrams.

In order to evaluate the two-dimensional spectrum in a quantitative way, the relative brightness of the spectrum has to be measured.

The information of brightness - distribution was obtained by using a photo multiplier which was connected to the frequency plane. By a step wise rotation of a narrow wedge filter the intensities can be easily recorded with respect to the direction.

In order to obtain information on the accuracy of this technique a lineament (Fig. 72) was optically evaluated. The result was compared with a conventional evaluation.

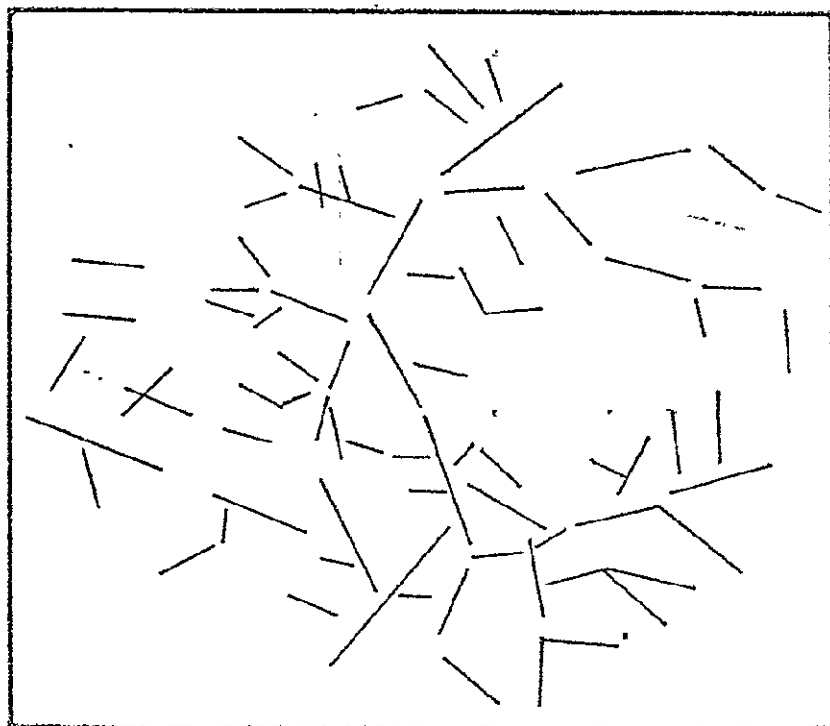


Fig. 72 Example of a lineament map

The comparison is exhibited by Fig.73 and shows a far-reaching agreement especially in the directional distribution of main lineaments.

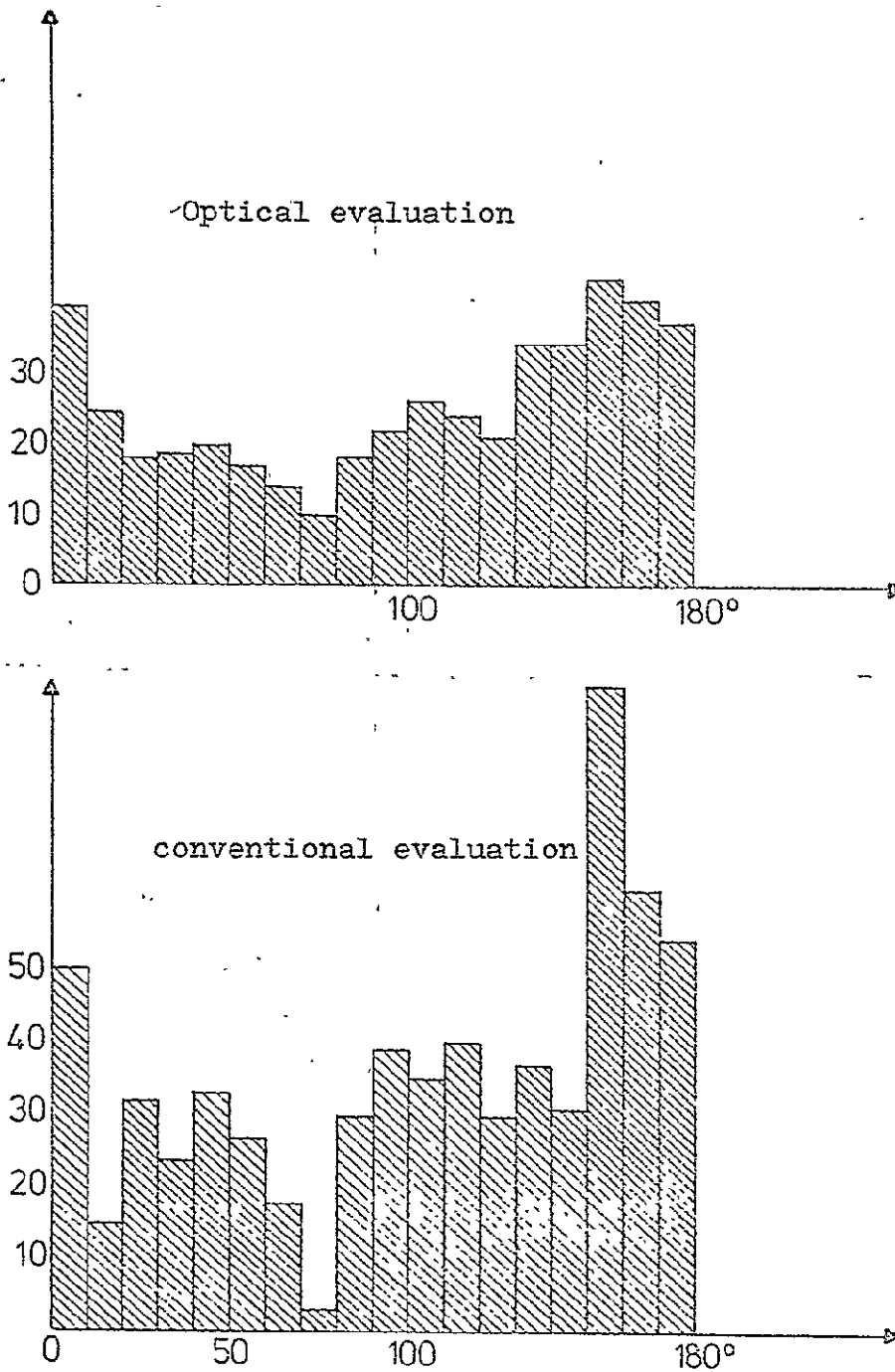


Fig. 73. Comparison optical/hand evaluation of a lineament map

REPRODUCIBILITY OF THE
ORIGINAL PAGE IS POOR

In a next step a small part out of a LANDSAT scene (Fig.74) was used. The distribution of image frequencies were directly measured and again compared with the lineament-distribution obtained by a pure interpretation.(Fig.75).



Fig. 74 LANDSAT MSS-6 Rhine Graben with test site for optical processing

REPRODUCIBILITY OF THE
ORIGINAL PAGE IS POOR

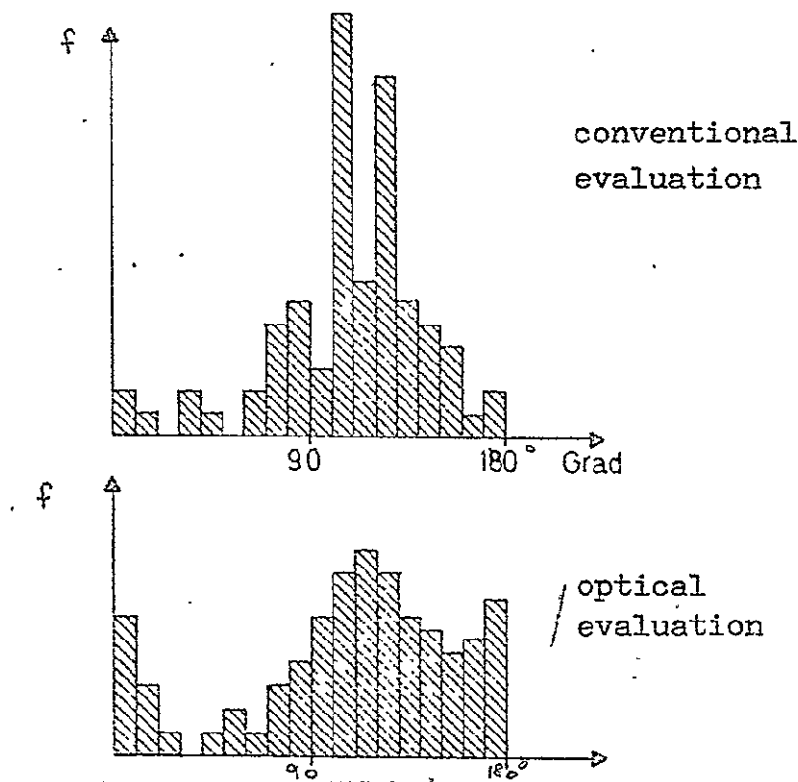


Fig. 75 Comparison optical/hand evaluation of test site

This figure demonstrates again, that it is possible to obtain information at least on the distribution of dominant linear features by applying optical processing techniques.

Above described good possibilities led to a more detailed evaluation taking into account the frequency distributions which can be derived from different spectral bands.

Fig. 76 demonstrates the frequency distributions of the same test area (Fig. 74) with respect to MSS bands 4, 5, 6 and 7. A good comparison of above readings is given by the characteristic peaks originated from the scan-lines. An effect which is distinctly expressed on MSS 4.

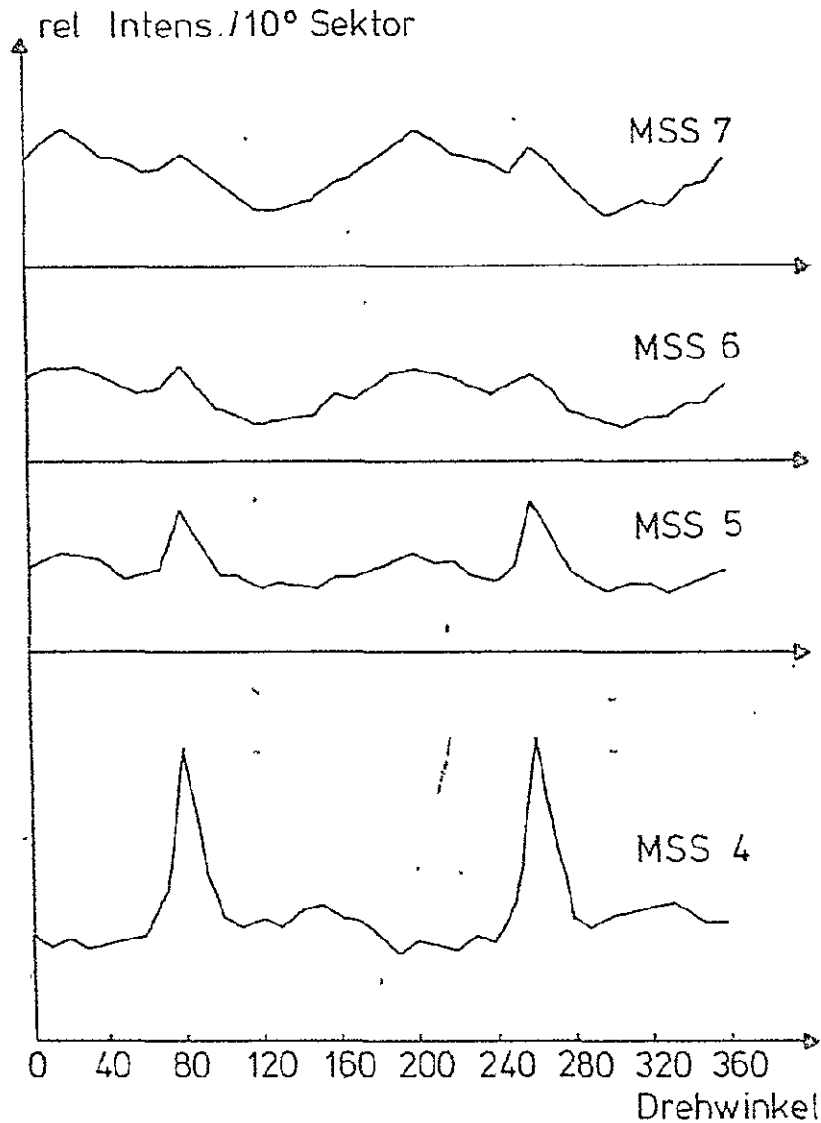


Fig. 76 Frequency distribution derived from
MSS bands 4, 5, 6 and 7

A comparative evaluation between MSS 7 and MSS 4 (Fig. 76) shows that two directions can be identified with respect to relative brightness differences.

Category I : Intensity MSS 7 MSS 4

Category II : Intensity MSS 7 MSS 4

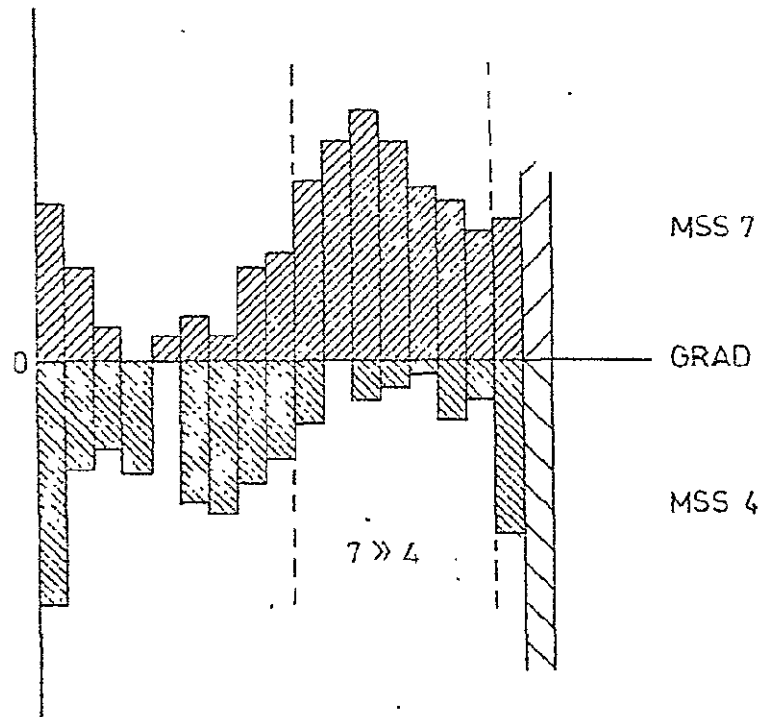


Fig. 77 Comparison Intensities band 7 versus band 4

These two characteristic intervals could be related to the dominant fracture system in the vicinity of the Rhine Graben. Category I corresponds to the Rhine Graben-parallel fracture system and Category II to the lineations which are \pm perpendicular to the parallel structures.

This example has to be regarded as an attempt to combine multispectral- with spatial- information on a more quantitative way.

REPRODUCIBILITY OF THE
ORIGINAL PAGE IS POOR

References to Part I, B: Geo-tectonic studies in Eastern Alps

- Anderson, E.M., 1951 The Dynamics of Faulting and Dyke-Formations with Application to Britain. Oliver and Boyd, Edinburgh, 2nd. ed. pp.10-11
- Aubouin, J., 1964 Esquisse Paleogeographique et Structurale des Chaines Alpines de la Mediterranee Moyenne. Geol. Rdsch vol 53, pp.480-534.
- Bodechtel, J. and Lammerer, B. 1973 New aspects on the tectonics of the Alps and the Appennines revealed by the ERTS-1 data. Proc. Symp. Significant Results Obtained from the ERTS-1 Goddard Space Flight Center, Maryland March 5-9, 1973, vol. I, Tech. Presentation Sect. A, pp.493-499.
- Bodechtel, J. and Nithack, J. 1974 Geologisch-tektonische Auswertung von ERTS-1 und SKYLAB Aufnahmen von Nord- und Mittelitalien. Geoforum 20, pp.11-24.
- Carte tectonique internationale de l'Europe, 1 : 2,500,000, No.10, Moscow, 1962.
- Ernst, W.G., 1975^a Systematics of large-scale tectonics and age progressions in Alpine and circum-Pacific blueschist belts. Tectonophysics, 26, pp.229-246.
- Ernst, W.G., 1975^b Interpretative synthesis of metamorphism in the Alps. In : W.G. Ernst (Editor) Subduction Zone Metamorphism ; Benchmark papers in Geology /19; Dowden Hutchinson & Ross Inc. , pp. 406-431.
- Farmer, I.W., 1968 Engineering Properties of Rocks E.&F.N. Spon Ltd. London, pp. 58-59.

- Freden, S.C. and Mercanti, E.P. 1973 Symposium on Significant Results Obtained from Earth Resources Technology Satellite - 1, vol. III, Discipline Summary Reports, 118 p., Goddard Space Flight Center, Greenbelt, NASA, Washington, D.C.
- Freden, S.C., Mercanti, E.P., and Friedman, D.B., 1974 Third Earth Resources Technology Symposium, vol. III, Discipline Summary Reports 155 p., Goddard Space Flight Center, Greenbelt, NASA, Washington, D.C.
- Gansser, A., 1968 The Insubric Line - a major geotectonic problem. Schweiz. Minerlog. Petrograph. Mittlgn., vol. 48, pp. 123-143.
- Illies, H., 1974 Intra-Plattentektonik in Mitteleuropa und der Rheingraben. Oberrhein. Geol. Abh., 23, pp. 1-24.
- 1975 Intraplate tectonics in stable Europe as related to plate tectonics in the Alpine system. Geol. Rdsch., vol. 64, pp. 677-699.
- Laubscher, H.P., 1971 The large-scale kinematics of the western Alps and the western Apennines and its palinspastic implications, Am. Jour. Sci., vol. 271, pp 193-226.
- Laubscher, H.P., 1973 Alpen und Plattentektonik-das Problem der Bewegungsdiffusion an kompressiven Plattengrenzen. Z. Deutsch. Geol. Ges. vol. 124, pp. 295-308.
- Price, N.J., 1959 Mechanism of jointing in rocks. Geol. Mag., vol. 96, pp. 149-167.
- 1966 Fault and Joint Development in Brittle and Semi-Brittle Rock. Pergamon Press, Great Britain.

- Ranalli, G., and
Chandler, T.E., 1975 The stress field in the Upper Crust as
determined from in-situ measurements.
Geol. Rdsch., vol. 64, pp. 653-674.
- Ritsema, A.R. 1969 Seismo-tectonic ^himplications of a
review of European earthquake mechanism.
Geol. Rdsch. vol.59, pp. 36-56.
- Senftle, E., and
Exner, Ch., 1973 Resente Hebung der hohen Tauern und
geologische Interpretation. Verh. Geol.
Bund. Anst., Vienna, No. 2, pp. 209-234.

REPRODUCIBILITY OF THE
ORIGINAL PAGE IS POOR.
3
BU